

Role of DNA damage repair pathways in chemoresistant leukemic cells

By

Sameer Jagannathrao Salunkhe

[LIFE09201204006]

TATA MEMORIAL CENTRE

MUMBAI

A thesis submitted to the

Board of Studies in Life Sciences

in partial fulfilment of requirements

for the Degree of

DOCTOR OF PHILOSOPHY

OF

HOMI BHABHA NATIONAL INSTITUTE


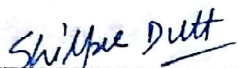
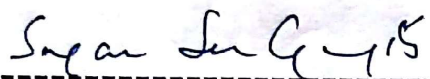
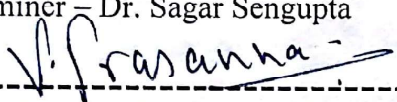
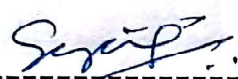
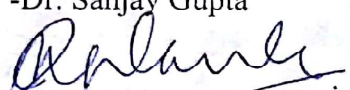


August, 2018

Homi Bhabha National Institute

Recommendations of the Viva Voce Committee


As members of the Viva Voce Committee, we certify that we have read the dissertation prepared by Mr. Sameer Jagannathrao Salunkhe entitled "**Role of DNA damage repair pathways in chemoresistant leukemic cells**" and recommend that it may be accepted as fulfilling the thesis requirement for the award of Degree of Doctor of Philosophy.

	24/8/18
Chairman – Dr. Sorab N. Dalal	Date:
	24/8/18
Guide/Convener – Dr. Shilpee Dutt	Date:
	24/8/18
External Examiner – Dr. Sagar Sengupta	Date:
	24/8/18
Member – Dr. Prasanna Venkatraman	Date:
	24/8/18
Member -Dr. Sanjay Gupta	Date:
	24/8/18
Technical Advisor –Dr. Sanjeev Galande	Date:

Final approval and acceptance of this thesis is contingent upon the candidate's submission of the final copies of the thesis to HBNI.

I hereby certify that I have read this thesis prepared under my direction and recommend that it may be accepted as fulfilling the thesis requirement.

Date: 24/08/2018
Place: Navi Mumbai


Dr. Shilpee Dutt.
Guide

STATEMENT BY AUTHOR

This dissertation has been submitted in partial fulfillment of requirements for an advanced degree at Homi Bhabha National Institute (HBNI) and is deposited in the Library to be made available to borrowers under rules of the HBNI.

Brief quotations from this dissertation are allowable without special permission, provided that accurate acknowledgement of source is made. Requests for permission for extended quotation from or reproduction of this manuscript in whole or in part may be granted by the Competent Authority of HBNI when in his or her judgment the proposed use of the material is in the interests of scholarship. In all other instances, however, permission must be obtained from the author.

Sameer Salunkhe

DECLARATION

I, hereby declare that the investigation presented in the thesis has been carried out by me. The work is original and has not been submitted earlier as a whole or in part for a degree at this or any other Institution / University.

Sameer Salunkhe

LIST OF PUBLICATIONS ARISING FROM THE THESIS

Journals:

1. **Salunkhe, S.**, Mishra, S. V., Nair, J., Ghosh, S., Choudhary, N., Kaur, E., Shah, S., Patkar, K., Anand, D., Khattry, N., Hasan, S. K. and Dutt, S., Inhibition of novel GCN5-ATM axis restricts the onset of acquired drug resistance in leukemia. **Int. J. Cancer**. 2018 May 15;142(10):2175-2185

Chapters in books and lectures notes: NA

Conferences:

1. **Sameer Salunkhe**, Shilpee Dutt. Understanding the mechanisms of survival of chemoresistant leukemic cells. XXXVIII All India Cell Biology Conference and International Symposium on. 'Cellular Response to Drugs' by CSIR-CDRI Lucknow. December 10-12, 2014. **(Poster presentation)**
2. **Sameer Salunkhe**, Ashwin Ramaswamy, Sanket Shah, Shilpee Dutt. Hyper phosphorylation of ATM Kinase is responsible for the early onset of acquired drug resistance in leukemia. 38th Annual conference of Mumbai Hematology Group, 14th-15th March 2015 **(Oral presentation- JC Patel award for best oral presentation)**.
3. **Sameer Salunkhe** , Sanket Shah, V.Devanand, Ashwin Ramaswami, Jyothi Nair, Smita Patkar, Syed Hasan, Navin Khattry and Shilpee Dutt*GCN5 mediated hyperactivation of ATM Kinase is responsible for the early onset of acquired drug resistance in leukemic minimal residual cells (MRD). -56th Annual meeting of the Indian Society of Haematology and Blood Transfusion (ISHBT) (5th-8th Nov 2015) **(Oral presentation)**
4. **Sameer Salunkhe**, Ekjot Kaur, Sanket Shah, Jyothi Nair, V.Devanand, Smita Patkar, Syed Hasan, Navin Khattry and Shilpee Dutt GCN5 mediated ATM activation a novel resistance mechanism that if targeted during early induction therapy eliminates the formation of MRD. at -TMC Platinum Jubilee Celebrations 1st Conference on A conference of new ideas in cancer - Challenging dogmas (26th to 28th February 2016). **(Poster presentation)**
5. **Sameer Salunkhe**, Jyothi Nair, Neha Choudhary, Samadri Ghosh, Ekjot Kaur, Sanket Shah, Ketaki Patkar, Dev Anand, Navin Khattry, Syed K Hasan, Shilpee Dutt. GCN5

regulates ATM mediated DNA repair responsible for onset of acquired resistance in leukemia. at “Annual meeting of American Association for Cancer Research (AACR)” in Washington DC, USA, April 1st to 5th, 2017. **(Poster presentation)**

6. **Sameer Salunkhe**, Jyothi Nair, Neha Choudhary, Samadri Ghosh, Ekjot Kaur, Sanket Shah, Ketaki Patkar, Dev Anand, Navin Khattry, Syed K Hasan, Shilpee Dutt. Inhibition of novel GCN5-ATM axis restricts the onset of acquired drug resistance in leukemia. International congress of cell biology (ICCB 2018) to be organized by CSIR CCMB Hyderabad to be held on (27th to 31st Jan 2018). **(Awarded for best poster presentation)- Awarded travel grant.**
7. **Sameer Salunkhe**, Jyothi Nair, Neha Choudhary, Samadri Ghosh, Ekjot Kaur, Sanket Shah, Ketaki Patkar, Dev Anand, Navin Khattry, Syed K Hasan, Shilpee Dutt. Inhibition of novel GCN5-ATM axis restricts the onset of acquired drug resistance in leukemia Poster presentation Indo-US conference on ‘Transcription, Chromatin Structure DNA Repair and Genomic Instability’, to be organized by IISc, Bangalore from March 6-10, 2018. **(Poster presentation)**

Others:

1. Mittra Indraneel**Sameer Salunkhe**. “Cell-Free Chromatin from Dying Cancer Cells Integrate into Genomes of Bystander Healthy Cells to Induce DNA Damage and Inflammation.” **Cell Death Discovery** 3 (2017): 17015–. PMC. Web. 10 Feb. 2018. doi: 10.1038/cddiscovery.2017.15

Navi Mumbai,

Date: 24.08.2018

Sameer Salunkhe

Dedicated To All My
Loved Ones

ACKNOWLEDGEMENTS

“The only journey is the one within”. The journey of Ph.D. was not an easy one but one step at a time made it possible. It is during my Ph.D. that I had the opportunity to grow into the person I always intended to be and thus, I would like to take this opportunity to thank all the people who were a part of this journey with me and made it a memorable one.

Firstly, I would be like to sincerely thank **Dr. Shilpee Dutt** my Ph.D. mentor, for her guidance and support all through my tenure. I am highly grateful to her for the motivation that she provided me in times of need and helped me sail my boat through the stormy sea. Our zealous and constructive discussions about science, academics, and research made my Ph.D. productive and me as an independent and rational thinker.

I would like to extend my gratitude towards **Dr. S.V. Chiplunkar** (Director, ACTREC), **Dr. Sudeep Gupta** (Deputy Director, ACTREC), **Dr. Rajiv Sarin** (Ex-Director, ACTREC), and **Dr. Surekha Zingde** (Ex-Deputy Director, ACTREC), for providing both research opportunity and excellent resources at ACTREC. I would also like to thank **CSIR** for promptly availing me the fellowship and ACTREC for all the required facilities. I am also thankful to the Homi Bhabha National Institute (**HBNI**) and Tata Memorial Centre (**TMC**) for proving me with the financial assistance to present my work at a prestigious international platform like AACR 2017.

I am extremely grateful to my thesis committee members: **Dr. Sorab Dalal** (Chairperson, ACTREC), **Dr. Prasanna Venkatraman** (ACTREC), **Dr. Sanjay Gupta** (ACTREC), **Dr. Sanjeev Galande** (Invitee, IISER Pune) and also to my ex-Chairperson **Dr. G.B. Maru** for their analytical and enlightening suggestions at regular intervals.

I am obliged to **Dr. Amit Dutt** who has made available his support in a number of ways. His insightful suggestions and constant encouragement helped me grow at both scientific as well as personal front. His subtle and thoughtful way of addressing scientific as well as non-scientific issues has taught me the finesse and craft of this field.

I would also like to show my gratitude to all my clinical collaborators **Dr. Syed Hasan** (ACTREC), and **Dr. Naveen Khattry** (ACTREC) for providing me with the AML patient samples. I am forever indebted to all the **patients** for agreeing to be a part of this study and making it possible.

I would also like to thank **Dr. Rahul Thorat** for helping me in developing leukemia mouse model. I am deeply thankful to **Dr. Vera Gorbunova** for HR and NHEJ activity vectors and **Dr. Ezra Burstein** for providing us with the GCN5 vectors for our important experiments.

I am thankful to the **staff** in common facility, microscopy, flow cytometry, animal house, sequencing, IT, library, steno-pool, administration and accounts for their constant help and support. A special thanks to **Retreat canteen** members for catering wonderful food.

The immense contribution made by the **all the lab members** have helped me to widen my research from various perspectives. They have been a true source of teamwork and fraternization. I am grateful to **Mr. Ganesh Bejjanki** for his excellent technical help. I would like to make a special mention about **Mrs. Smita Patkar** whose prompt action and assistance for every laboratory aspect have truly bolstered my research work. I would like to thank

Priya, Rachyata, Akruti, and Sanket for their valuable contribution during the initial years of my Ph.D.

I am grateful to all my trainees **Neha, Samadri, Naren, Ashwin, Rajeev** and **Gargi** without whom this work wouldn't have been possible. **Pratik, Nilesh** and **Pawan** for their support in different computational aspects of my work. I extend my thanks towards **Jacynth, Jyothi, Anagha, Saket, Tejashree, Shraddha, Mukul, Prajish, Prachi, Sanket, Asim, Trupti, Bhasker, Nilima, Suhail** and **Supriya** for maintaining a positive and fruitful atmosphere in the lab and making this venture pleasant for me.

"A journey is best measured in friends rather than miles". This journey wouldn't have been so lovely without the support of my batchmates **Pratik, Gopal, Saujanya, Bhavik, Arunabha, and Bhushan**. We all made great memories together that will stay with me forever.

I also owe my deepest thanks to all my friends outside the lab, especially **Shailesh** who understood and endured my frustrations and most importantly for being a true friend in times of need. I would like express appreciation to my beloved wife **Alokananda** for her forbearance whilst I undertook this project and helped me organize my life. Her true love, support and encouragement have helped me breeze through difficult times and made this thesis possible.

I am extremely blessed to be born to **my parents** whose sacrifices cannot be measured. Their faith in me and shield of prayers helped me pursue my dreams. Their love and inspiration gave me the strength to pick myself up after each fall and walk again. I cannot express how thankful I am to my sister **Poonam** for always being there in my absence and acting as an anchor for the family.

"I may not have gone where I intended to go, but I think I have ended up where I needed to be". With that, lastly I would like to thank the **God almighty** for his blessings and kindness that made me complete my Ph.D.

Sameer Salunkhe.

TABLE OF CONTENTS

CONTENTS	PAGE No.
ABBREVIATIONS	1
SYNOPSIS	3
LIST OF ILLUSTRATIONS	17
LIST OF TABLES	18
LIST OF FIGURES	19
CHAPTER 1: INTRODUCTION	21
1.1: Leukemia:	22
1.1.1: Risk factors/Causes for Leukemia:	22
1.1.2: Epidemiology:	22
1.1.3: Symptoms and Diagnosis:	24
1.1.4: Treatment:	25
1.1.5: DNA damaging drugs in leukemia chemotherapy:	26
1.1.5.1: Doxorubicin:	27
1.1.5.2: Mitoxantrone:	28
1.1.6: Therapy outcome:	29
1.1.7: Resistance to DNA damaging drugs:	30
1.1.7.1: Drug uptake and efflux:	31
1.1.7.2: Drug target alterations:	32
1.1.7.3: DNA damage and repair:	33
1.1.7.3.1: Homologous recombination (HR) repair:	36
1.1.7.3.2: Non-Homologous End Joining (NHEJ) repair:	38
1.1.7.3.3: Role of ATM in DNA double-strand break repair:	40
1.1.7.3.4: Mechanisms of ATM activation:	43
1.1.8: Current challenges in leukemia treatment are to:	44

1.2: Rationale:	45
1.3: The aim of the thesis:.....	45
1.3.1: Objectives:	45
CHAPTER 2: MATERIALS AND METHODS	46
2.1: Cell lines and media requirements:	47
2.2: STR profiling:	47
2.2.1: K562:	47
2.2.2: THP-1:	48
2.2.3: HL-60:	49
2.3: Development of an evolutionary model of drug resistance:	49
2.4: Generation of HL-60/MX2 cell line:	50
2.5: Drugs and MTT assay:	51
2.6: Clonogenic assay:.....	51
2.7: Cell cycle and Drug uptake:	51
2.8: Softwares:	51
2.9: Neutral comet assay/ Single cell gel electrophoresis assay:	52
2.10: DNA fragmentation Assay:	52
2.11: Western blotting:	52
2.12: Immunofluorescence and Image analysis:	53
2.13: GFP vector reactivation assay/ HR and NHEJ activity assay:	54
2.13.1: Purification of digested linearized plasmid using PCR clean-up kit:	54
2.13.2: NHEJ & HR Vector Transfection:	55
2.14: Quantitative real-time SYBR green PCR:	57
2.15: Transmission electron microscopy (TEM):	58
2.15.2: TEM image quantitation:.....	59
2.16: ATM kinase inhibitor (KU-55933):	59
2.17: GCN5 inhibitor (Butyrolactone 3 or BL-3 or MB-3):.....	59

2.18: Co-Immunoprecipitation of GCN5 and ATM:	60
2.19: siRNA knockdown of GCN5:	60
2.20: Plasmid isolation using NucleoSpin:	60
2.21: GCN5 overexpression:.....	61
2.22: GCN5/KAT2A metadata analysis:.....	61
2.23: Collection of AML patient samples and ethics statement:	61
2.24: Immunohistochemistry of GCN5 in AML bone marrow biopsies:	62
2.25: Statistics:	63
CHAPTER 3: RESULTS	65
3.1 Objective 1: Establishment and characterization of drug resistant cell lines.	66
3.1.1: Conventional drug resistant models and their limitations:.....	66
3.1.2: Establishment of the evolutionary model of drug resistance:	66
3.1.2.1: Clonogenic properties, cross resistance and reversible resistance of drug resistant cells:	68
3.1.2.2: Cell cycle profile of drug resistant cells:	70
3.2: Objective 2: Discerning the differences in DSB repair pathways between chemosensitive and chemoresistant population.	72
3.2.1 DNA damage and repair kinetics of HL-60/MX2 cells:	72
3.2.2 Absence of DNA damage in highly adapted populations:	73
3.2.3: Faster DNA repair kinetics in early stage drug resistant population:	74
3.2.4: EDRP harbors hyperactive ATM kinase signaling and favors HR repair:	77
3.2.5: ATM kinase inhibition efficiently eliminates EDRP cells, however, fails to sensitize LDRP cells:	80
3.2.6: Plausible reasons for failure of ATM kinase inhibitor in late stage drug resistant cells:....	80
3.2.7: LDRP display multifactorial drug resistance:	83
3.3: Mechanisms of ATM activation in EDRP cells:.....	87
3.3.1: EDRP show enrichment of euchromatin rich cells:.....	87
3.3.2: GCN5 is upregulated in all the drug resistant populations:	89
3.3.3: <i>GCN5</i> or <i>KAT2A</i> (Lysine Acetyltransferase 2A):	90

3.3.4: Role of GCN5 in Drug resistance and DNA repair:	91
3.3.5: Genetic or pharmacological inhibition of GCN5 perturbs ATM activation:.....	93
3.3.6: GCN5 colocalizes and interacts with ATM post doxorubicin treatment:	95
3.3.7: GCN5 overexpression is associated to high risk disease and poor patient survival:	96
CHAPTER 4: DISCUSSIONS AND CONCLUSIONS	101
4.1: Discussion:.....	102
4.2: Summary/ Outcome of the study:	105
BIBLIOGRAPHY	108
PUBLICATIONS	115



Homi Bhabha National Institute

SYNOPSIS OF Ph. D. THESIS

1. **Name of the Student:** Sameer Jagannathrao Salunkhe
2. **Name of the Constituent Institution:** Tata Memorial Centre, ACTREC
3. **Enrolment No. :** LIFE09201204006
4. **Title of the Thesis:** Role of DNA damage repair pathways in chemoresistant leukemic cells.
5. **Board of Studies:** Life Science

SYNOPSIS

Introduction:

Leukemia chemotherapy involves drugs that inhibit topoisomerases to induce DNA double strand breaks (DSBs) in rapidly dividing cells. However, despite initial remission most of patients experience relapse [8]. Apart from mechanisms like downregulation of topoisomerases [9] and upregulation of drug transporters [10], modulation of DNA repair pathway is known to play a major role in acquiring drug resistance in different cancer types [11, 12]. As topoisomerase inhibitors induce DNA DSBs, we focused on understanding the regulation of DNA repair mechanisms in chemoresistant leukemic cells.

ATM, a master regulator kinase involved in DNA DSBs repair [13] is known as an important mediator of drug resistance[14-16]. Although ATM can get activated by autophosphorylation, mechanisms like higher recruitment via Mre11 proteins, relaxed chromatin architecture, downregulation of its phosphatases (*WIP1* and *PP2CA*), direct acetylation by *TIP-60* and

Synopsis

HMOF induced H4K16ac mediated recruitment [13, 17-22] have been shown to further enhance its activity.

Extensive research on understanding the role of DNA DSB repair in chemoresistance in leukemia has been done using cell lines with high resistance indices based model systems. Since these model systems cannot be used for comparative studies between the early and late stages of drug resistance, there is limited knowledge regarding the evolution of DNA repair mechanism during acquired resistance. Therefore, we developed *in vitro* cellular models that allowed us to examine regulation of DNA repair from an initial drug tolerant state to late drug resistant state. We found that with continuous drug treatment, LDRP evolved such that topoisomerase inhibitors failed to induce significant DNA damage and ATM activation, rendering these cells ineffective against ATM inhibitor. However, during early stages of acquired resistance *GCN5/KAT2A* (a lysine acetyltransferase) was upregulated in chemoresistant leukemic cells. Upon drug treatment GCN5 facilitated higher ATM activation leading to faster DNA repair. Inhibition of GCN5 inhibited ATM activation and sensitized EDRP to doxorubicin treatment thus demonstrating that targeting early events during acquired resistance would have maximum clinical benefit. Furthermore, *GCN5* expression could be used as a potential biomarker to detect onset of resistance during induction therapy. Accordingly, inhibition of GCN5 during early stages is a novel approach to prevent emergence of difficult to treat stable resistant leukemic clones.

Taken together, for my thesis, I want to identify the differences in DNA double strand break (DSB) repair pathways innately present or acquired during chemotherapy that influence the efficiency and choices of DSB repair pathways in chemoresistant resistant leukemic cells. Specifically, in this study I would focus on differential DSBR pathways helping survival of chemoresistant cells and would try to identify critical change for their survival.

Aim: To understand the role of DNA double strand break repair pathways in chemoresistant leukemic cells.

Specific Objectives:

1. Establishment of chemoresistant cell lines to lethal dose of DNA damaging drugs for acquired resistance.

2. Discerning the differences in DSB repair pathways between chemosensitive and chemoresistant population.

Objective 1: Establishment of chemoresistant cell lines to lethal dose of DNA damaging drugs for acquired resistance.

Work plan: Two Leukemic cell lines K-562, THP-1 and HL-60 will be used for studying the mechanisms of chemo-resistance against two DNA damaging drug i.e. Doxorubicin and mitoxantrone. In order to study the drug resistance, an *in vitro* chemo-resistant model will be established by treating the cells with repeated cycles of IC-90 conc. of drugs until the cells are able to survive the IC-90 concentration of the drug.

Work done:

3.1 Recapitulating clinical scenario of acquired resistance in a cellular model.

We modeled acquired resistance to DNA damaging agent doxorubicin using leukemic cell lines K562 and THP-1. First, the lethal dose (where ≥ 90 % cells die) of doxorubicin for K562 and THP-1 was determined to be 2.5 μ M and 1.4 μ M respectively by cell viability assay. Cells were then treated with their respective lethal dose of doxorubicin for 48 h. We found that a small percentage (<10%) of cells survived (persisters or residual cells, equivalent to the minimal residual disease observed in the patients) high concentrations of doxorubicin in both the cell lines. These persisters were allowed to grow. The first relapsed population (R) was termed K562-R1 and THP-1 R1. K562 cells were treated with doxorubicin for 10 cycles (over 8 months) while THP-1 for 7 cycles (over 6 months) to obtain the cells with the high drug resistance index. We collected the relapsed cells after every round of drug treatment i.e., R1, R2, R5, R7 and R10 for K562 and R1, R2, R3, R5 and R7 for THP-1 cell line. Resistance to doxorubicin for each population was analyzed by MTT cell viability assay. We found that R1 population of K562 and R1 and R2 population of THP-1 cell line showed similar sensitivity to doxorubicin as the parent population. However, K562-R2 cells (1.97-fold resistance) and THP-1-R3 cells (1.46-fold resistance) were earliest relapses that showed significantly better survival to doxorubicin than their respective parent populations. Since K562-R2 and THP-1-R3 were the first populations to show significant resistance to doxorubicin, we refer to these populations as Early Drug Resistant Population (EDRP) cells and K562-R10 and THP-1-R7 as Late Drug Resistant Population (LDRP) cells. EDRP and

LDRP of both the cell lines were analyzed for their clonogenic ability in the presence of IC90 concentration of doxorubicin. Both EDRP and LDRP formed significantly higher number of colonies compared to parent cells, indicating the enrichment of cells with colony forming capacity (unlimited cell growth) in these populations. Similar results were obtained with HL-60 and its mitoxantrone resistant sub-cell line HL-60/MX2 (representing LDRP of HL-60) which is 35 fold more resistant than parent HL-60 cells [23] . We further tested the cross resistance of K562, K-EDRP and K-LDRP to DNA damaging drugs daunorubicin and cytarabine and found that both the populations were resistant to daunorubicin whereas cytarabine resistance was shown only by K-LDRP

Interestingly, the chemoresistant populations showed reversibility to resistance when cultured in drug free media. EDRP cells showed loss of resistance faster (10-12 days) than LDRP cells (30-40 days) . Similarly, chemoresistance is shown to be reversible in HL-60/MX2 cells as well (ATCC CRL 2257). These data are suggestive of non-genetic mechanisms of acquired chemoresistance, especially during early stages of drug resistance.

Objective 2: Discerning the differences in Double Strand Break (DSB) repair pathways between chemosensitive and chemoresistant population.

Work done:

3.2 EDRP show faster DNA repair while LDRP do not incur significant DSBs post doxorubicin treatment.

To investigate the alteration in DNA repair, we first checked for double strand breaks (DSBs) induced by doxorubicin at different time points (5min, 6h and 12h) post drug removal (PDR) using neutral comet assay. Interestingly LDRP showed minimal induction of DSBs while EDRP populations from both the cell lines (K562 and THP-1) showed DSBs similar to the parent population. However, by 12h EDRP could resolve most of DSBs compared to parent cells suggesting faster DNA repair. Similar to LDRP of K562 and THP-1, post mitoxantrone treatment, HL-60/MX2 cells also induced minimal DNA DSBs

Phosphorylation of H2AX is the first cellular response to the induction of DSBs and the rate of appearance and resolution of γ -H2AX is considered to be a measure of DSB repair efficiency of a cell [24]. Therefore, we analyzed the activation of γ -H2AX at different time

points following the drug treatment. We found that immediately after drug removal compared to the parent cells, EDRP cells showed increased H2AX phosphorylation which was mostly resolved by 12h PDR confirming faster DNA repair in EDRP cells. Concordant with comet assay, LDRP cells showed significantly less induction of γ -H2AX indicating inability of doxorubicin to induce DNA DSBs in these cells. Similarly, HL-60/MX2 cells also did not show significant induction of γ -H2AX and p-Chk2 upon mitoxantrone treatment. These data demonstrate that topoisomerase inhibitors were unable to induce DSBs in LDRP cells. We then sought to elucidate the mechanism of DSB repair in EDRP cells.

3.3 EDRP harbors hyperactive ATM kinase signaling.

Because cell cycle arrest and DNA repair is interlinked, we analyzed cell cycle profile of parent and EDRP with and without doxorubicin treatment. Post drug treatment, K562 and THP-1 parent and respective EDRP cells showed S and G2/M arrest at 24 and 48 h respectively. Although, the parent populations remained arrested, EDRP cells could overcome S and G2/M cell cycle arrest. Similarly, mitoxantrone treatment induced cell cycle arrest in HL-60 cells but not in HL-60/MX2 cells. These data demonstrate that EDRP cells were able to resolve cell cycle arrest and do not elicit an apoptotic response.

ATM (ataxia telangiectasia mutated) is a sensor kinase that phosphorylates H2AX following DNA DSBs [13]. To investigate whether increased γ -H2AX in EDRP cells could be attributed to ATM activation, levels of p-ATM were analyzed at different time points post doxorubicin treatment. Concordant with γ -H2AX activation kinetics, immunofluorescence and western blot analysis of p-ATM showed more than 2 fold increase in ATM activation in K-EDRP compared to the parent K562 cells. Furthermore, downstream targets of ATM, like p-NBS1 (Ser343), p-BRCA1 (Ser1524) and p-Chk2 (Thr68), also showed higher activation in EDRP cells compared to the parent K562 cells. Additionally Mcl-1L, an anti-apoptotic protein, whose expression is controlled by ATM [25] showed upregulation in K-EDRP cells. Similar results were obtained for parent THP-1 and T-EDRP. We then wanted to assess the choice of repair pathway (HR or NHEJ) and its efficiency in EDRP cells. For which we used HR and NHEJ vector activity assay [5]. Results showed significantly higher HR activity in K-EDRP cells compared to K562 cells. Further we also found higher recruitment of Rad51, an HR specific protein in K-EDRP compared to the parent K562, these data are in agreement with previous reports where ATM is shown to prefer resolution of DNA DSBs via HR pathway [26].

3.4 ATM kinase inhibition eliminates EDRP but not LDRP cells.

The data presented above demonstrates hyperactivation of ATM during the onset of acquired resistance. Accordingly, inhibition of ATM should induce death in residual cells and prevent emergence of chemoresistance. To test this, parent cells, EDRP and LDRP of K562 and THP-1 were treated with 10 μ M of ATM kinase inhibitor (KU55933) [27] in combination with different concentrations of doxorubicin (0 to 10 μ M). ATM kinase inhibitor induced complete cell death in K-EDRP at 2.5 μ M doxorubicin concentration but only 40% cell death in K-LDRP cells. Importantly, ATM inhibitor reduced the IC₉₀ concentration of doxorubicin for K-EDRP from 6.93 μ M to 1.39 μ M. Similar results were obtained with THP-1 EDRP and LDRP. As expected, ATM kinase inhibitor in combination with mitoxantrone did not show significant cell death in HL-60/MX2 cells. Specificity of ATM kinase inhibitor was confirmed by quantification of p-ATM and p-Chk2. The differential response of EDRP and LDRP cells to ATM kinase inhibitor is attributed to the fact that, only EDRP but not LDRP cells show the activation of ATM with doxorubicin treatment. This was expected as the LDRP cells showed minimum DNA damage to the drug treatment. In order to understand how LDRP cells escape DNA damage, we reasoned that this could be because of loss of its molecular target or over expression of drug efflux proteins. Therefore, we checked the expression of *TOP2 β* (molecular target of doxorubicin and mitoxantrone) and drug efflux pump protein *ABCB1* (*MDR1*) in all the three population of cells parent, EDRP and LDRP. No significant differences were seen in the transcripts of *TOP2 β* in parent and EDRP. However, *TOP2 β* was found to be significantly downregulated in LDRP of both K562 and THP-1 cell line. Similarly, HL-60/MX-2 cells also showed downregulation of *TOP2 β* . We further examined the drug accumulation capacity of the parent, EDRP and LDRP of K562 and THP-1 cells. For which cells were treated with IC₉₀ concentrations of doxorubicin and intracellular doxorubicin was measured using flow cytometry at 480nm (excitation wavelength) and 570nm (emission wavelength) [28]. Intracellular drug concentrations were found to be comparable in parent and EDRP but reduced in LDRP cells indicating either reduced uptake or faster efflux of drug by LDRP. We found no significant difference in the transcript levels of *ABCB1* (i.e. *MDR1*) in parent and EDRP, but they were markedly elevated in LDRP suggesting that reduced drug accumulation in LDRP cells could be due to faster efflux of the drug. Collectively, these data showed that LDRP cells had evolved multiple mechanisms to escape drug induced DNA damage. However, given the central role of ATM

activation in mediating chemoresistance in EDRP, we deemed it important to further understand the mechanism of higher ATM activation in EDRP cells.

3.5 EDRP cells show GCN5 upregulation.

ATM activation is known to be controlled by the Mre11-Rad50-NBS1 (MRN) sensor complex [17]. However, we did not find either differential expression or recruitment of Mre11 between parent K562 and K-EDRP, ruling out the possibility of MRN complex mediating differential recruitment of ATM at DSBs in EDRP. We then reasoned that downregulation of ATM phosphatases (*WIP1* and *PP2CA*) could also maintain high levels of p-ATM[13]. However, no differences in the transcript levels of *WIP1* and *PP2CA* in EDRP cells with respect to parent population were observed. It is also known that chromatin relaxation triggers higher ATM activation [13]. We therefore, did immunofluorescence staining for HP1 alpha (heterochromatin associated protein), indeed we found significant reduction in the levels of HP1 alpha in K-EDRP compared to the K562 population. Additionally, transmission electron microscopy of the K562 and K-EDRP also confirmed euchromatization of K-EDRP cells compared to parent population. Open chromatin in K-EDRP was further confirmed by the presence of increased levels of H3K4me2 and downregulation of H4K20me2 and H3K27me2. HATs (Histone Acetyl Transferases) and HDACs (Histone deacetylases) are important in defining chromatin architecture and DNA repair response [29], also higher expression of *TIP60* and *HMOF* are known to activate ATM. Therefore, to define which HAT/HDAC could be responsible for euchromatization in EDRP cells, we analyzed the transcript levels of *P300*, *GCN5*, *TIP60*, *HMOF*, *HDAC* and *HDAC2* in all the chemoresistant populations. We found *GCN5* to be overexpressed in all the different populations of chemoresistant cell lines (K562, THP-1 and HL-60). To examine the expression of *GCN5* in AML patient samples, peripheral blasts of 44 AML patients at baseline (at diagnosis) were collected and immunophenotypically characterized. Patient information is provided in Supplementary Table 4. Immunophenotyping by multiparametric flow cytometry (MPFC) was used to classify these patients into MRD positive and MRD negative cohorts post induction and consolidation therapy. Baseline samples were then analyzed for *GCN5* expression by SYBR green based quantitative real time PCR using *RPL19* as internal control. Absolute Δ ct values were used to compare the expression differences of *GCN5* between MRD positive (n=22) and MRD negative (n=22) patients. We found that MRD positive patients had significantly higher expression of *GCN5* compared to MRD negative patient samples. Consequently, protein levels of GCN5 were also significantly

higher in MRD positive (n=18) AML baseline bone marrow biopsies compared to MRD negative (n=11) samples as shown by immunostaining. Additionally, we analyzed two AML microarray datasets GSE12417-GLP96(n=163) [30] and GSE5122(n=58) [31] using PrognoScan[32] and found that *GCN5* overexpression significantly (Minimum p value= 0.000432 and p= 0.046) correlates with poor patient survival. These results suggest that *GCN5* expression could be used to predict therapy response in AML patients.

3.6 *GCN5* mediated ATM hyperactivation causes onset of acquired drug resistance in leukemia.

Although *GCN5* upregulation was associated with chemoresistant population however, to analyze if *GCN5* also contributed to the chemoresistance, we treated EDRP of K562 and THP-1 with different concentrations of *GCN5* inhibitor (Butyrolactone 3) alone and in combination with doxorubicin. Indeed, inhibition of *GCN5* significantly sensitized K-EDRP to doxorubicin. Importantly Butyrolactone 3 had no effect on the viability of peripheral blood mononuclear cells (PBMCs) at 100 μ M concentration. Furthermore, *GCN5* inhibition also sensitized K-EDRP cells to daunorubicin suggesting that *GCN5* plays a role in resistance to daunorubicin. We next examined whether *GCN5* inhibition is linked with ATM activation in leukemia cells. For this we treated parent and EDRP cells with *GCN5* inhibitor prior to doxorubicin treatment. *GCN5* inhibition led to decreased p-ATM and p-Chk2 in doxorubicin treated EDRP and parent cells. To confirm, that decreased p-ATM was due to loss of *GCN5* and not because of off target effect of the inhibitor, we performed siRNA mediated knockdown of *GCN5* in THP-1 cell line. Indeed, THP-1 *GCN5* knockdown cells showed reduced p-ATM post doxorubicin treatment compared to control siRNA. Similar results were also observed in HL-60, KG-1 (leukemic cell lines) and 293FT (Non-transformed cell line) demonstrating that interaction of *GCN5* and ATM is not restricted to a specific cell type.

3.7 *GCN5* colocalizes and interacts with ATM post doxorubicin treatment.

To further confirm that *GCN5* over expression can induce higher ATM activation, we overexpressed Flag-tagged and GFP-tagged *GCN5* in 293FT cells. These cells when treated with doxorubicin showed higher ATM activation compared to doxorubicin treated non *GCN5* overexpressing 293FT cells. Next to understand, if the direct interaction of *GCN5* with ATM enhances its recruitment, we first performed colocalization of *GCN5* and p-ATM (S1981) in K562 cells following doxorubicin treatment. *GCN5* and p-ATM showed overlapping foci, suggestive of their physical interaction. To further examine if *GCN5* and ATM physically

interact, we immunoprecipitated GCN5 from doxorubicin treated THP-1 and Flag-GCN5 overexpressing 293FT cells. p-ATM (S1981) was co-immunoprecipitated with GCN5 from both the cell lines. These data confirm that GCN5 physically interacts with ATM kinase post doxorubicin treatment, although we cannot rule out the plausibility of other proteins in the complex that could be mediating the interaction of GCN5 and ATM. Taken together, this is the first study that shows GCN5 interacts with ATM and inhibition of GCN5 activity inhibits ATM activation.

4. Conclusion and Discussion

Collectively, we show that early drug resistant cells survive by modulating DNA repair via higher activation of ATM kinase mediated by GCN5. Accordingly, these cells can be efficiently targeted by GCN5 and ATM inhibitors. In contrast, LDRP cells undergo several rounds of drug selection and acquire more than one bona fide drug-resistance mechanisms and therefore do not respond to ATM inhibitor. These findings provide a plausible mechanistic explanation for the failure of DDR inhibitors that are tested in clinical trial for the relapse, refractory and advanced stage patients.

We observed that both early and late acquired drug resistance was reversible in absence of drug which indicates non-genetic routes of resistance. We demonstrate that modulation of DNA repair pathway is the first response of the cells towards development of resistance to DNA damaging drugs and over multiple rounds of drug treatment, there is a gradual accumulation of molecular events that leads to difficult to treat highly resistant cells. At least during the early drug resistant stage as defined by our studies there are no multiple clones with different mechanisms of resistance, because ATM inhibitor with doxorubicin in EDRP kills all the cells. However, we cannot rule out the fact that there are different mechanisms in different clones all requiring ATM activation for their survival. GCN5 is a lysine acetyl transferase involved in post translational modification of multiple histone and non-histone proteins. GCN5 acts as a transcription activator and is a part of human ATAC and STAGA complex [33]. GCN5 have been shown to interact with DNA repair proteins like DNA-PK, Ku70/80, H2AX [34] and also have been reported to be involved nucleotide excision repair [35]. This is the first report showing GCN5 is required for efficient ATM activation. However, our understanding of GCN5 and ATM interaction is inadequate and requires further investigation. This study identifies two important candidates (ATM and GCN5) that can be targeted during early stages of acquired resistance to prevent relapse. Recently, GCN5

is shown as potential therapeutic target against AML and ALL *in vivo* [36, 37]. Moreover, our data demonstrate GCN5 to be an important drug target that precludes leukemia drug resistance. Most importantly, we also demonstrate that GCN5 expression can be used as an indicator to detect onset of acquired drug resistance. We show that ATM inhibition in the EDRP along with doxorubicin not only induce apoptosis in EDRP but also significantly lower the concentration of doxorubicin required to induce complete cell death thus, increasing the efficacy of doxorubicin many folds. In conclusion, our data provides mechanistic explanation to clinical observations and demonstrate that preventing emergence of resistance by targeting early drug resistant population would be more effective therapeutic approach in leukemia treatment. We believe these findings are clinically significant and warrant further studies to establish their *in vivo* significance.

References

1. Chen, X., et al., *Relation of clinical response and minimal residual disease and their prognostic impact on outcome in acute myeloid leukemia*. J Clin Oncol, 2015. **33**(11): p. 1258-64.
2. Harker, W.G., et al., *Alterations in the topoisomerase II alpha gene, messenger RNA, and subcellular protein distribution as well as reduced expression of the DNA topoisomerase II beta enzyme in a mitoxantrone-resistant HL-60 human leukemia cell line*. Cancer Res, 1995. **55**(8): p. 1707-16.
3. Marin, J.J., et al., *Role of drug transport and metabolism in the chemoresistance of acute myeloid leukemia*. Blood Rev, 2016. **30**(1): p. 55-64.
4. Elliott, S.L., et al., *Mitoxantrone in combination with an inhibitor of DNA-dependent protein kinase: a potential therapy for high risk B-cell chronic lymphocytic leukaemia*. Br J Haematol, 2011. **152**(1): p. 61-71.
5. Bian, K., et al., *ERK3 regulates TDP2-mediated DNA damage response and chemoresistance in lung cancer cells*. Oncotarget, 2016. **7**(6): p. 6665-75.
6. Paull, T.T., *Mechanisms of ATM Activation*. Annu Rev Biochem, 2015. **84**: p. 711-38.
7. Sun, H., et al., *Aurora-A controls cancer cell radio- and chemoresistance via ATM/Chk2-mediated DNA repair networks*. Biochim Biophys Acta, 2014. **1843**(5): p. 934-44.
8. Yoon, J.H., et al., *Role of autophagy in chemoresistance: regulation of the ATM-mediated DNA-damage signaling pathway through activation of DNA-PKcs and PARP-1*. Biochem Pharmacol, 2012. **83**(6): p. 747-57.
9. te Raa, G.D., et al., *Assessment of p53 and ATM functionality in chronic lymphocytic leukemia by multiplex ligation-dependent probe amplification*. Cell Death Dis, 2015. **6**: p. e1852.

Synopsis

10. Lee, J.H. and T.T. Paull, *ATM activation by DNA double-strand breaks through the Mre11-Rad50-Nbs1 complex*. Science, 2005. **308**(5721): p. 551-4.
11. Shreeram, S., et al., *Wip1 phosphatase modulates ATM-dependent signaling pathways*. Mol Cell, 2006. **23**(5): p. 757-64.
12. McConnell, J.L., et al., *Identification of a PP2A-interacting protein that functions as a negative regulator of phosphatase activity in the ATM/ATR signaling pathway*. Oncogene, 2007. **26**(41): p. 6021-30.
13. You, Z., et al., *Rapid activation of ATM on DNA flanking double-strand breaks*. Nat Cell Biol, 2007. **9**(11): p. 1311-8.
14. Gong, F. and K.M. Miller, *Mammalian DNA repair: HATs and HDACs make their mark through histone acetylation*. Mutat Res, 2013. **750**(1-2): p. 23-30.
15. Sun, Y., et al., *A role for the Tip60 histone acetyltransferase in the acetylation and activation of ATM*. Proc Natl Acad Sci U S A, 2005. **102**(37): p. 13182-7.
16. Harker, W.G., et al., *Multidrug resistance in mitoxantrone-selected HL-60 leukemia cells in the absence of P-glycoprotein overexpression*. Cancer Res, 1989. **49**(16): p. 4542-9.
17. Podhorecka, M., A. Skladanowski, and P. Bozko, *H2AX Phosphorylation: Its Role in DNA Damage Response and Cancer Therapy*. J Nucleic Acids, 2010. **2010**.
18. Jang, E.R., et al., *ATM modulates transcription in response to histone deacetylase inhibition as part of its DNA damage response*. Exp Mol Med, 2010. **42**(3): p. 195-204.
19. Mao, Z., et al., *DNA repair by homologous recombination, but not by nonhomologous end joining, is elevated in breast cancer cells*. Neoplasia, 2009. **11**(7): p. 683-91.
20. Morrison, C., et al., *The controlling role of ATM in homologous recombinational repair of DNA damage*. EMBO J, 2000. **19**(3): p. 463-71.
21. Hamilton, G., et al., *ATM regulates a RASSF1A-dependent DNA damage response*. Curr Biol, 2009. **19**(23): p. 2020-5.
22. Kim, D.W., et al., *siRNA-based targeting of antiapoptotic genes can reverse chemoresistance in P-glycoprotein expressing chondrosarcoma cells*. Mol Cancer, 2009. **8**: p. 28.
23. Bhoumik, A., et al., *Regulation of TIP60 by ATF2 modulates ATM activation*. J Biol Chem, 2008. **283**(25): p. 17605-14.
24. Metzeler, K.H., et al., *An 86-probe-set gene-expression signature predicts survival in cytogenetically normal acute myeloid leukemia*. Blood, 2008. **112**(10): p. 4193-201.
25. Raponi, M., et al., *Identification of molecular predictors of response in a study of tipifarnib treatment in relapsed and refractory acute myelogenous leukemia*. Clin Cancer Res, 2007. **13**(7): p. 2254-60.

Synopsis

26. Mizuno, H., et al., *ProgenoScan: a new database for meta-analysis of the prognostic value of genes*. BMC Med Genomics, 2009. **2**: p. 18.
27. Nagy, Z. and L. Tora, *Distinct GCN5/PCAF-containing complexes function as co-activators and are involved in transcription factor and global histone acetylation*. Oncogene, 2007. **26**(37): p. 5341-57.
28. Chatr-Aryamontri, A., et al., *The BioGRID interaction database: 2017 update*. Nucleic Acids Res, 2017. **45**(D1): p. D369-D379.
29. Zhao, M., et al., *PCAF/GCN5-Mediated Acetylation of RPA1 Promotes Nucleotide Excision Repair*. Cell Rep, 2017. **20**(9): p. 1997-2009.
30. Tzelepis, K., et al., *A CRISPR Dropout Screen Identifies Genetic Vulnerabilities and Therapeutic Targets in Acute Myeloid Leukemia*. Cell Rep, 2016. **17**(4): p. 1193-1205.
31. Holmlund, T., et al., *GCN5 acetylates and regulates the stability of the oncoprotein E2A-PBX1 in acute lymphoblastic leukemia*. Leukemia, 2013. **27**(3): p. 578-85.

Publications in Referred Journal:

Published—

Salunkhe, S., Mishra, S. V., Nair, J., Ghosh, S., Choudhary, N., Kaur, E., Shah, S., Patkar, K., Anand, D., Khattry, N., Hasan, S. K. and Dutt, S., Inhibition of novel GCN5-ATM axis restricts the onset of acquired drug resistance in leukemia. **Int. J. Cancer**. Accepted Author Manuscript. doi:10.1002/ijc.31242

Accepted— N.A

Communicated/In preparation—

Other Publications—N/A

Book Chapter: N.A

Conference/Symposium (Oral/Poster presentation)

8. **Sameer Salunkhe**, Shilpee Dutt. Understanding the mechanisms of survival of chemoresistant leukemic cells. XXXVIII All India Cell Biology Conference and International Symposium on. 'Cellular Response to Drugs' by CSIR-CDRI Lucknow. December 10-12, 2014. **(Poster presentation)**
9. **Sameer Salunkhe**, Ashwin Ramaswamy, Sanket Shah, Shilpee Dutt. Hyper phosphorylation of ATM Kinase is responsible for the early onset of acquired drug resistance in leukemia. 38th Annual conference of Mumbai Hematology Group, 14th-15th March 2015 **(Oral presentation- JC Patel award for best oral presentation)**.
10. **Sameer Salunkhe** ,Sanket Shah, V.Devanand, Ashwin Ramaswami, Jyothi Nair,

Synopsis

Smita Patkar, Syed Hasan, Navin Khattry and Shilpee Dutt*GCN5 mediated hyperactivation of ATM Kinase is responsible for the early onset of acquired drug resistance in leukemic minimal residual cells (MRD). -56th Annual meeting of the Indian Society of Haematology and Blood Transfusion (ISHBT) (5th-8th Nov 2015)

(Oral presentation)

11. **Sameer Salunkhe**, Ekjot Kaur, Sanket Shah, Jyothi Nair, V.Devanand, Smita Patkar, Syed Hasan, Navin Khattry and Shilpee Dutt GCN5 mediated ATM activation a novel resistance mechanism that if targeted during early induction therapy eliminates the formation of MRD. at -TMC Platinum Jubilee Celebrations 1st Conference on A conference of new ideas in cancer - Challenging dogmas (26th to 28th February 2016). **(Poster presentation)**
12. **Sameer Salunkhe**, Jyothi Nair, Neha Choudhary, Samadri Ghosh, Ekjot Kaur, Sanket Shah, Ketaki Patkar, Dev Anand, Navin Khattry, Syed K Hasan, Shilpee Dutt. GCN5 regulates ATM mediated DNA repair responsible for onset of acquired resistance in leukemia. at “Annual meeting of American Association for Cancer Research (AACR)” in Washington DC, USA, April 1st to 5th, 2017. **(Poster presentation)**
13. **Sameer Salunkhe**, Jyothi Nair, Neha Choudhary, Samadri Ghosh, Ekjot Kaur, Sanket Shah, Ketaki Patkar, Dev Anand, Navin Khattry, Syed K Hasan, Shilpee Dutt. Inhibition of novel GCN5-ATM axis restricts the onset of acquired drug resistance in leukemia. International congress of cell biology (ICCB 2018) to be organized by CSIR CCMB Hyderabad to be held on (27th to 31st Jan 2018). **(Award for best Poster presentation)- Awarded travel grant.**
14. **Sameer Salunkhe**, Jyothi Nair, Neha Choudhary, Samadri Ghosh, Ekjot Kaur, Sanket Shah, Ketaki Patkar, Dev Anand, Navin Khattry, Syed K Hasan, Shilpee Dutt. Inhibition of novel GCN5-ATM axis restricts the onset of acquired drug resistance in leukemia Poster presentation Indo-US conference on ‘Transcription, Chromatin Structure DNA Repair and Genomic Instability’, to be organized by IISc, Bangalore from March 6-10, 2018. **(Poster presentation)**



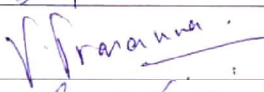


Synopsis

novel GCN5-ATM axis restricts the onset of acquired drug resistance in leukemia Poster presentation Indo-US conference on 'Transcription, Chromatin Structure DNA Repair and Genomic Instability', to be organized by IISc, Bangalore from March 6-10, 2018. (Poster presentation)

Signature of Student

Date 18/1/18

Doctoral Committee:

S. No.	Name	Designation	Signature	Date
1.	Dr. Sorab N Dalal	Chairman		18.1.18
2.	Dr. Shilpee Dutt	Guide & Convener		18.1.18
3.	Dr. Prasanna Venkatraman	Member		18.1.18
4.	Dr. Sanjay Gupta	Member		18.1.18
5.	Dr. Sanjeev Galande	Technical Advisor		18.1.18

Forwarded Through:



Dr. S.V. Chiplunkar
Director, ACTREC
Chairperson,
Academic & training Program, ACTREC
Dr. S. V. Chiplunkar
Director
Advanced Centre for Treatment, Research &
Education in Cancer (ACTREC)
Tata Memorial Centre
Kharghar, Navi Mumbai - 410 210



Prof. K. Sharma
Director, Academics
T.M.C.
PROF. K. S. SHARMA
DIRECTOR (ACADEMICS)
TATA MEMORIAL CENTRE,
PAREL, MUMBAI

Version approved during the meeting of Standing Committee of Deans held during 29-30 Nov 2013

ABBREVIATIONS

ABC- Adenosine triphosphate Binding Cassette

ALL- Acute Lymphoblastic Leukemia

AML- Acute Myeloid Leukemia

Ara-C- Cytarabine

ATAC- Ada2a-containing (ATAC) complex

ATCC- American type culture collection

ATM- Ataxia-telangiectasia mutated

BCA- Bicinchonic Acid Assay

BL-3/MB3- Butyrolactone 3

BLM- Bleomycin

BSA- Bovine Serum Albumin

CBC- Complete blood count

CLL-Chronic Lymphocytic Leukemia

CML-Chronic Myeloid Leukemia

Co-IP- Co-Immunoprecipitation

CR- Complete remission

DAPI- 4',6-diamidino-2-phenylindole

DDR-DNA Damage Response

DMEM- Dulbecco's Modified Eagle Medium

DNA- Deoxyribonucleic acid

DSB- Double-Strand Breaks

DSBR-Double strand break repair

EDRP- Early drug resistant population

ELN- European Leukemia NET

GCN5- general control non-depressible 5

HP1A- heterochromatin protein 1 (HP1) alpha isoform

HR- Homologous Recombination

Abbreviations

IHC- Immunohistochemistry

Kb- Kilobase

kDa- Kilo Dalton

LA- Luria Agar

LB- Luria Broth

LDRP- Late drug resistant population

MDR- Multi-Drug Resistance

MPFC- Multiparametric flow cytometry

MRD- Minimal residual disease

MRN- Mre11-Rad50-Nbs1

MTT- (3-(4,5-Dimethylthiazol-2-yl)-2,5-Diphenyltetrazolium Bromide

NHEJ- Non-Homologous End Joining

NSCLC- Non small cell lung cancer

OTM- Olive tail movement

PBS- Phosphate Buffer Saline

PDR- Post drug removal

PIKK- Phosphatidylinositol 3-kinase-related kinase

Puro- Puromycin

RPM- Rotation Per Minute

RPMI- Roswell Park Memorial Institute Medium

SDS-PAGE- Sodium Dodecyl Sulfate Polyacrylamide Gel Electrophoresis

SEER- Surveillance, Epidemiology, and End Results Program

SN-38- Irinotecan metabolite

STAGA- SPT3-TAF9-GCN5 acetylase complex

TBST- Tris-Buffered Saline and Tween 20

LIST OF ILLUSTRATIONS

Illustration 1: Incidence and mortality of various cancers in the world and India. Y-axis represents absolute numbers versus different types of cancers arranged in descending order of occurrence (Source: GLOBOCAN-2012 IACR).....	24
Illustration 2: SEER statistics for (A) 5-year survival, (B) age-based incidence and (C) mortality rates for leukemia.....	24
Illustration 3: A. Different types of leukemia B. DNA damaging drugs used for the treatment and C. Types of DNA lesions induced by chemotherapy.	27
Illustration 4: Structure of Doxorubicin, Daunorubicin, and Mitoxantrone [2]	28
Illustration 5: Mechanisms of multidrug resistance (MDR) in tumor cell [6].....	31
Illustration 6:P-gp/ABCB1/MDR1 major in drug efflux and resistance.....	32
Illustration 7: General mechanism of action of TOP2 inhibitors figure modified from [7]....	33
Illustration 8: Therapeutic targets in the DSB repair pathway [1].....	35
Illustration 9: Homologous recombination repair [1]	37
Illustration 10: Non-Homologous end Joining pathway for DNA repair [1]	39
Illustration 11: Domain architecture of ATM protein along with their associated modifications [3]	41
Illustration 12: ATM signaling pathways and functions [4]	42
Illustration 13: NHEJ and HR activity vectors [5].....	56
Illustration 14: Mechanisms of ATM activation.....	87
Illustration 15: X-ray crystallographic structure of GCN5 bound to acetyl coenzyme A (AcCoA)	90
Illustration 16: Expression of KAT2A in various cancer types: Data Source: ©2015 Broad Institute of MIT & Harvard. (http://firebrowse.org).....	91

LIST OF TABLES

Table 1: Estimated New Cancer Cases and Deaths by Sex, USA, 2016[38]	23
Table 2: Response criteria in acute myeloid Leukaemia (AML) as reported by the International Working Group and the European Leukaemia Net(ELN)[45].....	29
Table 3: List of cell lines with STR data.....	47
Table 4: List of antibodies and dilutions used.	53
Table 5: Reaction mix for 1ug of plasmid restriction digestion with IsceI.	54
Table 6: : List of primers used for SYBR green based real-time PCR.	58
Table 7: Clinical Characteristics of 44 Patients with Acute Myeloid Leukemia grouped on the basis of post induction and post-consolidation MRD status.	64

LIST OF FIGURES

Figure 1: Mutation profile of DNA repair genes in leukemia cell lines	48
Figure 2: Schema for development of an evolutionary model of drug resistance:	50
Figure 3: Establishment and validation of drug resistance model.	67
Figure 4: HL-60/MX2 drug resistance model and validation.....	69
Figure 5: Cross resistance and resistance reversibility of EDRP and LDRP cells.	70
Figure 6: Cell cycle profile of EDRP of THP-1, K562, HL-60, and HL-60/MX2.....	71
Figure 7: Levels of DNA double strand breaks in HL-60/MX2 cells post mitoxantrone (100nM for 2h) treatment.	72
Figure 8: Neutral comet assay in THP-1 and K562 EDRP and LDRP cells.	75
Figure 9: γ -H2AX staining in EDRP and LDRP of K62 and THP-1 cells.	76
Figure 10: Hyperactive ATM kinase signaling in EDRP cells.....	78
Figure 11: EDRP cells follows HR directed DSB repair.	79
Figure 12: Differential response of early and late stage drug resistant populations to ATM kinase inhibition with DNA damaging drugs.	81
Figure 13: ATM activation kinetics in LDRP cells post drug treatment.	82
Figure 14: Expression of ABCB1, TOP2 β and drug accumulation in early and late stage drug resistant populations.....	84
Figure 15: LDRP represents multifactorial drug resistance.	85
Figure 16: EDRP cells harbors euchromatin rich cells.	88
Figure 17: GCN5 is overexpressed by all the drug resistant populations	89
Figure 18: GCN5 inhibition sensitizes EDRP cells to doxorubicin.....	92
Figure 19: Pharmacological inhibition of GCN5 inhibits ATM activation and downstream pathway in cell type independent manner.	93
Figure 20: Genetic perturbation of GCN5 influences ATM activation.	95
Figure 21: GCN5 interacts with ATM post DNA damage.....	96

List of Figures

Figure 22: Expression of GCN5/KAT2A in baseline samples of MRD(+) and MRD(-) AML patient samples.....	97
Figure 23: GCN5 protein expression by IHC in bone marrow biopsies of AML patient samples.	98
Figure 24: High-risk AML patient show GCN5 upregulation and poor survival.....	99
Figure 25: Proposed model for acquired drug resistance in leukemia.	103

CHAPTER 1: INTRODUCTION

1.1: Leukemia:

Leukemia is the cancer of the blood and bone marrow and is caused by the increased production of abnormal white blood cells. These aberrant white blood cells are not able to fight infections invading the body and impair the ability of the bone marrow to produce erythrocytes also known as red blood cells and platelets. Leukemia can be either acute or chronic. The progression of chronic leukemia is slower than acute leukemia, thus requiring immediate treatment. Leukemia is also classified as lymphocytic or myelogenous. Lymphocytic leukemia refers to abnormal and increased cell growth in the bone marrow cells that become lymphocytes, a type of white blood cell that plays a role in the immune system. In myelogenous leukemia, abnormal cell growth occurs in the marrow cells that mature into red blood cells, white blood cells, and platelets. The four broad classes of leukemia include Acute lymphoblastic leukemia (ALL), Acute myelogenous leukemia (AML), Chronic lymphocytic leukemia (CLL), Chronic myelogenous leukemia (CML). Leukemia occurs in both adults and children. ALL is the most common form of childhood leukemia, and AML is the second most common. Decades of research have improved outcomes for children diagnosed with ALL. However, AML treatment still remains a major clinical problem.

1.1.1: Risk factors/Causes for Leukemia: Most causes of leukemia are not known. However, the disease has been linked to; Exposure to large amounts of high energy radiation, Occupational exposure to the chemical benzene, Viral infections, Cigarette smoking, Previous chemotherapy, Human T-cell leukemia virus 1 (HTLV-1), Myelodysplastic syndromes, Down syndrome and other genetic diseases and Family history.

1.1.2: Epidemiology: **New Cases:** In USA 2017, 62,130 people are expected to be diagnosed with leukemia. **Prevalence:** There are an estimated 363,794 people living with, or in remission from, leukemia. **Survival:** The overall five-year relative survival rate for

leukemia from 2006 to 2012 is 62.7 percent. From 2006-2012, the five-year relative survival rates in different types of leukemia were

1. CML - 65.9 percent
2. CLL - 85.1 percent
3. AML - 26.8 percent
4. ALL- 70.7 percent

Deaths: In 2017, 24,500 people are projected to die from leukemia (14,300 males and 10,200 females). In 2009-2013, leukemia was the sixth most common cause of cancer deaths in women and fifth most common in men.

Table 1: Estimated New Cancer Cases and Deaths by Sex, USA, 2016[38]

Type	Estimated new cases			Estimated deaths		
	Both Genders	Male	Female	Both Genders	Male	Female
Leukemia	60,140	34,090	26,050	24,400	14,130	10,270
Acute lymphoblastic leukemia	6,590	3,590	3,000	1,430	800	630
Chronic lymphocytic leukemia	18,960	10,830	8,130	4,660	2,880	1,780
Acute myeloid leukemia	19,950	11,130	8,820	10,430	5,950	4,480
Chronic myeloid leukemia	8,220	4,610	3,610	1,070	570	500
Other leukemia	6,420	3,930	2,490	6,810	3,930	2,880

As evident from table 1, AML contributes the maximum to the number of leukemia incidence and the mortality. Adult AML has worst survival rates of <20% and its therapy hasn't changed since last 40 years [39]. With respect to the number of incidence and mortality due to all the cancers, leukemia ranks 11th in the world while it ranks 9th in India.

Introduction

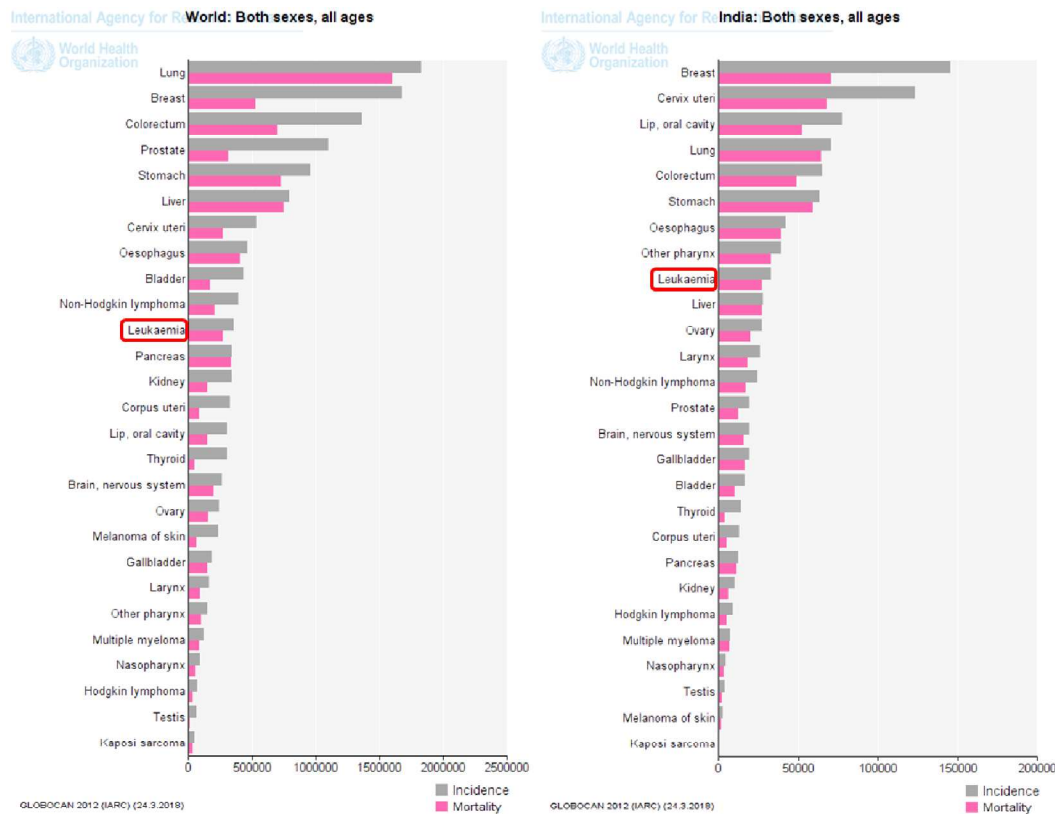


Illustration 1: Incidence and mortality of various cancers in the world and India. Y-axis represents absolute numbers versus different types of cancers arranged in descending order of occurrence (Source: GLOBOCAN-2012 IACR)

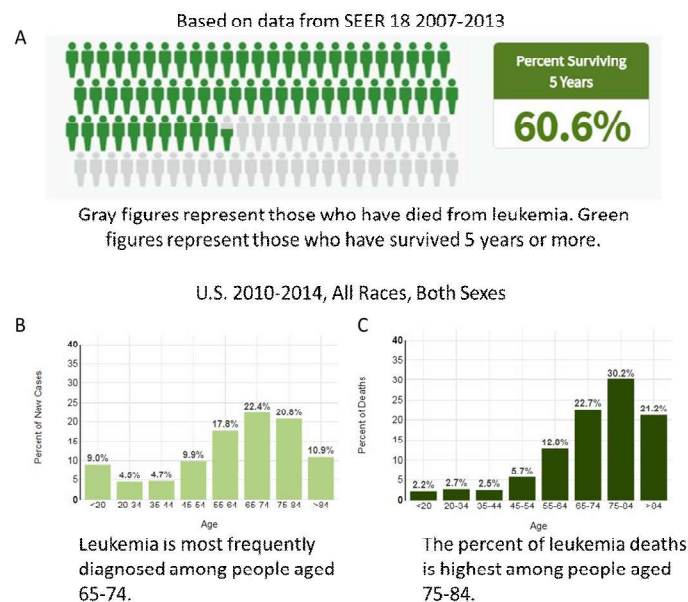


Illustration 2: SEER statistics for (A) 5-year survival, (B) age-based incidence and (C) mortality rates for leukemia.

1.1.3: Symptoms and Diagnosis: Swollen tonsils, Paleness, Fever, chills, night sweats and other flu-like symptoms, enlarged liver and spleen, Weakness and fatigue, Swollen or

bleeding gums, Bone pain, Pinhead-size red spots on the skin. Initial blood test (complete blood count [CBC]) presenting an atypical white cell count may indicate the need for a bone marrow biopsy to ratify the diagnosis and to identify the specific type of leukemia. Leukemic cells are tested for their presence in the bone marrow tissue (biopsy) sample from a pelvic bone. The cells also are examined for chromosomal abnormalities. Generally, diagnosis is confirmed by detecting cells based antigens on the cell surface, using a process called Immunophenotyping. Karyotyping is done to identify structural and numeral changes in chromosomes. Often polymerase chain reaction (PCR) may be done; to look for certain changes in the important genes like *NPM1*, *BCR-ABL* etc.

1.1.4: Treatment: Leukemia Treatment depends on the type of leukemia, certain features of the leukemic cells, the extent of the disease, and whether leukemia has been treated before. Following are the types;

Chemotherapy: It is the major treatment modality for leukemia. Chemotherapy is administered in cycles, a treatment period followed by a recovery period, and the next cycle until leukemic blasts are either eliminated or reduced significantly. Chemotherapy acts on rapidly proliferating cancer cells thus stopping them from growing or multiplying. Some of the rapidly dividing healthy cells such as epidermal and gametic cells are destroyed as well, which causes the side effects. Different types of drugs are used for the different types of leukemia.

Bone Marrow Transplants: Bone Marrow Transplants are well proven to improve the overall health and long-term survival of leukemia patient [40]. This is an expensive procedure and difficult to find the right donor (can be syngeneic or allogeneic). Bone marrow transplant helps patients tolerate otherwise intolerable doses of toxic chemotherapy. It is performed when leukemia is in remission or relapses during or after treatment. As chemotherapy also

kills normal cells in the bone marrow, making the bone marrow transplant necessary in order to make up for the destruction of normal cells.

Surgery: As leukemia cells are spread throughout the body, surgery is unlikely to be an option for leukemia patients. However, sometimes surgery can be used to remove spleen as blood cells accrue there, which causes the spleen swelling and pain.

1.1.5: DNA damaging drugs in leukemia chemotherapy: Treatment of leukemia majorly involves chemotherapy which can be a combination of various drugs. Depending upon the type of leukemia, conventional or targeted therapies are preferred for leukemia treatment. There are very few cancers with successful targeted therapies for e.g. in CML patients “Imatinib”, is an effective targeted therapy [41], whereas, for most of the leukemias, conventional chemotherapy involving DNA damaging drugs like 1. Anthracyclines: Doxorubicin, Daunorubicin, Mitoxantrone, and Idarubicin is the preferred treatment. Although as mentioned before, DNA damaging drugs do not specifically kill cancer cells, however for most of the leukemias chemotherapy is the best possible therapy available. Unfortunately, as cancer cells divide rapidly and acquire genetic heterogeneity the likelihood of a cancer population to have innately resistant genotype for a particular type of drug (Targeted/ or conventional) by permutation and combination is high. This is also one of the major reasons for the failure of several attempted targeted and conventional chemotherapy. Development of resistance is also a major clinical challenge in leukemia treatment.

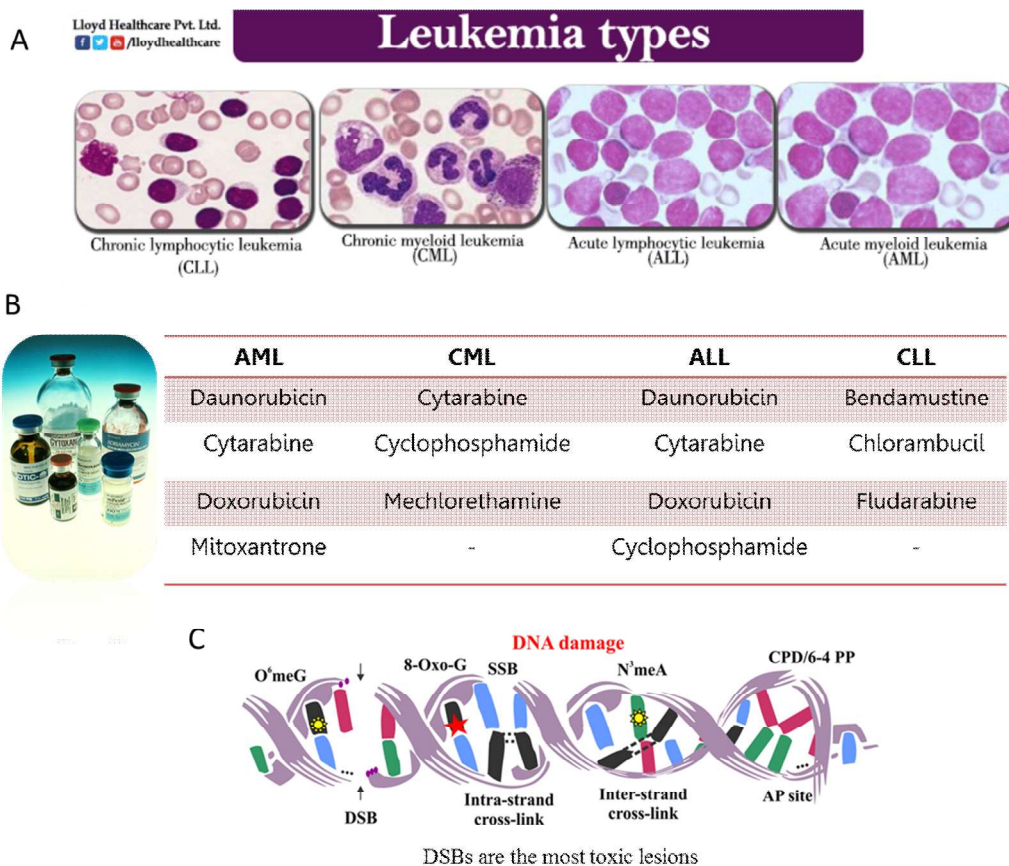


Illustration 3: A. Different types of leukemia B. DNA damaging drugs used for the treatment and C. Types of DNA lesions induced by chemotherapy.

1.1.5.1: Doxorubicin: Doxorubicin is a common bacterial antibiotic widely used in the treatment of cancer. The immediate precursor of Doxorubicin is daunorubicin. Doxorubicin is essentially a 14-hydroxylated version of daunorubicin. A number of different wild-type strains of *Streptomyces* produce Daunorubicin making it more abundantly found as a natural product. Doxorubicin is used to treat different cancers like leukemia, Hodgkin's lymphoma, bladder, ovarian, breast, stomach, and lung. Doxorubicin interacts with DNA by intercalating between base pairs of DNA thus inhibiting replication and transcription. It also inhibits the function of topoisomerase II, an enzyme responsible for relaxing the supercoils in DNA for transcription. Doxorubicin stabilizes topoisomerase II complex preventing the DNA from releasing the tension generated due to supercoiling [42]. This breaks the DNA double helix. Apart from above mentioned mechanisms, it is also known to increase free radical production

in the cells. Doxorubicin fluorescence can be used to determine its concentration in a cell [43].

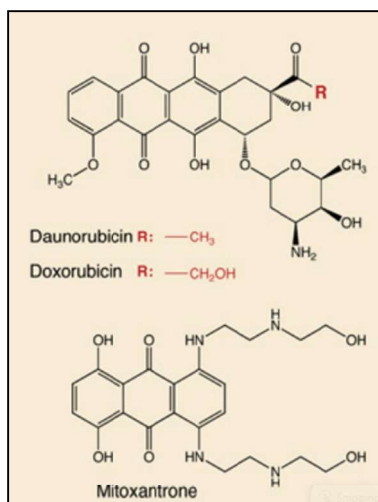


Illustration 4: Structure of Doxorubicin, Daunorubicin, and Mitoxantrone [2]

1.1.5.2: Mitoxantrone: Mitoxantrone is an antineoplastic drug. Mitoxantrone is a type II topoisomerase inhibitor; and has a similar mode of action like doxorubicin but is less toxic to humans and animals compared to doxorubicin [44]. It intercalates between DNA bases through hydrogen bonding causing crosslinks and strand breaks and thus disrupts DNA synthesis and DNA repair in both healthy cells and cancer cells. It is generally used to treat metastatic breast cancer, acute myeloid leukemia, and non-Hodgkin's lymphoma. It is known to improve the survival rate of children suffering from acute lymphoblastic leukemia relapse.

1.1.6: Therapy outcome: Therapy outcome is determined by various pathological interpretations, here for example in case of AML therapy response is defined as below

Complete remission (CR): No signs and symptoms of the disease after treatment. Less than 5 percent blast cells in the marrow. Blood cell counts recovered to normal ranges.

Table 2:Response criteria in acute myeloid Leukaemia (AML) as reported by the International Working Group and the European Leukaemia Net(ELN)[45]

Outcome	Definition
Complete remission (CR)*	Bone marrow blasts < 5%; absence of blasts with Auer rods; absence of extramedullary disease; absolute neutrophil count > $1.0 \times 10^9/l$; platelet count > $100 \times 10^9/l$; independence of red cell transfusions
CR with incomplete recovery (CRi)	All CR criteria except for residual neutropenia (< $1.0 \times 10^9/l$) or thrombocytopenia (< $100 \times 10^9/l$)
Morphological leukaemia-free state	Bone marrow blasts < 5%; absence of blasts with Auer rods; absence of extramedullary disease; no haematological recovery required
Partial remission (PR)	Relevant in the setting of Phase 1 and 2 clinical trials only; all haematological criteria of CR; a decrease of bone marrow blast percentage to 5% to 25%; and decrease of pretreatment bone marrow blast percentage by at least 50%
Cytogenetic CR (CRc)	Reversion to a normal karyotype at the time of morphological CR (or CRi) in cases with an abnormal karyotype at the time of diagnosis; based on the evaluation of 20 metaphase cells from bone marrow
Resistant disease (RD)	Failure to achieve CR or CRi (general practice; Phase 2/3 trials), or failure to achieve CR, CRi, or PR (Phase 1 trials); only includes patients surviving ≥ 7 days following completion of initial treatment, with evidence of persistent leukaemia by blood and/or bone marrow examination
Death in aplasia	Death occurring ≥ 7 days following completion of initial treatment while cytopenic; with an aplastic or hypoplastic bone marrow obtained within 7 days of death, without evidence of persistent leukaemia
Death from indeterminate cause	Death occurring before completion of therapy, or < 7 days following its completion; or deaths occurring ≥ 7 days following completion of initial therapy with no blasts in the blood, but no bone marrow examination available
Relapse	Bone marrow blasts $\geq 5\%$; or reappearance of blasts in the blood; or development of extramedullary disease

Refractory (resistant) disease: Failure to achieve a CR (i.e., failure to achieve significant reduction <5% of blast cells in bone marrow post-chemotherapy) is described as a refractory disease (also referred to as primary induction failure). However, patients who achieve CR

post second cycle of induction therapy are not considered to have refractory disease. Resistance to chemotherapy is closely associated with unfavorable cytogenetic and molecular features of blast cells.

Minimal residual disease (MRD): It refers to the persistence of leukemia cells that cannot be identified under the microscope. The sensitivity of techniques for detection of MRD (e.g. multiparametric flow cytometry, polymerase chain reaction, DNA sequencing) is greater than that of bone marrow morphology, but the standards for defining MRD depend on the specific methodology that is utilized.

Relapsed disease: Relapse describes the reappearance of leukemia cells in the bone marrow, peripheral blood, or elsewhere (extramedullary disease) after the attainment of a CR. However, the significance of the reappearance of AML detected only by polymerase chain reaction (PCR) analysis is uncertain.

1.1.7: Resistance to DNA damaging drugs: Drug resistance is a major problem that limits the success of chemotherapies used in cancer treatment. Cancer cells may be intrinsically resistant to chemotherapy prior to treatment or resistance can also be developed during the course of the treatment by tumors that are originally sensitive to chemotherapy. A discouraging property of such acquired resistance is that the tumors not only become resistant to the drugs originally used to treat them but may also become cross-resistant to other drugs with similar as well as altered mechanisms of action. As chemoresistance causes therapy failure, clearly, if drug resistance could be overcome, the survival would highly be improved. Drug resistance can occur at many layers, including increased drug efflux, drug inactivation, alterations in drug target, processing of drug-induced damage, and evasion of apoptosis. Although there are multiple ways by which leukemic cells would acquire drug resistance to

DNA damaging drugs, our focus has been mainly on widely reported mechanisms like Drug efflux, alteration in target molecule and DNA repair.

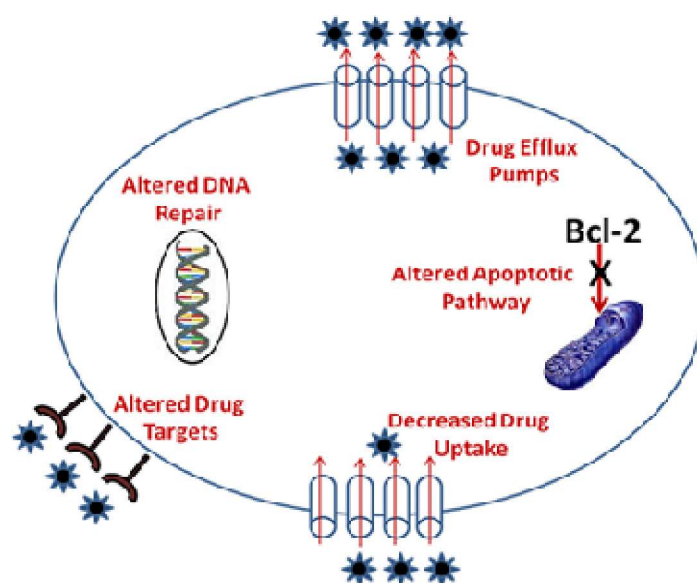


Illustration 5: Mechanisms of multidrug resistance (MDR) in tumor cell [6].

1.1.7.1: Drug uptake and efflux: Amongst various mechanisms overexpression of membrane transporter such as P-glycoprotein (*MDR1* or *ABCB1*), that efflux the chemotherapeutic drugs out of the cell is highly reported for drug resistance [46]. It is a 170 kDa membrane protein from ATP-binding cassette superfamily and a key drug transporter reported to be overexpressed in different types of cancers. Inhibition of P-gp efflux function has been shown to reverse the MDR of cancer [47, 48]. However, almost all the P-gp inhibitors that have been tested in clinical trials, to date none of them are approved for human use [49, 50]. First generation P-gp inhibitors, including verapamil and cyclosporine A, were not specific to P-gp, therefore, caused an unpredictable pharmacokinetics [51, 52]. The second generation inhibitors biricodar, valspodar, and dexverapamil are more potent than the first generation inhibitors and less toxic, but are, found to interact with drug metabolizing enzymes such as *CYP3A4*, thus affecting drug metabolism [53].

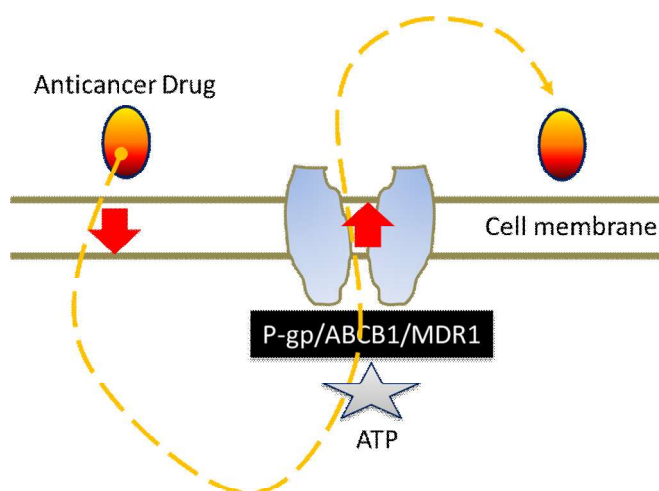


Illustration 6: P-gp/ABCB1/MDR1 major in drug efflux and resistance.

The third generation inhibitors tariquidar, elacridar, and zosuquidar showed acceptable toxicity with the highest potency of P-gp inhibition in phase I clinical trials [54-56], but phase III studies of tariquidar in combination with carboplatin/paclitaxel or with vinorelbine had to be barred early, because of toxicity issues [54].

1.1.7.2: Drug target alterations: Activity or expression level of topoisomerase II enzyme plays a key role in tumor cells which have acquired resistance to inhibitors of topoisomerases like doxorubicin and mitoxantrone [57, 58]. DNA damaging drugs like doxorubicin, mitoxantrone and daunorubicin work by stabilizing the covalent enzyme-associated DNA complexes, these drugs swing the DNA cleavage/religation balance of the enzyme reaction to the cleavage state [59]. These drugs are able to convert biological intermediate of topoisomerase II activity into a toxin one ultimately leading to DNA breaks which result in cellular poisoning [60]. Drug response and resistance can be affected by alterations in the drug target, such as mutations or changes in expression level. Downregulation of Doxorubicin target, which is Topoisomerase 2 β (*TOP2 β*) [61] [62, 63] is well reported in the literature and is a major cause for Doxorubicin resistance.

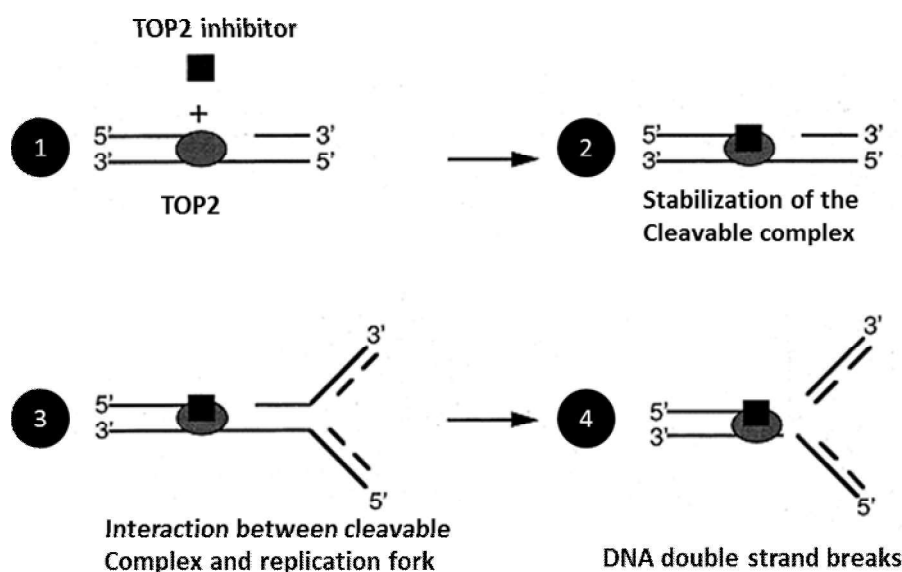


Illustration 7: General mechanism of action of TOP2 inhibitors figure modified from [7]

1.1.7.3: DNA damage and repair: A cell responds to DNA damage by either being able to repair DNA and survival or not able to repair their DNA and induce apoptosis; therefore, the DNA repair ability of a cancer cell is a key determinant for success of DNA-damaging drugs. Accordingly, inhibiting DNA damage repair in cancer cells is an obvious therapeutic strategy to combine with DNA-damaging agents. Moreover, cancers frequently have a dysfunction in at least one DNA damage repair pathway, which can lead to complete dependence on an alternative repair pathway that is functionally redundant in normal cells and therefore can be inhibited to induce cancer-cell-specific death; this is called as synthetic lethality. Most prominent example of synthetic lethality is the inhibition of PARP in *BRCA1* deficient cancer cells [64, 65]

Various targets in the DNA repair pathway have been shown to be therapeutically important and work at the level of sensors, mediators, and a downstream effector such as cell cycle regulators like p53 and checkpoint kinases. Inhibition of these targets not only sensitizes chemoresistant populations but also drastically decreases the drug doses. Inhibition of DNA repair protein is tricky and manifestations of the effects are context dependent. Genetic or

pharmacological inhibition of ATM sensitizes p53-deficient cells to the DNA intercalating drug doxorubicin but induce doxorubicin resistance in p53-proficient cells [66]. This striking difference in the outcome is because ATM inhibition reduces p53-dependent apoptosis in p53-proficient cells, whereas it magnifies mitotic catastrophe in p53-deficient cells with a dysfunctional G1/S checkpoint. Lack a functional G1/S checkpoint in various cancers is attributed to the defects in the p53 pathway, this makes them sensitive to G2/M checkpoint inactivation via inhibition of ATM or other DNA damage checkpoint proteins such as Chk1, and WEE1, which are lately understood to be required for G2/M checkpoint induction and DNA repair in mouse glioblastoma cells after treatment with temozolomide or ionizing radiation [67]. Inhibition of downstream repair pathways also has been shown for NHEJ and HR specific proteins. Inhibition of DNA-PKcs, hPNKP [68] as well as ligase 4 [69] inhibits entire NHEJ repair pathway. Researchers have been successful in targeting not only the DNA repair enzymes but also adaptor proteins like RPA. TDRL-505(RPA-DNA interaction inhibitor) prevents cell cycle progression, induces cytotoxicity, and increases the efficacy of the chemotherapeutic DNA damaging agent's cisplatin and etoposide *in vitro*[70].

Introduction

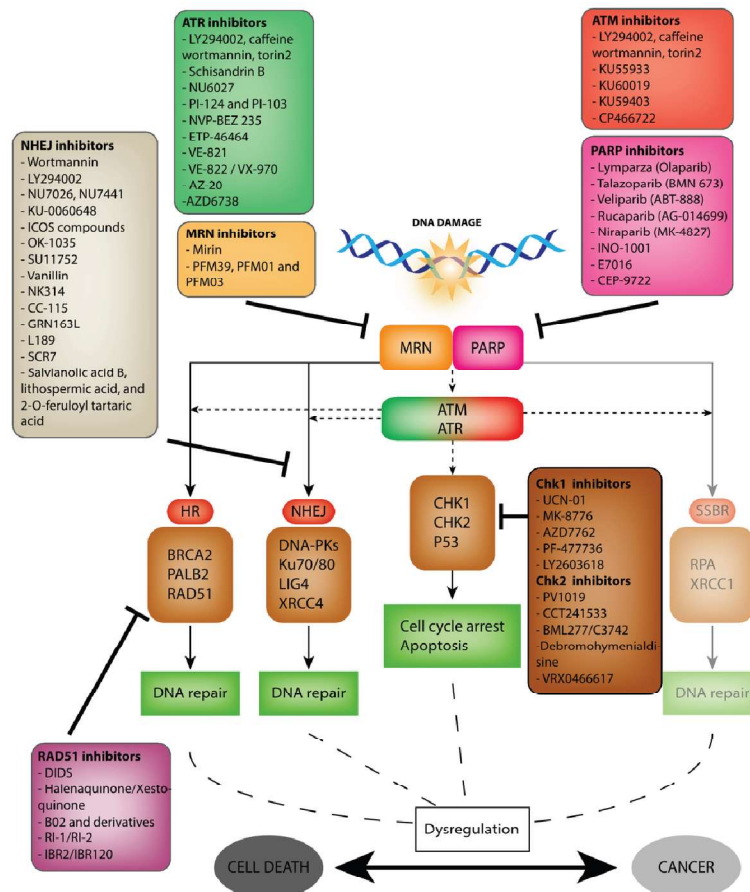


Illustration 8: Therapeutic targets in the DSB repair pathway [1]

DNA repair is closely orchestrated with chromatin modifiers, inhibition of the activities of such proteins also opens up important therapeutic opportunity in cancer treatment [71]. Several of class I and II histone deacetylases (HDAC) are also shown to be important targets for the abrogation of repair response [72, 73]. Hence, HDAC inhibitors such as vorinostat might be used as chemosensitizers. However recent report suggests that use of HDAC inhibitors led to upregulation of *ABCB1* which in turn caused drug resistance [74].

We focused our interest on understanding the role of the DSB repair pathway in resistance to DNA damaging agents as we believe that modulation of DNA repair response is crucial for the survival of drug resistant populations. Apart from being essential for the survival of drug resistant cells, the DSB repair pathway involves many targetable proteins like kinases, ligases, phosphatases, methyltransferases, acetyl-transferases etc.

DNA Double-strand break repair pathway: Activation of DNA repair is initiated after successful detection of DSBs by sensor proteins. For DSBs, Ku (comprising the Ku70/Ku80 protein heterodimer) and MRN (Nbs1, Mre11, and Rad50) are the principal sensor protein complexes. Ku binds DNA DSBs within seconds, and aids as a scaffold for ensuing recruitment of classical non-homologous end-joining (NHEJ) proteins [75]. However, most of the therapy-induced DSBs are repaired by ATM kinase signaling pathway [76]. The MRN complex plays key roles in triggering full activation of the ATM kinase, the initiation of DNA end-resection, and favoring of DNA repair via HR[77]. Choice of DNA repair pathway either by HR or NHEJ and the mechanisms is an intense area of active research, which is influenced by the chromatin context, transcriptional status, cell cycle stage and extent of end-resection [78]. The MRN complex (Nbs1, Mre11, and Rad50) is necessary for the DSB repair; telomere maintenance and checkpoint control and is a critical component in both (HR and NHEJ) repairs pathways. MRN complex mediated enhanced DNA repair is critical in driving chemoresistance [79]. The deficiency of ATM, Mre11, or Rad50 led to a 2–5-fold sensitization of leukemia cells to chemotherapy [80]. Downstream repair of DSBs is taken care by classical HR or NHEJ pathways.

1.1.7.3.1: Homologous recombination (HR) repair: It uses a complementary DNA strand to repair the damaged DNA. This mode of DNA repair is referred to as error-free mechanism and is important for repair of DNA damage caused by either IR or replication fork arrest. Because HR uses homologous sequences in the genome e.g. sister chromatids, homologous chromosomes or repeated regions, to prime the repair synthesis it is called error-free repair. Accordingly, HR is most active in late S/G2 phase of the cell cycle [81]. As HR uses a template for the recovery of damaged DNA, which can result in loss of heterozygosity, is an important feature of HRR repair.

Introduction

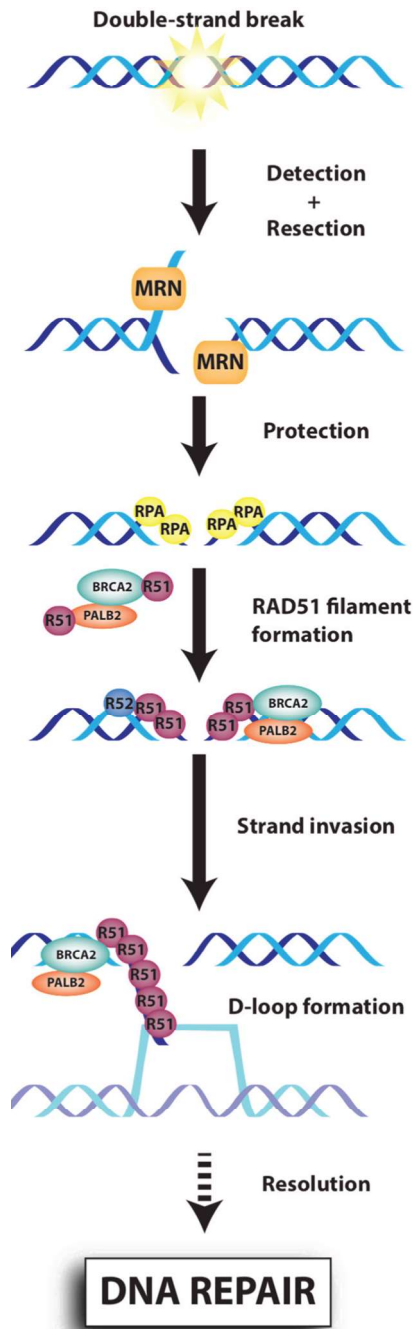


Illustration 9: Homologous recombination repair [1]

In this pathway, DSBs are followed by extensive 5' to 3' end processing resulting from the activities of the recruited exonucleases i.e. Mre11, present as a complex with Mre11/Rad50/Nbs1, collectively called MRN complex. Added roles of MRN complex include recruitment of ATM via its NBS1 subunit, which is known to be a substrate for ATM phosphorylation [82] and unwinding of DNA via ATPase activity of its Rad50 subunit [83]. After the 5' to 3' end resection, the exposed single strands recruit RPA protein, which covers

the resected single-stranded DNA and also recruit Rad51 [84]. With the support of HR facilitator proteins, such as Brca2, PALB2, and the Rad51 paralogs (RAD51B, C, D, XRCC2 and XRCC3), Rad51 is recruited to the DSB sites and polymerizes onto the resection-generated ssDNA ends, forming a nucleoprotein filament that promotes strand invasion and exchange between homologous DNA sequences [85-87]. The nucleoprotein filament searches the nearby sequences to find a homologous sequence which is later occupied with the help of Rad54, an ATPase related to DNA helicases [88]. Next Rad52, can interact with both double and single-stranded DNA by recruitment which forms a seven-monomer ring structure at the nucleoprotein filament [89]. All these initial events result in strand invasion of the DNA overhangs and pairing with homologous sequences. Using this sequence as a DNA template, DNA polymerase starts filling the gaps of the resected 5' to 3' DNA ends of the damaged homolog. At this point, there is a formation of an intermediate DNA structure, called Holliday junction [90]. Holliday junction can be resolved non-crossing over mode by separation of the two pairs of strands or by resolvases mediated endonucleolytic cleavage resulting in a crossing over [91].

1.1.7.3.2: Non-Homologous End Joining (NHEJ) repair: It is the predominant type of repair mechanism of DSBs in mitotically replicating cells and has been studied in greater detail. The hallmark of NHEJ is its ability to ligate non-ligatable DNA ends. This mode of DNA repair is often described as error-prone. Here, post DSB induction, a heterodimeric protein KU comprising Ku70 and Ku80 subunits, binds to the ends of DNA breaks and covers a region of 16-18bp [92].

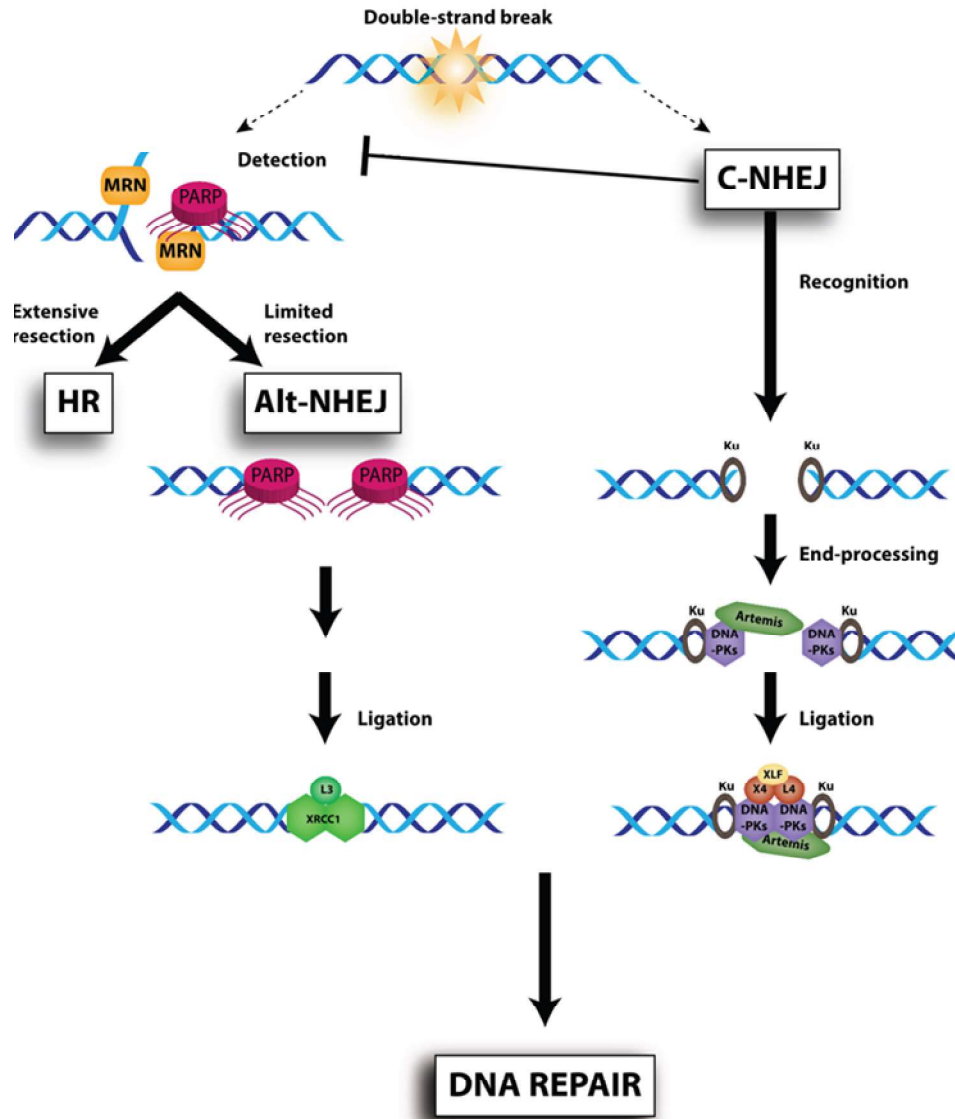


Illustration 10: Non-Homologous end Joining pathway for DNA repair [1]

This recruits its catalytic subunit called DNA-PKcs to the DNA end which displaces the KU dimer inside and binds at the extreme ends of broken DNA [93], setting up the formation and activation of the trimeric DNA-PK holoenzyme, a key enzyme in NHEJ repair. This further recruits WRN, which is a 3' to 5' exonuclease [94]. Artemis, which has specific 5' to 3' exonuclease as well as endonucleolytic activity on 5' and 3' hairpins and overhangs [95] and the replication protein A (RPA) which binds and subsequently stabilizes single-stranded DNA intermediates formed during DSBs and thus prevents complementary DNA from reannealing [96]. Next, the exonucleases can digest and prepare the damaged DNA ends

suitable for ligation. Further, DNA-PK phosphorylates XRCC4, a binding partner of DNA ligase IV, which is then recruited to the damaged DNA ends. DNA polymerases POL μ or POL λ fill up the DNA gaps produced by the damage [97] while XRCC4-Ligase IV complex ligates the nicks [98]. DNA-PK then autophosphorylates itself, leading to its detachment from the DNA lesion [99]

1.1.7.3.3: Role of ATM in DNA double-strand break repair: ATM belongs to phosphatidylinositol-3 kinase-like kinase (PIKK) superfamily of large proteins having phosphatidylinositol-3/4 kinase (PI3K/PI4K) catalytic domain thus functioning as an important kinase in DDR signal transduction. ATM serves as a DSBs sensor protein which activates downstream mediators and effector proteins. The ATM function is emphasized by its loss in, Ataxia Telangiectasia (A-T) disorder also called as Louis-Barr syndrome, caused by hereditary mutations in the *ATM* gene. The disease is characterized by ataxia, referring to uncoordinated body movements and telangiectasia, which means enlarged blood capillaries that, can be seen under the skin. Other characteristic features of A-T include immune deficiency, hypersensitivity to ionizing radiation, and a predisposition to certain cancers [100]. An interesting observation in some A-T patients is the loss of the distal 11q region of the chromosome that harbors key DNA damage response genes including *ATM*, *MRE11*, *CHK1*, and *H2AX* in several hematological malignancies and solid tumors. Cancer predisposition is one of the major complications in A-T with the homozygous A-T patients having a lifetime risk of 30-40 % [101]. In line with the finding that A-T patients have a weak immune system, the most common malignancy linked with A-T patients is that of the immune system (Leukemias and Lymphomas) with the most common being non-Hodgkin's lymphoma (~45%) followed by acute lymphoblastic leukemias (~20%). The *ATM* gene is located on chromosome 11 (11q22-23). It belongs to the class of housekeeping genes [102].

ATM gene consists of 66 exons which span around 150 Kb of the whole genomic DNA, with a coding sequence of 9168bp [103].

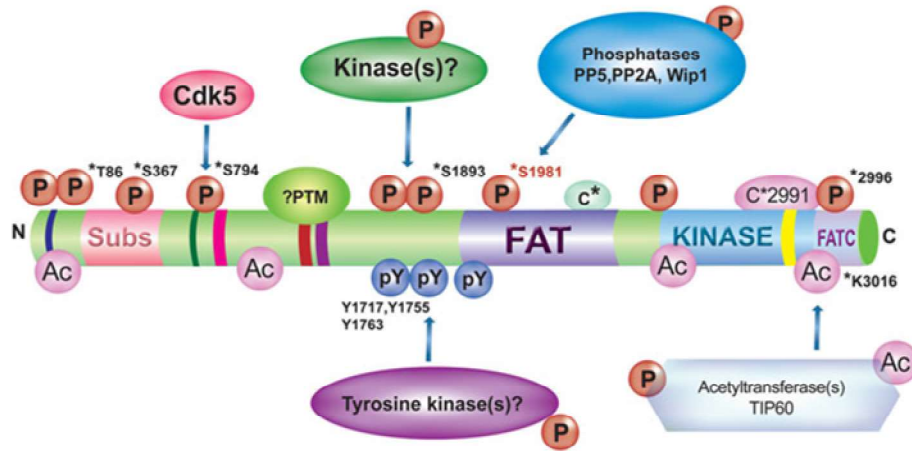


Illustration 11: Domain architecture of ATM protein along with their associated modifications [3]

The 3-D crystal structure of this protein is as yet, unknown. The kinase role of ATM is retained by 350 amino acid long, PI3K/PI4K domain spanning from amino acids 2712 to 2962. It has a FAT domain (FRAP, ATM, and TRRAP) from 1960 to 2566 amino acids and a C-terminal FAT domain (FATC domain) from 3024 and 3056 [104]. Apart from that, a leucine zipper motif between residues 1217-1238 [104, 105] and a ten amino acids long, proline-rich c-Abl (a tyrosine kinase) interacting region between residues 1373 – 1382 have been identified [106].

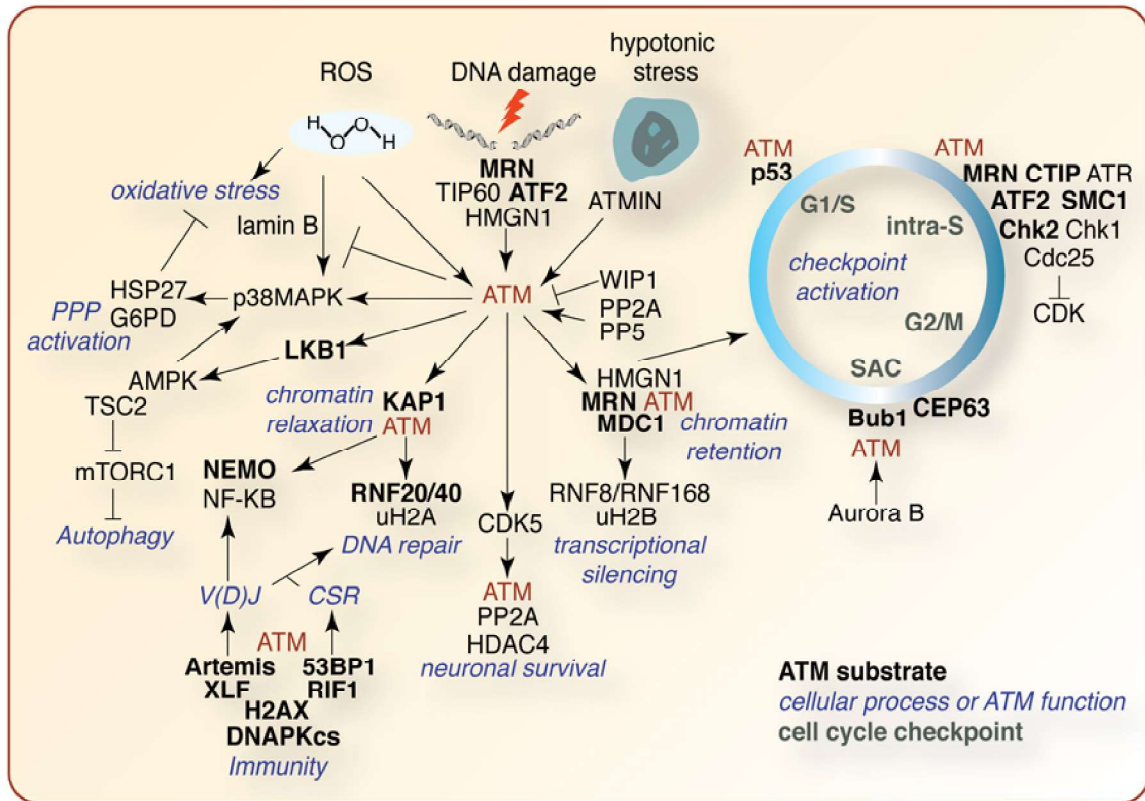


Illustration 12: ATM signaling pathways and functions [4]

ATM is a constitutively expressed protein, remains in an inactive homodimer state. In this form, the kinase domain of one molecule is covered by other. Upon DNA DSBs, the ATM molecules undergo rapid autophosphorylation at residues Ser367, Ser1893, and Ser1981, the last serine being in the FAT domain [107, 108]. This autophosphorylation leads to dimer dissociation and the discharge of kinase active monomers [107]. Simultaneously, a change in the higher order of chromatin structure is initiated, which leads to unwinding and relaxation of the local DNA super-coil. This causes exposure of a variant form of histone H2A called H2AX [107]. The exposed H2AX is a substrate for ATM and triggers its activation. Activated ATM now phosphorylates H2AX at serine 139, also called as γ -H2AX. H2AX is considered as the earliest substrate of ATM after DSBs and hence γ -H2AX formation represents one of the earliest events after DNA damage [109]. γ -H2AX acts as a docking site for a variety of other proteins involved in the DNA damage response pathway which in turn recruit additional ATM molecules to amplify its signal and form discrete ATM foci at the

broken DNA ends. Proteins involved in the formation of ATM foci include MRN complex (MRE11, RAD50, and NBS1), MDC1, RPA, RAD51, RAD52, RAD54, BRCA1, and BLM1.

1.1.7.3.4: Mechanisms of ATM activation: ATM lies at the center of nearly all DSB-induced alterations to chromatin structure at the break site. These chromatin changes include (i) histones post-translational modifications [110], [86] recruitment/eviction and modification of chromatin architectural components and (iii) changes in nucleosome occupancy/spacing due to the ATP-dependent chromatin remodeling machinery [111].

ATM, a master regulator kinase involved in DNA DSBs repair [13] is known as an important mediator of drug resistance [14-16]. Although ATM can get activated by autophosphorylation, other mechanisms like higher recruitment via Mre11 proteins [17], downregulation of its phosphatases (*WIP1 and PP2CA*) [18, 19] also enhance ATM activation and sustainment. ATM recruitment to the DSB is highly dependent upon chromatin architecture around DNA DSBs. ATM is known to be directly acetylated by *TIP-60* at residue 3016 which is known to facilitate its autophosphorylation, whereas *HMOF* is known to induce H4K16ac which opens up the chromatin for ATM recruitment and activation [13, 20-22].

Electron microscopy demonstrated the generation of DSB leads to a rapid, ATP dependent, local relaxation of chromatin [112]. Various studies have classified epigenetic events that lead to higher ATM activation. For e.g. HMGN1 dependent H3K14ac leading to global scale chromatin relaxation is required for ATM activation [113]. ATM also promotes heterochromatin repair by phosphorylating serine 824 of the KRAB-Associated Protein 1 (KAP-1), a widely known transcriptional repressor and a bona fide heterochromatin constituent [114]. Knockdown of HP-1 alpha also uplifts the recruitment of ATM to the DSBs [115]

Intensive combination chemotherapy regimens for acute myeloid leukemia (AML) have improved the outcome of patients, and about 80% of younger patients with newly diagnosed AML may achieve complete remission (CR). However, the majority of patients who achieve CR with initial chemotherapy will eventually relapse [116]. Drug resistance is a major problem that limits the success of chemotherapies used in cancer treatment. Cancer cells may be intrinsically resistant to chemotherapy prior to treatment or can also be developed during treatment by tumors that are originally sensitive to chemotherapy [117]. As mentioned before cells with acquired resistance can also become cross-resistant to other drugs with similar as well as altered mechanisms of action. Intensifying chemotherapy is not the answer as it leads to increased cardiotoxicity, including cardiomyopathy and congestive heart failure (CHF) [118, 119]. As chemoresistance causes therapy failure, clearly, if drug resistance could be overcome, the survival would highly be improved. Drug resistance can occur at many layers, including increased drug efflux, drug inactivation, alterations in drug target, processing of drug-induced damage, and evasion of apoptosis. Although there are multiple ways by which leukemic cells could acquire drug resistance to DNA damaging drugs,

1.1.8: Current challenges in leukemia treatment are to:

1. Identify novel therapeutic targets or bring up the efficacy of currently available therapeutics.
2. Minimize the toxic side effects due to high dose chemotherapy.
3. Improve disease prognostication.
4. Understand the mechanisms of early-stage drug resistance.

The focus of my thesis is to understand the modulation of DNA repair pathways involved in mediating resistance to leukemic cells.

1.2: Rationale: Acquired drug resistance is an evolutionary and complex process. Relapse leukemia is highly resistant and refractory to treatment. We hypothesized that instead of targeting the late resistant leukemic cells, targeting the earliest phase of resistance would provide a much needed therapeutic window for treatment. However, **earliest changes acquired during the evolution of drug resistance are poorly understood. Since most of the chemotherapeutic drugs work by damaging their DNA we postulated that DNA double-strand break repair plays the key mechanisms for the survival of early drug resistant cells and targeting it would have maximum therapeutic value.**

1.3: The aim of the thesis: To understand the role of DNA double-strand break repair pathways in chemoresistant leukemic cells.

1.3.1: Objectives:

3. Establishment of chemoresistant cell lines to a lethal dose of DNA damaging drugs for acquired resistance.
4. Discerning the differences in DSB repair pathways between chemosensitive and chemoresistant population.

CHAPTER 2: MATERIALS AND METHODS

2.1: Cell lines and media requirements: Cells lines, cell culture: K562, THP-1, KG-1 and HL-60 cell lines were obtained from NCCS Pune, HL-60/MX2 cell line was obtained from ATCC (CRL 2257™). All the cell lines were maintained in RPMI with 10% FBS and antibiotics. 293FT cells (A kind gift from Dr. Amit Dutt, ACTREC) were cultured in DMEM with 10% FBS and antibiotics.

2.2: STR profiling: Cell lines were authenticated by STR profiling using PROMEGA STR profiling kit using 10 markers.

Table 3: List of cell lines with STR data

% Match	ATCC Number	Designation	D5S818	D13S317	D7S820	D16S539	vWA	TH01	AMEL	TPOX	CSF1PO	D21S11
100	TIB-202	THP-1 Acute Monocytic Leukemia Human	11,12	13	10	11,12	16	8,9,3	X,Y	8,11	11,13	30,31,2
100	CCL-243	K-562 Leukemia (CML) Human	11,12	8	9,11	11,12	16	9,3	X	8,9	9,10	29,30,31
100	CCL-240	HL-60 Promyelocytic Leukemia Human	12	8,11	11,12	11	16	7,8	X	8,11	13,14	29,30
100	CRL-2257	HL-60/MX2 Mitoxant. Resist. HL-60 Human	12	8,11	11,12	11	16	7,8	X	8,11	13,14	29,30
100	CCL-246	KG-1 Leukemia (AML) Human	13	11,12	8,10	10,11	14,19	7,8	X,Y	7,9	7	28,29
100	CRL-12013	2A Embryonic kidney Human	8,9	12,14	11	9	16,19	7,9,3	X	11	12	30,2

2.2.1: K562: Established from the pleural effusion of 53-year-old female with chronic myelogenous leukemia in terminal blast crisis. Population highly undifferentiated and of the granulocytic series. It can be used as a highly sensitive target for the *in vitro* natural killer assay. Recent studies have shown the K562 blasts are multipotential, hematopoietic malignant cells that spontaneously differentiate into recognizable progenitors of the erythrocyte, granulocyte, and monocytic series. The cells are non-adherent and rounded, are positive for the *BCR-ABL* fusion gene, and bear some proteomic resemblance to both undifferentiated granulocytes and erythrocytes.

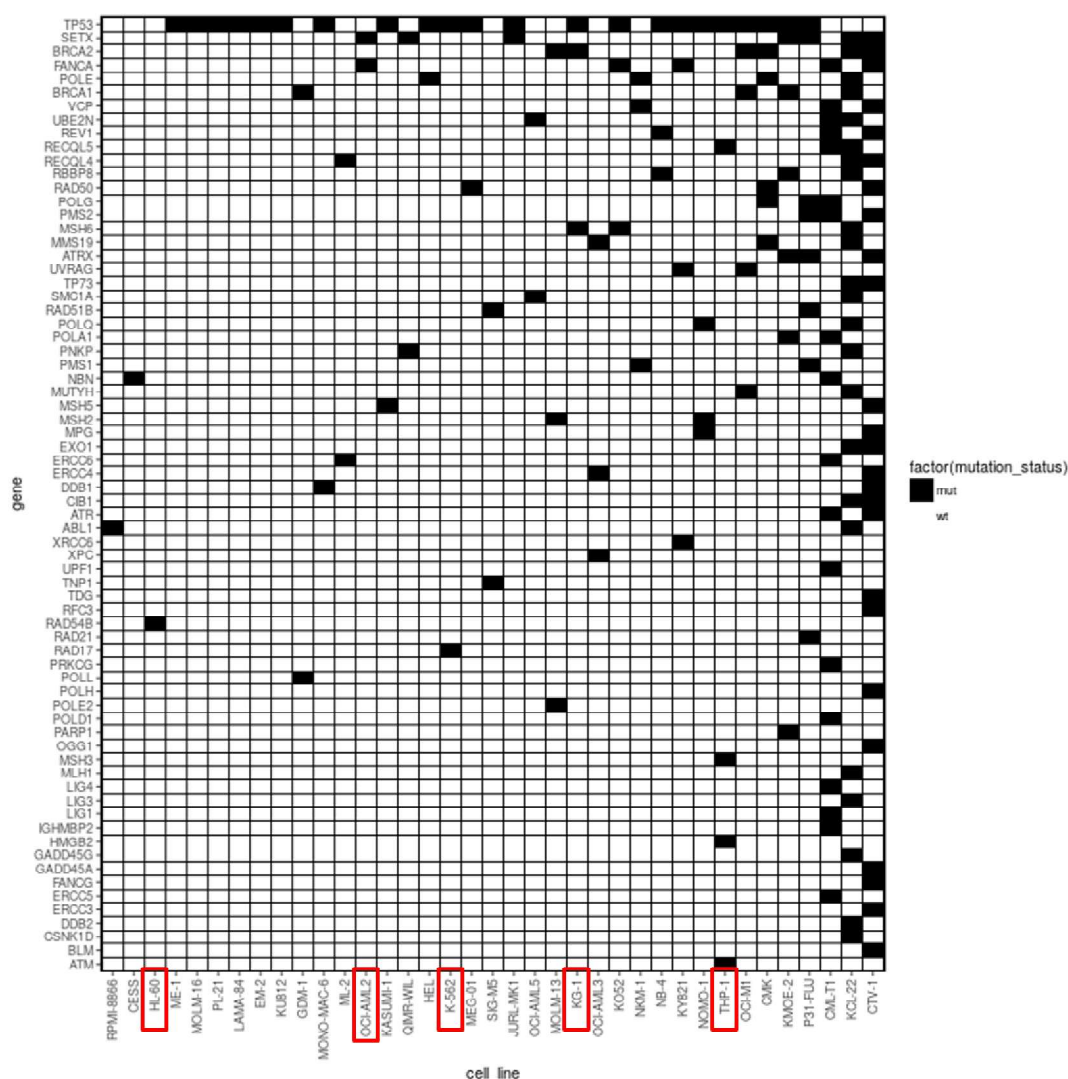


Figure 1: Mutation profile of DNA repair genes in leukemia cell lines

The figure represents a spectrum of mutation in DNA repair gene in all the AML cell lines. The cell lines those are used in this study are boxed in the red color. (Data analysis from- <http://www.broadinstitute.org/ccle>)

2.2.2: THP-1: Cell line derived from the peripheral blood of a 1-year-old male with acute monocytic leukemia (M5b subtype). They resemble native monocyte-derived macrophages with respect to numerous criteria. THP-1 cells have Fc and C3b receptors and lack surface and cytoplasmic immunoglobulin. THP-1 is near-diploid and consists of two related subclones with a number of aberrations, including der(1)t(1;12), der(20)t(1;20), deletions 6p, 12p, and 17p, trisomy 8, and monosomy 10. It also possesses the t(9;11) translocation,

associated with AML M5 and duplication of the 3' portion of *MLL* in the derivative 9 chromosomes and a deletion of the 5' portion of the *AF9* gene involved in the translocation.

2.2.3: HL-60: The HL-60 (Human promyelocytic leukemia cells) cell line is a leukemic cell line. The cell line was derived from a 36-year-old woman with acute promyelocytic leukemia at the National Cancer Institute. HL-60 cells are predominantly a neutrophilic promyelocyte (precursor) The HL-60 cell genome contains an amplified c-myc proto-oncogene; c-myc mRNA levels are correspondingly high in undifferentiated cells but decline rapidly following induction of differentiation. These features have made the HL-60 cell line an attractive model for studies of human myeloid cell differentiation. Chromosomal aberrations include a derivative of chromosome 7 that resulted from translocations of chromosome arms 5q and 16q to 7q. Interstitial deletions of the q arm of chromosome 5 have been associated with AML.

2.3: Development of an evolutionary model of drug resistance: We modeled acquired resistance to DNA damaging agent doxorubicin using leukemic cell lines K562 and THP-1. The overall schema for the development of the resistance model is shown in Figure 2. First, the lethal dose (where $\geq 90\%$ cells die) of doxorubicin for K562 and THP-1 was determined to be 2.5 μ M and 1.4 μ M respectively by cell viability assay. Cells were then treated with their respective lethal dose of doxorubicin for 48 h. We found that a small percentage (<10%) of cells survived (persisters or residual cells, equivalent to the minimal residual disease observed in the patients) high concentrations of doxorubicin in both the cell lines.

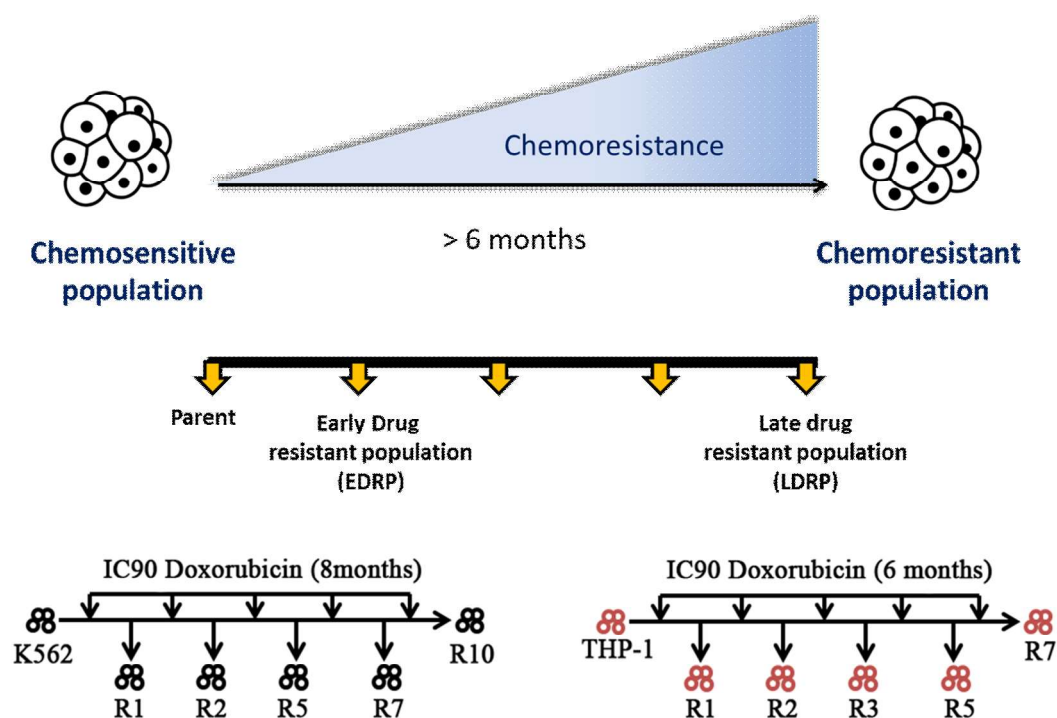


Figure 2: Schema for development of an evolutionary model of drug resistance:

The schema represents the development of acquired chemoresistance model using K562 and THP-1 cell lines. Cell lines were made resistant to doxorubicin with >6-month treatment. Different relapse populations were collected and tested for the drug resistance to define early and late stage drug resistant cells.

These persisters were allowed to grow. The first relapsed population (R) was termed K562-R1 and THP-1 R1. K562 cells were treated with doxorubicin for 10 cycles (over 8 months) while THP-1 for 7 cycles (over 6 months) to obtain the cells with the high drug resistance index. We collected the relapsed cells after every round of drug treatment i.e., R1, R2, R5, R7 and R10 for K562 and R1, R2, R3, R5 and R7 for THP-1 cell line. Resistance to doxorubicin for each population was analyzed by MTT cell viability assay.

2.4: Generation of HL-60/MX2 cell line: Exponentially growing HL-60 cells given 1ng/ml Mitoxantrone for 3day and cells were outgrown in the drug free medium for 3-7 days. Such 21 cycles were given to the cells until they became resistant to 20ng/ml mitoxantrone. These

cells are called MX-1 cells. The further treatment made cells resistant to 100ng/ml over 6 months. The clonal population was selected after limiting dilution in soft agar under drug pressure. Cells capable of growing at 200ng/ml are called HL-60/MX2 cells.[23]

2.5: Drugs and MTT assay: Approximately 5×10^3 cells were treated with doxorubicin (Pfizer Laboratories), mitoxantrone (Sun Pharmaceuticals), KU55933 (Calbiochem), Daunorubicin (Pfizer Laboratories), Cytarabine (Fresenius Kabi), and Butyrolactone 3 (ab141255) at different concentrations. The assay was performed as per manufacturer's instructions (Himedia)

2.6: Clonogenic assay: 1×10^3 cells were treated with the drug and seeded directly in 1ml of methyl cellulose agar (1.6%) with 1 ml of 2X RPMI containing 20% FBS and a 2X antibiotic cocktail in 1:1 ratio. Colonies (>40 cells) were scored under an inverted optical microscope (Olympus model IX 51) on the 12th day.

2.7: Cell cycle and Drug uptake: Cells treated with an IC₉₀ dose of doxorubicin were acquired at different time points and washed with $1 \times$ PBS and fixed with 70% cold ethanol overnight at 4°C. Fixed cells were then washed with PBS and incubated with RNase A (40 µg/ml) and propidium iodide (40 µg/ml) for 30 min at 37°C. These cells were acquired on FACS Caliber (BD Biosciences). Cell cycle analysis was done using ModFitLT 2.0 program. For drug uptake, cells were analyzed by flow cytometry at 480/580 nm wavelengths.

2.8: Softwares: Flow Cytometry: Cell quest, Modfit 2.0 and Flow jo

Image processing: ImageJ, LSM image browser, LAS AF Lite, Photoshop CS3, Foci Counter, Open Comet.

Graphs and statistics: Graph pad prism 5, MS-Excel 2010,

Citation manager: Endnote X6,

2.9: Neutral comet assay/ Single cell gel electrophoresis assay: Modified from E. Boutet-Robinet et al [120] Frosted glass slides were coated with 1% Agarose and kept for drying overnight. Approximately 10000 cells were mixed in 100µl 0.5% LMPA at 42 °C and spread homogeneously on the surface of agarose coated slides with the help of a coverslip. Slides were kept on ice for 30min to solidify the LMPA. Coverslips were then removed gently without disturbing the gel layer. Slides were then incubated in pre-cooled lysis buffer containing 2.5 M NaCl, 100 mM EDTA, 10 mM Tris, 0.05 mg/ml Proteinase K, along with freshly added 1% Triton X-100 and 10% DMSO, pH 8.5 for 1h at 4⁰C. The slides were then electrophoresed in fresh 1X TAE, pH 8.5 at 15V for 10-15 minutes at room temperature. Slides were immediately dehydrated in 100% ethanol for 20 minutes, allowed to dry at room temperature and were stained with 2.5 µg/ml Propidium Iodide for 5 minutes. After a single rinse in fresh milli-Q water, images were acquired at 20X magnification on a fluorescence microscope. Comets were scored in terms of percentage DNA in tail using the OpenComet software. At least 50 cells were counted and the median value was plotted against the respective time points.

2.10: DNA fragmentation Assay: 1*10⁶ cells were treated with Mitoxantrone for 6h and DNA was extracted. 200ng of DNA was loaded on 2% Agarose gel and run at 80V till 3/4 length of gel and visualized with ethidium bromide.

2.11: Western blotting: Cells were lysed in 1X laemmli lysis buffer, proteins separated on SDS-PAGE and transferred on to nitrocellulose membrane. Membranes were probed with different primary antibodies (Table 4). Blots were developed using ECL reagent (Thermo Fischer). Densitometric analysis was done using ImageJ software. Image densitometry was performed as described in ImageJ User Guide – NIH.

Table 4: List of antibodies and dilutions used.

Sr. No.	Antibody and dilutions	Cat no.(company)	Specification
1	γ -H2AX(S139) (1:1000 WB) (1:400 IF)	CST Kit #9947	Rabbit IgG 15kDa
2	Total ATM (1:1000)	CST Kit #9653	Rabbit IgG 350kDa
3	p-ATM(S1981) (1:800) WB	CST Kit #9653	Rabbit IgG 350kDa
4	p-Chk2(T68) (1:1000 WB)	CST Kit #9947	Rabbit IgG 62kDa
5	Total Chk2(1:1000)	ab47571	Rabbit IgG 61kDa
6	p-BRCA1(S1524)(1:1000)	CST Kit #9947	Rabbit IgG 220kDa
7	Mre11(1:1000) (1:200 IF)	CST Kit #9653	Rabbit IgG 81kDa
8	P-p95/NBS1 (Ser343) (1:1000)	CST Kit #9653	Rabbit IgG 95kDa
9	GCN5(IF1:100), (WB 1:1000) (IHC:100)	CST Kit #3305	Rabbit IgG 94kDa
10	p-ATM(s1981) (IF 1:100)	abcam(19304)	Mouse IgG 350kDa
11	Rad51 (IF 1:100)	abcam133534	Rabbit IgG 37kDa
12	H3K27me2(WB 1:1000)	H3 me CST Kit #9847	Rabbit IgG 17kDa
13	H3K4me2(WB 1:1000)	H3 me CST Kit #9847	Rabbit IgG 17kDa
14	H4K20me2(WB 1:1000)	H3 me CST Kit #9847	Rabbit IgG 17kDa
15	Total H4(WB1:1000)	ab10158	Rabbit IgG 11kDa
16	Beta Actin(1:4000)	Sigma A5316	Mouse IgG 42kDa
17	Anti-rabbit IgG, HRP-linked (1:2500)	CST Kit #7074	Rabbit IgG
18	Anti-mouse IgG, HRP-linked (1:2500)	CST KIT 7076P2	Mouse IgG
19	MCL1 L(1:1000)	Santacruz	Mouse IgG
20	HP1 alpha (1:500) IF	ab77256	Goat IgG 22kDa
21	Alexa Fluor® 488 conjugate(1:100)	A11034	Rabbit IgG
22	Alexa Fluor® 568 conjugate(1:100)	A11004	Mouse IgG
23	Vinculin	CST#4650	Rabbit IgG 124kDa
24	Alexa Fluor® 633 conjugate(1:150)	A-21070	Rabbit IgG
25	Rabbit IgG isotype	Millipore 12-370	Rabbit IgG

2.12: Immunofluorescence and Image analysis: Co-localization/Immunofluorescence:

Around 0.5×10^6 K562 cells treated with $2.5 \mu\text{M}$ of doxorubicin for 2h was taken and fixed with 100% methanol for 2h in -20°C and dispensed on a poly-lysine coated coverslips. Dual staining for with anti-GCN5 and anti-p-ATM (S1981) was performed. Cells were then permeabilized for 30 min in 0.5% Triton-X-100 (Sigma) in PBS at 4°C . After one wash with PBS, the coverslips were incubated for one hour at 37°C in blocking solution (3% BSA with 0.1% Tween-20 in PBS). For each coverslip, $15 \mu\text{l}$ of primary antibody was spotted on parafilm kept on a smooth surface. The coverslip was incubated overnight in a humid chamber at 4°C . Next coverslips were washed 3 times 10 min each with 1X PBS. The coverslips were then incubated with $15 \mu\text{l}$ secondary antibody at room temperature for 1h

using the same technique as that from primary antibody. Following incubation, the coverslips were washed 3 times with 1X PBS. The coverslips were then mounted with 15µl vectashield mounting media containing 1.5µg DAPI/ml on a clean slide and sealed with nail polish. Images were acquired using a confocal microscope (Zeiss LSM 780). Images were processed using LSM image browser. Foci were counted with Foci counter software. The intensity of the staining was calculated by using ImageJ software.

2.13: GFP vector reactivation assay/ HR and NHEJ activity assay: Plasmid isolation of NHEJ and HR vector: A good quality plasmid DNA was subjected to the restriction digestion as mentioned below.

Protocol: Make a high-quality preparation of NHEJ or HR reporter plasmid. Measure plasmid concentration and purity by absorbance at 260/280 nm. Linearize 1 µg of the reporter plasmid by digesting with 5 U of I-sce1 in 50µl (total volume of the reaction) for 1 hours in 37°C incubator. Confirm the yield and digestion by running a small aliquot (1µl) on a gel, along with an undigested reporter construct. The linearized reporter construct can be stored at -20°C.

Table 5: Reaction mix for 1ug of plasmid restriction digestion with I-sce1.

NHEJ or HR plasmid	1ug
Cut smart buffer 10x (NEB)	5ul
Restriction enzyme I-sce1 5U/ul(NEB)	1ul
Milli-Q	-----
Total	50ul

2.13.1: Purification of digested linearized plasmid using PCR clean-up kit: Purify DNA from the digestion solution with PCR clean-up kit by MN. Measure DNA concentration and purity by absorbance at 260/280 nm. Usually, you will lose 20-30% of DNA during

purification. Confirm the yield and digestion by running a small aliquot (1µl) on a gel, along with an unpurified reporter construct. The purified linearized reporter construct can be stored at -20°C.

2.13.2: NHEJ & HR Vector Transfection: HR and NHEJ activity assay vectors were a kind gift from Dr. Vera Gorbunova (University of Rochester Department of Biology). K562 Cells were transfected with 1µg of I-SceI endonuclease digested vectors with X-treme GENE HP DNA Transfection Reagent (Roche). Transfection was done in three biological replicates including Td-Red as transfection control in individual plates.

The NHEJ reporter cassette contains a *GFP* gene with 3 kb intron from the *Pem1* gene (GFP-*Pem1*). The *Pem1* intron contains an adenoviral exon flanked by recognition sequences for HindIII and I-SceI endonucleases for induction of DSBs (Illustration 13A). These sites are in inverted orientation. I-SceI has a non-palindromic recognition sequence; hence two inverted sites generate incompatible DNA ends. The intact NHEJ cassette is GFP negative. As I-SceI induces DSBs, the adenoviral exon is removed and NHEJ restores the *GFP* gene. The HR cassette is again based on the GFP-*Pem1*. In the HR cassette, the first exon of the GFP-*Pem1* contains a 22 bp deletion with the insertion of three restriction sites, I-SceI/HindIII/I-SceI. The deletion guarantees that GFP cannot be rebuilt by an NHEJ event. The first copy of GFP-*Pem1* is trailed by a promoter-less/ATG-less first exon and intron of GFP-*Pem1*.

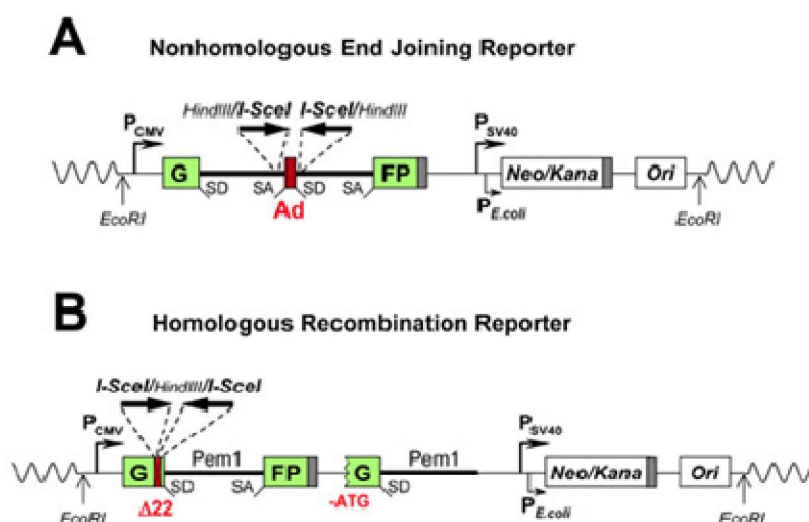


Illustration 13: NHEJ and HR activity vectors [5]

Upon a DSB by I-SceI digestion the functional *GFP* gene is reconstituted by homology mediated repair using downstream GFP-Pem1 exon. Since the second copy of the GFP gene is lacking the first ATG codon and the second exon, crossing over or single-strand annealing will not restore the GFP activity (Illustration 13 B).

- In preparation for transfection, seed 30,000 cells/100ul of RPMI CM in 96-well plate. Grow the cells to 70-80% confluence. It is critical for the best transfection efficiency to bring the cells into logarithmic growth. Actively growing culture contains cells in M stage.
- Make a transfection complex containing 0.5 µg of linearized kit purified reporter constructs of NHEJ and HR in the presence of 0.5µl of X-treme gene HP reagent in 50ul of opti-MEM. Also, transfect cells with 0.5ug of TdRed plasmid as a control.
- Put 10µl of above-prepared transfection complex into each well containing 30,000 cells in 100ul of RPMI complete medium
- After 72 hours of transfection verify the efficiency of transfection and expression of GFP and TdRed proteins by a fluorescent inverted microscope with filters for detection of GFP

and TdRed Flow cytometry was done after 72h Post-transfection. Percent repair efficiency was calculated by taking the ratio of % GFP (HR or NHEJ) cells to % Td-Red cells.

Calculations: Tdred was used as a control for transfection to calculate the competency of each cell type for transfection. Average transfection efficiency of Td-Red in respective cell type was used as the denominator for calculating the HR or NHEJ repair efficiencies. For example, from three independent experiments avg. transfection efficiency of Td-Red in K562 cells was 10.12% while in K-EDRP was 8.07%. Similarly, the GFP positive cells after transfection with NHEJ vector in K562 and K-EDRP cells was 5.07% and 3.49% respectively. Hence NHEJ efficiency of these cell types was calculated as NHEJ repair efficiency= (% NHEJ (GFP) cells/ (Td-Red efficiency) *100 i.e. for K562= (5.07/10.12) *100=50% and for K-EDRP= (3.49/8.07) *100= 43.24%. Calculations for HR efficiency were also made following the same method.

2.14: Quantitative real-time SYBR green PCR: Quantitative real-time SYBR green PCR: RNA was extracted using TRI Reagent (Thermofisher) and cDNA made using Superscript III First-Strand kit (Invitrogen). SYBR green real-time PCR was performed using SYBR green (Roche) in a Roche Life Cyclor 480. GAPDH or RPL19 was used as internal control. Primer sequences are given in the table below.

Table 6: : List of primers used for SYBR green based real-time PCR.

Sr. No	Primer name	Primer Sequence
1	RPL19 F	CAAGCGGATTCTCATGGAACA
2	RPL19 R	TGGTCAGCCAGGAGCTTCTT
3	GCN5/KAT2A F	TTCAAGCTACTGCGGAAATG
4	GCN5/KAT2A R	CACAAAGTTCAGCACACCCT
5	GAPDH F	AATCCCATCACCATCTTCCA
6	GAPDH R	TGGACTCCACGACGTACTCA
7	TOP2B F	TCCAACCAGATCTGTCCAAA
8	TOP2B R	CGAAATCCATTTACAGGCAA
9	ABCB1F	TCCTTCATCTATGGTTGGCA
10	ABCB1 R	TAGCGATCTTCCCAGAACCT
11	HMOF F	TCCAGTCTCGAGTGAACGAC
12	HMOF R	TTGTCTACCCACTCGTCCAG
13	P300 F	TTCTGAGGCGACAGAATCAC
14	P300 R	TCTGCCATCTCTCCACTGTC
15	TIP60 F	AAACGTCTGGATGAATGGGT
16	TIP60 R	CCTTCCGTTTCACCTCTCTC
17	HDAC2 F	GGAGGAGGTGGCTACACAAT
18	HDAC2 R	GGCAACTCATTGGGAATCTC
19	HDAC1 F	CATTAAATTCTTGCGCTCCA
20	HDAC1 R	CCAACGTTGAATCTCTGCAT
21	PP2CA F	CCAGCTAGTGATGGAGGGAT
22	PP2CA R	GGGTCAAACCTGCAAGAAAGAG
23	WIP1 F	GCACTTGGTGATTTGTGGAG
24	WIP1 R	TTGTGCTTCTGAGGGTCAAG

2.15: Transmission electron microscopy (TEM): Cells were harvested and washed with phosphate-buffer saline, following the cells were fixed with 3% glutaraldehyde for 2 hours at 4°C. The cells were then washed 3 times with 0.1M sodium cacodylate buffer for 5 minutes and centrifuged at 3000rpm. Post fixation, cells were treated with 0.1% osmium tetra oxide for 1 hour at 4°C, followed by 3 washes with 0.1M sodium cacodylate buffer. Subsequently, the cells were dehydrated in increasing percentage of absolute alcohol: 30% absolute alcohol- 15 minutes, 50% alcohol- 15 minutes, 70% alcohol- 30 minutes, 90% alcohol-15 minutes and finally in 100% absolute alcohol for 60 minutes. Dehydrated cells were then incubated with absolute alcohol and araldite A (1:1 ratio) for 30 minutes at 60°C, araldite A for 30 minutes at 60°C, araldite B for 30 minutes at 60°C and the finally in araldite B for 48-72 hours at 60°C

for polymerization and embedding of the cells. Ultrathin sections of 70nm were then made using Leica Ultramicrotome (UC7). The sections were then stained in 10% of alcoholic uranyl acetate for 10 minutes followed by 3 minutes incubation with lead acetate. The sections were then washed with CO₂ free distill water to remove any unbound stain. The imaging was then carried out on transmission electron microscope (Jeol 1400 plus).

2.15.2: TEM image quantitation: Images were analyzed on the basis of their gray-scale intensity using MATLAB (Mathswork) computing software. To obtain the distribution of gray scale values at a given offset, the gray-level co-occurrence matrix (GLCM) was used [16]. For a gray-scale, images were divided into 8 image grey levels (0 to 31, 32-63...224-255) in which image darkness is inversely proportional to grey level values. The GLCM described here is used for a series of "second order" texture calculations. It means that the relationship between groups of two pixels in the original image has been considered in the calculation. The GCLM mean of co-occurrence of pixels value with a neighbor was calculated based on the equation;

$$\mu_i = \sum_{j=0}^{N-1} j(P_{i,j}) \quad \mu_j = \sum_{i=0}^{N-1} i(P_{i,j})$$

2.16: ATM kinase inhibitor (KU-55933): ATM inhibitor KU-55933, is one of the most used in laboratories to inhibit ATM kinase activity. KU-55933 is a cell-permeable, potent, selective and ATP-competitive inhibitor of ATM. KU-55933, with an IC₅₀ of 13 nmol/L and a K_i of 2.2 nmol/L *in vitro*, showed a >100-fold higher potency against ATM compared to other PIKK family members, with no selectivity toward a panel of 60 unrelated protein kinases [121]. Nonetheless, KU-55933 can induce cell death in senescent breast, lung, and colon carcinoma cells through p21, in an ATM-dependent manner [122].

2.17: GCN5 inhibitor (Butyrolactone 3 or BL-3 or MB-3): It is (2R,3S)-rel-Tetrahydro-4-methylene-5-oxo-2-propyl-3-furancarboxylic acid. Synthesized by Markus Biel [123]. It

inhibits acetyltransferase activity of GCN5 ($IC_{50} = 100 \mu M$). Also shows weak inhibition of CBP ($IC_{50} = 1.75-2mM$).

2.18: Co-Immunoprecipitation of GCN5 and ATM: Co-IP was performed using cell lysates from THP-1 and Flag-GCN5 overexpressing 293FT cells treated with $5\mu M$ doxorubicin for 2h. Cells were treated with 2% PFA for 15 min; unbound PFA was quenched with 0.3M glycine solution. Cells were washed with PBS and lysed in EBC lysis buffer (50 mM Tris, pH 7.5, 150 mM NaCl, 0.5% NP-40, 1 mM PMSF, 1 mM Complete protease inhibitors (Roche Diagnostics) and 1 mM Phosphatase Inhibitor Cocktail III (Sigma). Protein concentration was done by routine BCA assay. Approximately 300 μg of lysates were incubated with 5 μg GCN5 antibody in 300 μl of 20mM Na-phosphate buffer (pH=7) overnight on rotating shaker at 4°C. Appropriate IgG Isotype control was taken. Next day equilibrated agarose-G beads were added to immuno-complexes and incubated for 2h on rotating shaker at 4°C. The mixture was centrifuged at 4000rpm to collect the pellet. Bead pellet was washed thrice with Na-phosphate buffer. The sample was boiled in 1X laemmli buffer for 10 min at 100°C and loaded on 10% SDS-PAGE and probed with anti-GCN5 and anti p-ATM (S1981) antibodies.

2.19: siRNA knockdown of GCN5: THP-1 cells were seeded at 0.3 million/ml density in a 6 well. Next day cells were transfected with siRNA (Invitrogen Cat no. 4390824) at 30pmols per well concentration using standard 6 well protocol for RNAiMax reagent. Cells were collected 72h post-transfection. Cell lysates were tested for GCN5 knockdown by western blot.

2.20: Plasmid isolation using NucleoSpin: In brief to explain the principle of the plasmid isolation, the bacterial cells were resuspended in Buffer A1 (provided in the kit) in which RNase A was mixed (provided in the kit). Plasmid DNA was extracted from the cells by alkaline lysis (Buffer A2). Buffer A3 neutralizes the resulting lysate and creates conditions by

which binding of plasmid DNA binds to the silica membrane of the NucleoSpin® Plasmid/Plasmid(NoLid) or NucleoSPin® Plasmid QuickPure column. After binding, contaminants like salts, metabolites and soluble macromolecular cellular components which affect the later transfections were removed by washes with ethanolic buffer(A4). Pure plasmid DNA is finally eluted under ionic strength conditions with alkaline buffer AE(5mM tris/HCl, pH 8.5).

2.21: GCN5 overexpression: GFP-GCN5 was purchased from Addgene (plasmid # 65386). pEBB Flag GCN5 was a gift from Dr. Ezra Burstein (UT Southwestern Medical Centre). 293FT cells were transfected with GCN5 overexpression vectors using lipofectamine 3000 reagents according to manufacturer's protocol.

2.22: GCN5/KAT2A metadata analysis: For *GCN5* expression and survival freely available AML gene expression datasets were used. Survival plots were made using prognoscan online tool whereas for representing *GCN5* expression in high and low-risk group SurveExpress was used.

2.23: Collection of AML patient samples and ethics statement: Blood samples from AML patients were accrued after approval by the institutional ethics committee (TMC-IEC III) DCGI registration number: IEC III:- ECR/149/Inst/MH/2013. A written informed consent in a language understood by the patients was obtained from all the patients and/ or patient's relatives/guardians prior to sample collection. Blood samples were processed and human investigations were performed according to the relevant guidelines and experimental procedure approved by TMC-IEC III. **Patient samples:** Following FAB diagnosis, AML cases were characterized by immunophenotyping using multiparametric flow cytometry. Detailed patient information (Table 7). Patients cytogenetic classification was done on the basis of WHO guidelines as follows

Favorable (good) prognostic abnormalities:

1. t(8;21) (AML M2)
2. Inversion of chromosome 16 or t(16;16) (AMML M4 eos)
3. t(15;17) (APML M3)

Intermediate prognostic abnormalities:

1. Normal karyotype

Unfavorable (poor) prognostic abnormalities:

1. Deletion/loss of chromosome 5 or 7 – may be secondary to alkylating agent chemotherapy
2. Translocation or inversion of chromosome 3
3. t(6;9)
4. t(9;22) - transformed CML or de novo AML or ALL
5. Chromosome 11q23 abnormalities – secondary to topoisomerase inhibitor chemotherapy
6. Monosomal karyotype involving a monosomy (loss of an entire chromosome) plus additional structural aberrations or more than a single monosomy
7. Complex karyotype often involving ≥ 3 chromosomal abnormalities (no specific AML type)

Note: In patients with normal karyotype the following have prognostic implications:

- Mutation in the FLT3 gene results in a poorer outcome. 1 in 3 patients have an internal tandem duplication (ITD) mutation in the FLT3 gene which results in a poorer outcome, especially when both alleles are involved (resulting in a high FLT3-ITD/normal FLT3 ratio).
- Patients with mutations in the NPM1 gene (and no other abnormalities) have a better prognosis, as do patients with mutations in both alleles of the CEBP α gene (so called biallelic gene mutations).

2.24: Immunohistochemistry of GCN5 in AML bone marrow biopsies: Thin sections of 4 μ M thickness were made using microtome from AML bone marrow paraffin embedded blocks. These sections were fixed on poly-L-lysine coated glass slides. Slides were kept at 60°C for 30 min in the oven. Slides were immediately transferred to xylene jar 3 times for 10 min each. Glass slides were then passed through 100%, 90% and 70% ethanol solution for 10 min each. Sectioned were given a tap water wash for 15 min. Sections were then kept in Tris-EDTA buffer (pH=9) for antigen retrieval. Sections were boiled in a pressure cooker till 2 whistles. Glass slides were taken out and allowed to slowly cool down. Blocking of 1:50 horse serum was added to sections in a moist chamber for 30 min at room temperature. Anti-

GCN5 antibody at 1:100 dilution prepared in PBS was added to sections and kept for overnight incubation. Next day sections were washed with PBS 10 min for 3 times to remove primary antibody. Secondary antibody tagged to 633 Alexa dye at (1:150 dilution in PBS) was added on sections for 1h at RT in a moist chamber. The secondary unbound antibody was removed by 3 PBS wash 10 min each. Sections were then mounted in mounting medium with DAPI covered with a coverslip and sealed with nail polish. Slides were stored in dark at 4°C for imaging. Median fluorescence intensity was calculated using ImageJ software.

2.25: Statistics: The two-tailed Student's t-test was applied for statistical analysis. Results were considered significant in all experiments at * means $P < 0.05$, ** means $P < 0.01$ and *** means $P < 0.001$. Survival analysis: Survival analysis in PrognoScan employs the minimum P-value approach to find the cutpoint in continuous gene expression measurement for grouping patients. First, patients are ordered by expression value of a given gene. Next, patients are divided into two (high and low) expression groups at all potential cutpoint, and the risk differences of the two groups are estimated by log-rank test. Then, the optimal cutpoint that gives the most pronounced P-value (P_{min}) is selected.

Table 7: Clinical Characteristics of 44 Patients with Acute Myeloid Leukemia grouped on the basis of post induction and post-consolidation MRD status.

No.	Hospital No.	Pt No.	Age	Gender	Date of induction	TLC cu.mm	Cytogenetic Risk	Post Induction Flow MRD	Post Consolidation flow MRD	Last updated status	Treatment
1	CJ/22706	9	18	F	30-09-12	6800	INTERMEDIATE	9.5	3.63	Relapsed/died	7+3
2	CJ/50041	17	39	M	20-11-12	30000	GOOD	5.38	2.13	Alive	7+3
3	CJ/27752	18	19	F	16-11-12	32400	GOOD	0.28	0.07	Relapsed/died	7+3
4	CJ/29494	19	47	M	17-11-12	5320	INTERMEDIATE	N/A	51	Alive	7+3
5	CJ/29044	20	37	M	22-11-12	119900	INTERMEDIATE	N/A	1.76	Relapsed/died	7+3
6	CJ/30688	21	37	F	03-12-12	77200	INTERMEDIATE	Negative	Negative	Alive	7+3
7	CJ/29609	22	40	M	03-12-12	21800	GOOD	0.65	0.4	Relapsed	7+3
8	CJ/30236	23	27	M	05-12-12	15700	GOOD	2.8	0.35	Relapsed	7+3
9	CJ/30658	25	24	M	17-12-12	90930	POOR	0.12	0.02	Relapsed/died	7+3
10	CJ/33198	31	22	F	05-01-13	26300	GOOD	Negative	Negative	Alive	7+3
11	CK/2117	40	58	M	09-02-13	38300	INTERMEDIATE	1.3	Negative	Alive	7+3
12	CK/3596	41	29	M	06-03-13	7100	POOR	38	N/A	Refractory disease	7+3
13	Ck/7458	52	22	F	23-04-13	23600	POOR	1.07	1.66	Relapsed/died	7+3
14	Ck/7246	53	37	M	21-04-13	130000	GOOD	N/A	0.37	Alive	7+3
15	Ck/13578	62	16	M	13-06-13	18200	GOOD	Negative	Negative	Alive	7+3
16	CK/14223	63	23	M	27-06-13	12330	POOR	N/A	85	Relapsed	7+3
17	CK/16487	65	18	M	23-07-13	49210	INTERMEDIATE	Negative	Negative	Relapsed/died	7+3
18	CK/21598	69	32	M	23-08-13	123000	INTERMEDIATE	Negative	Negative	Relapsed/died	7+3
19	CK/21415	72	35	M	02-09-13	6300	INTERMEDIATE	8.5	0.69	Relapsed/died	7+3
20	CK/20239	73	45	M	07-09-13	6000	INTERMEDIATE	13	N/A	Refractory	7+3
21	CK/21960	74	18	F	17-09-13	2900	INTERMEDIATE	0.12	0.02	Relapsed/died	7+3
22	CK25193	83	18	F	19-10-13	1100	POOR	0.94	N/A	Alive/refractory	7+3
23	CK17125	84	23	M	20-07-13	2680	GOOD	Negative	Negative	Alive	7+3
24	CK50140	85	30	F	15-11-13	113000	POOR	Negative	Negative	Relapsed/died	7+3
25	CK28755	87	42	M	21-11-13	1000	POOR	3.16	0.25	Alive	7+3
26	CK32438	89	37	M	07-01-14	4300	INTERMEDIATE	1.32	N/A	Refractory disease	7+3
27	CK33041	92	18	F	14-01-14	92800	POOR	35	N/A	died	7+3
28	CL221	93	18	M	02-02-14	22700	INTERMEDIATE	Negative	Negative	Alive	7+3
29	CL2372	95	21	M	06-02-14	35700	INTERMEDIATE	2.26	Negative	Alive	7+3
30	CL7779	104	16	M	09-04-14	178900	INTERMEDIATE	Negative	Negative	Relapsed/died	7+3
31	CL10255	110	54	F	12-05-14	12230	GOOD	Negative	Negative	Relapsed	7+3
32	CL15457	114	20	M	N/A	8600	INTERMEDIATE	Negative	Negative	relapsed	7+3
33	CL18282	118	31	F	13-08-14	N/A	INTERMEDIATE	Negative	Negative	ALIVE	7+3
34	CL29173	128	24	M	29-10-14	10130	INTERMEDIATE	Negative	Negative	ALIVE	7+3
35	CL29433	130	31	M	07-11-14	34200	POOR	Negative	Negative	ALIVE	7+3
36	CL32379	133	15	F	25-11-14	28600	GOOD	Negative	Negative	ALIVE	7+3
37	CJ31151	135	20	M	20-11-14	31340	GOOD	Negative	Negative	ALIVE	7+3
38	CL33649	137	30	M	29-11-14	41100	INTERMEDIATE	Negative	Negative	ALIVE	7+3
39	CM467	138	42	F	30-01-15	1580	INTERMEDIATE	N/A	1.41	ALIVE	7+3
40	CL32323	140	26	M	11-12-14	7700	GOOD	Negative	Negative	ALIVE	7+3
41	CL34088	141	15	M	22-12-14	20600	GOOD	Negative	Negative	ALIVE	7+3
42	CL32644	142	32	M	26-12-14	3100	INTERMEDIATE	Negative	Negative	ALIVE	7+3
43	CM3067	149	49	M	22-02-15	117900	INTERMEDIATE	Negative	Negative	ALIVE	7+3
44	CM2268	152	22	M	15-02-15	1110	INTERMEDIATE	Negative	Negative	ALIVE	7+3

CHAPTER 3: RESULTS

3.1 Objective 1: Establishment and characterization of drug resistant cell lines. This objective mainly focuses on the development and characterization of the chemoresistant model. It involves major/critical work done, rationale and comparison with conventional resistance models. Establishment of the chemoresistant model is the strenuous and lengthy procedure. As it's an adaptive process, it takes months of continuous culturing of cells in the presence of a drug of interest.

3.1.1: Conventional drug resistant models and their limitations: Understanding drug resistance mechanism using cell line models has been in practice for many years now. Development of drug resistance is an adaptive response to a particular class of chemotherapeutics and is a fairly complex and multistep process of biological change. Making of drug resistance models is time consuming and laborious process and involves continuous treatment of escalating doses of chemotherapeutics to the cancer cells over a period of 6 months to 2 years. Starting with measurement of the dose-response using MTT assays, a semi-lethal concentration of the drug is selected to start the treatment and multiple cycles of drug treatment makes cells non-responder to the drug by virtue of cellular alterations. Next, the escalated doses are used over multiple cycles of treatment to establish a resistance model with high resistance indices (Fold resistance). Such model systems are reasonably stable for their resistance and are widely accepted for understanding the mechanisms of drug resistance. However, as this process is essentially a complex and multistep evolutionary process, we hypothesized that there would be distinct differences in cellular response to chemotherapeutics during onset (Early) and established (Late) stages. Assuming that early stage mechanisms are the roots of advanced stage resistance, targeting these changes could offer more effective treatment targets.

3.1.2: Establishment of the evolutionary model of drug resistance: To test our hypothesis we used leukemia cell lines like K562 and THP-1 and measured the IC90 dose of

Results

doxorubicin using MTT assay. The IC₉₀ dose was chosen as it reduces the entire heterogeneous population to a very small subset of highly resistant cells that grow back to form relapse which is used for the next cycle of treatment. Again, the IC₉₀ dose is also important in leukemia as it mimics patient treatment. Leukemia patients are treated with maximum tolerable doses of DNA damaging drugs and declared in complete remission when blasts are < 5%. This lead to the generation of multiple relapse population (named as R1, R2.....Rn) over a period of 6-8 months during which we could achieve early as well as late stage drug resistant cells.

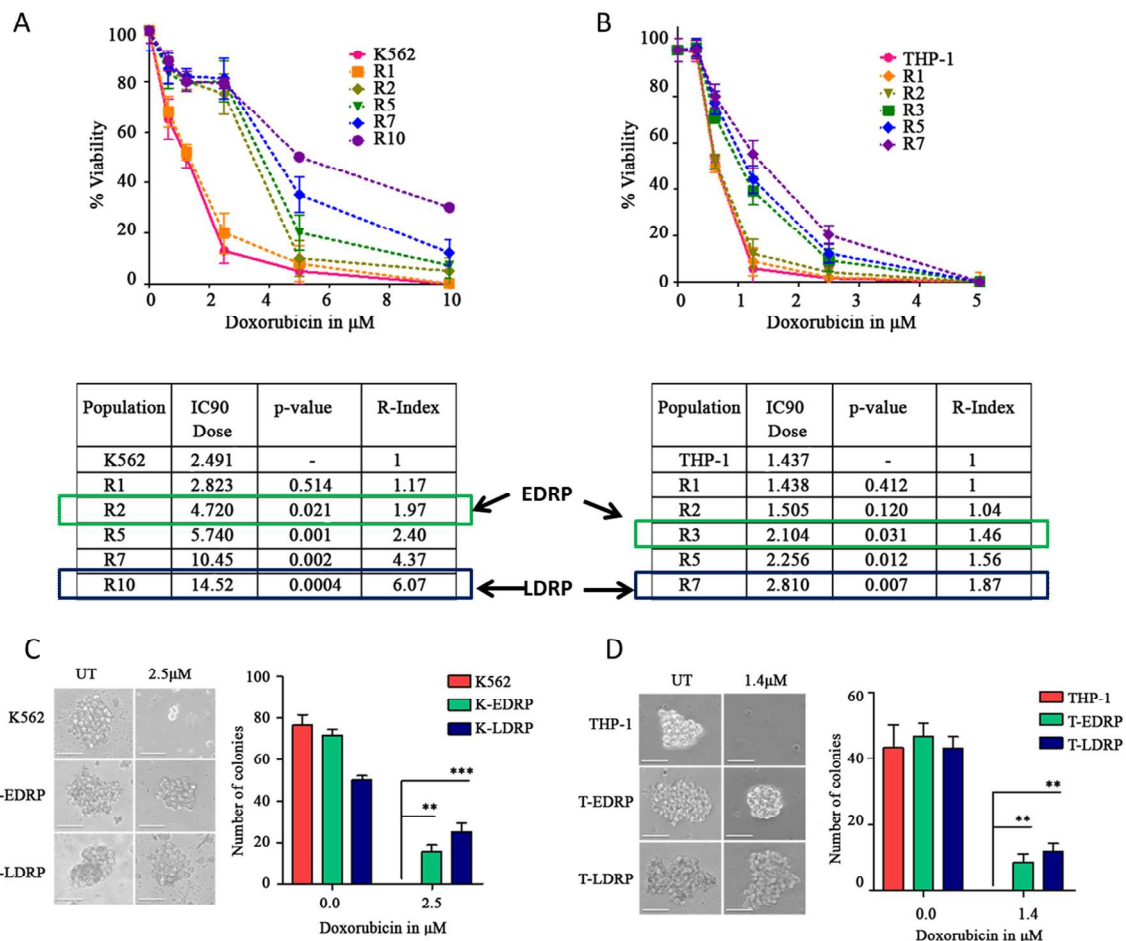


Figure 3: Establishment and validation of drug resistance model.

(A and B) Cytotoxicity evaluation by MTT assay after treatment of K562, THP-1 and its resistant derivatives to increasing concentrations of doxorubicin for 48 hours. X-axis scales are different for A and B. Table depicts resistance indices of different resistant populations

*developed from K562 and THP-1 cells following increasing cycles of doxorubicin treatment. (C and D) Representative images for a typical cell colony observed by bright-field microscopy (20X Objective) at day 10-12 of growth in soft agar are shown. (Scale bar=50µm) Bar graph quantifies the number of colonies formed in different cell populations after doxorubicin treatment. Y-Axis scales are different for C and D. Results in each bar and line graph are the composite data from three independent experiments performed in triplicate (mean± SEM); * denotes $p \leq .05$, ** denotes $p \leq .01$, *** denotes $p \leq .001$. PDR- Post drug removal.*

We found that R1 population of K562 and R1 and R2 population of THP-1 cell line showed similar sensitivity to doxorubicin as the parent population. However, K562-R2 cells (1.97 fold resistance) and THP-1-R3 cells (1.46 fold resistance) were earliest relapses that showed significantly better survival to doxorubicin than their respective parent populations (Figure 3A and B). Since K562-R2 and THP-1-R3 were the first populations to show significant resistance to doxorubicin, we refer to these populations as **Early Drug Resistant Population (EDRP)** cells and K562-R10 and THP-1-R7 as **Late Drug Resistant Population (LDRP)** cells.

3.1.2.1: Clonogenic properties, cross resistance and reversible resistance of drug resistant cells: Both the EDRP and LDRP cells were analyzed for their clonogenic ability in the presence of an IC90 concentration of doxorubicin. As shown in Figure 3C and D, both EDRP and LDRP formed a significantly higher number of colonies compared to parent cells, indicating the enrichment of cells with colony forming capacity (indefinite cell growth) in these populations. We confirmed the drug resistance of HL-60 and its mitoxantrone resistant sub-cell line HL-60/MX2 (representing LDRP of HL-60) which is 35 fold more resistant than parent HL-60 cells (Figure 4A). HL-60/MX2 cells are cross resistant to cytarabine (Figure 4B) and multiple other drugs like m-AMSA, Teniposide, Etoposide, Daunorubicin etc. [23].

Results

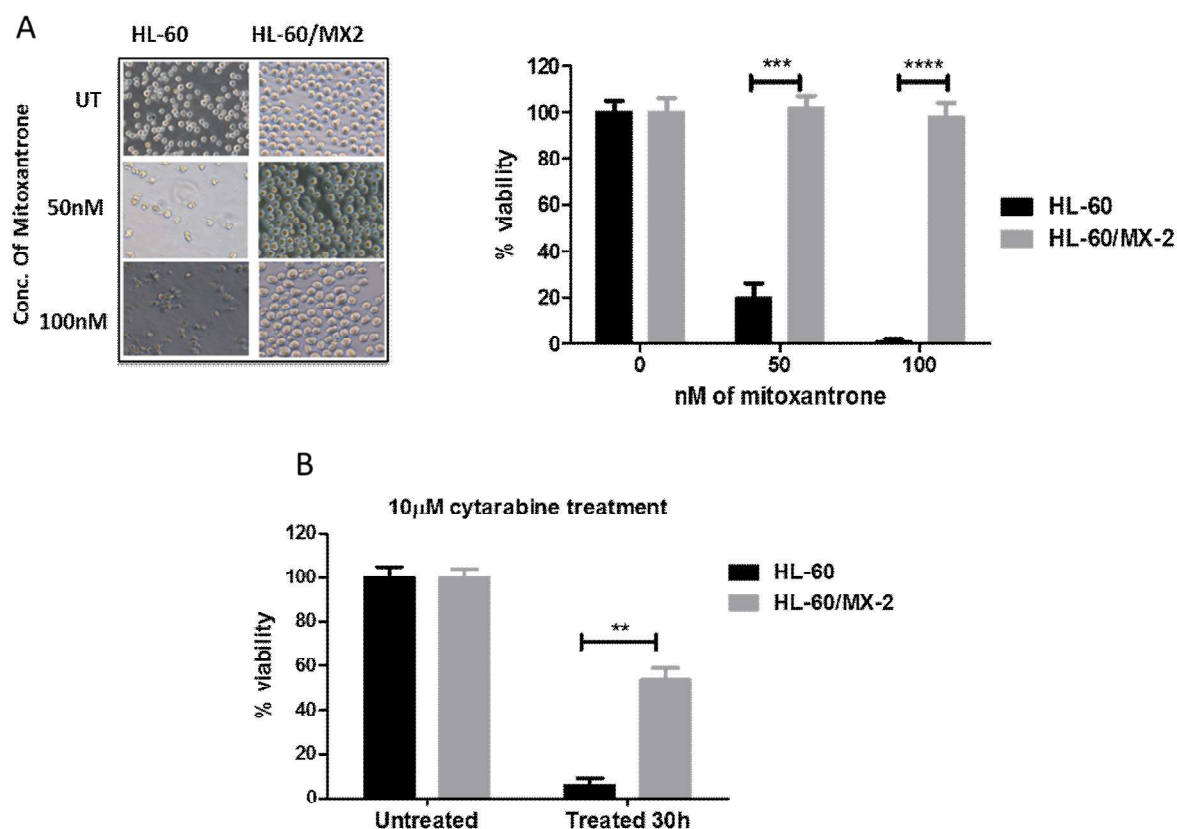


Figure 4: HL-60/MX2 drug resistance model and validation

(A) Trypan blue viability count of HL-60 and HL-60/MX2 cells treated with 50 and 100 nM conc. of mitoxantrone for 30h. **(B)** Trypan blue viability count of HL-60 and HL-60/MX2 cells treated with 10 μ M conc. of cytarabine for 30h.

Further, we tested the cross-resistance of K562, K-EDRP, and K-LDRP to therapeutically relevant DNA damaging drugs such as daunorubicin and cytarabine and found that both the populations were resistant to daunorubicin whereas cytarabine resistance was shown only by K-LDRP suggesting a better adaptation of LDRP to a class of drug (Figure 5A and B). Interestingly, all the chemoresistant populations showed reversibility to resistance when cultured in drug-free media. EDRP cells showed loss of resistance faster (10-12 days) than LDRP cells (30-40 days) (Figure 5C).

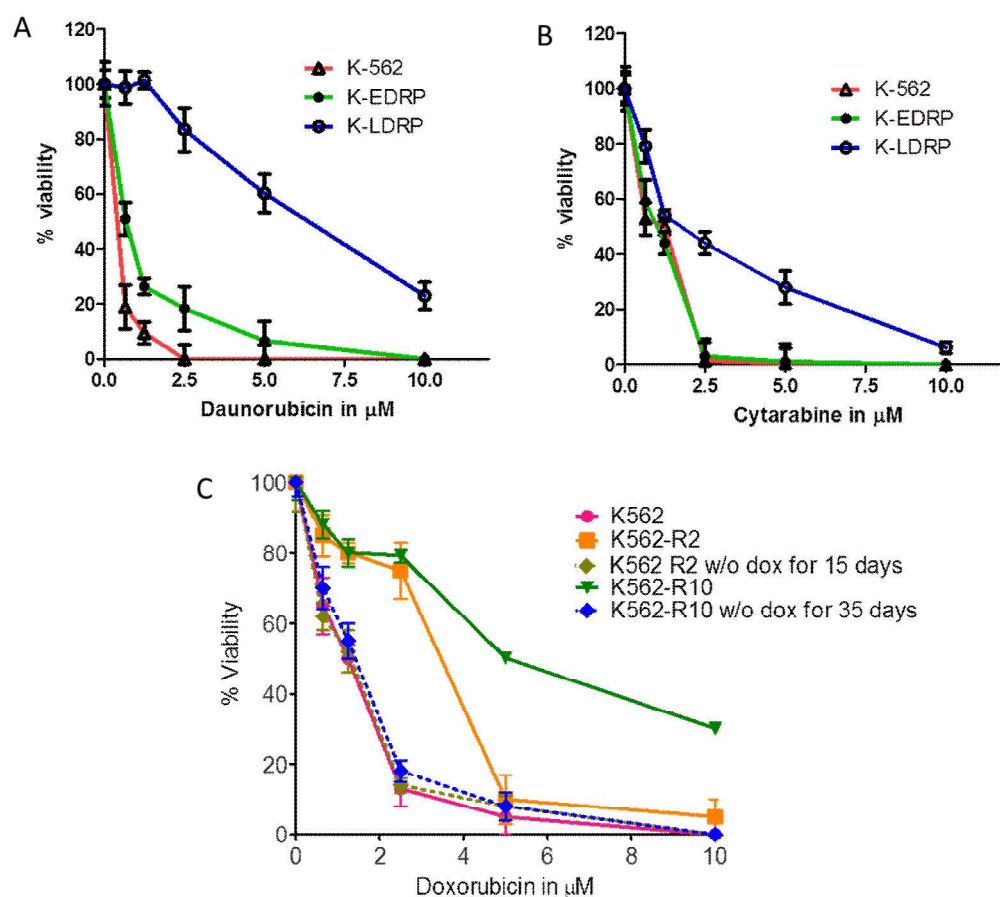


Figure 5: Cross resistance and resistance reversibility of EDRP and LDRP cells.

(A and B) The line graph shows MTT viability assay for K562, K-EDRP, and K-LDRP when treated with different concentrations of daunorubicin and cytarabine for 48h. *(C)* MTT assay of K-EDRP and K-LDRP cells when kept in doxorubicin free medium for 15 and 35 days. Results in line graph are the composite data from three independent experiments (mean \pm SEM)

Similarly, chemoresistance is shown to be reversible in HL-60/MX2 cells as well (ATCC CRL 2257). These data are suggestive of non-genetic (epigenetic) mechanisms of acquired chemoresistance, during both early and late stages of drug resistance.

3.1.2.2: Cell cycle profile of drug resistant cells: Cell cycle phases and DNA repair are interlinked and variation in cell cycle phases affect DNA repair pathways. Moreover, cell

Results

cycle arrest is an indicator of functional checkpoint system whereas recommencing a normal proliferation signals faithful DNA repair. As we are more focused to understand early stage resistance, we analyzed cell cycle profile of parent and EDRP with and without doxorubicin treatment. Post drug treatment, K562 and THP-1 parent and respective EDRP cells showed S and G2/M arrest at 24 and 48 h respectively. Although the parent populations remained arrested, EDRP cells could overcome S and G2/M cell cycle arrest (Figure 6A and B). Similarly, mitoxantrone treatment induced cell cycle arrest in HL-60 cells but not in HL-60/MX2 cells (Figure 6C). These data demonstrate that EDRP cells were able to resolve cell cycle arrest efficiently and did not elicit cell death.

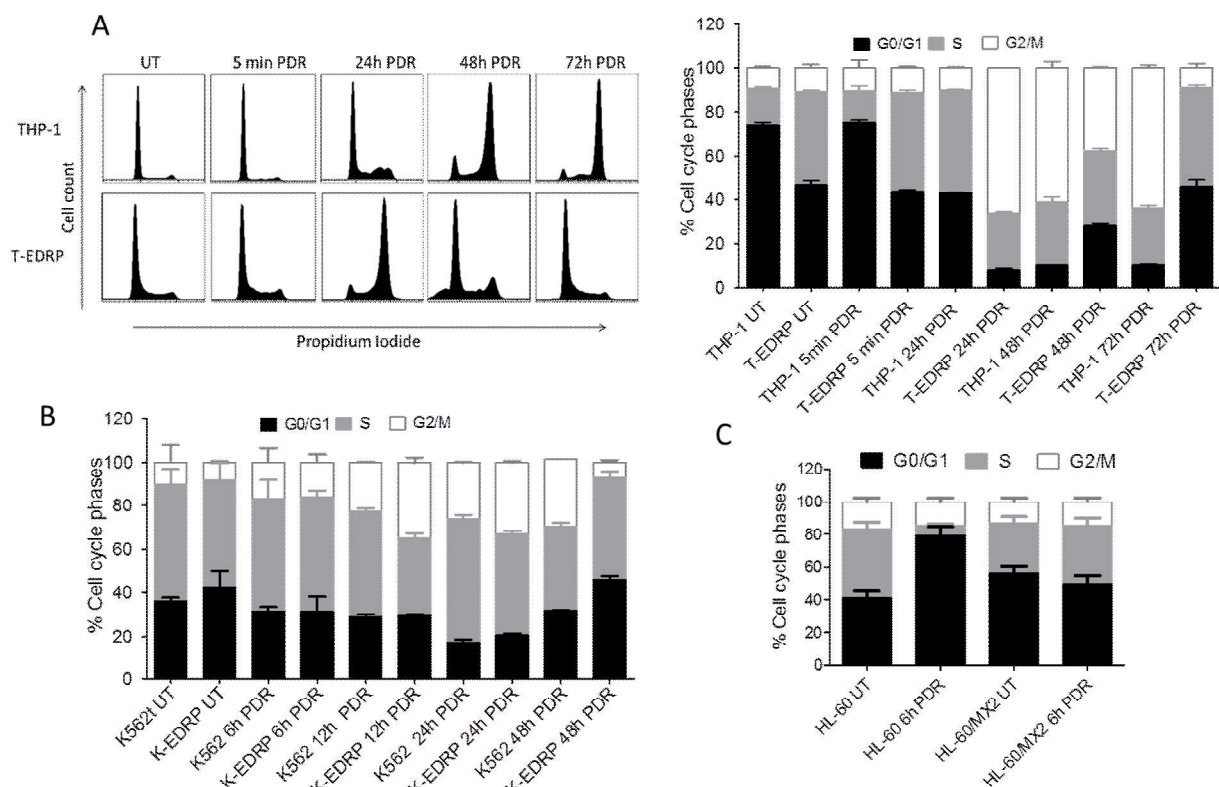


Figure 6: Cell cycle profile of EDRP of THP-1, K562, HL-60, and HL-60/MX2.

(A and B) Bar graph represents cell cycle profiles of THP-1, K562 and their EDRP cells at indicated time point pre and post doxorubicin treatment. (C) Cell cycle profile of HL-60 and HL-60/MX2 at indicated time points pre and post mitoxantrone (100nM) treatment.

3.2: Objective 2: Discerning the differences in DSB repair pathways between chemosensitive and chemoresistant population.

3.2.1 DNA damage and repair kinetics of HL-60/MX2 cells: To understand the role of DSB repair pathway proteins in the survival of drug resistant population we first performed DSB repair kinetics in HL-60/MX2 population (As these cells were readily available and establishment other resistance models was in progress). We used untreated and 2h mitoxantrone treated cells from HL-60 and HL-60/MX2. These cells were used for 1. DNA fragmentation assay and 2. Neutral comet assay. Experimental data from both the experiments indicate that mitoxantrone fails to induce significant levels of DNA damage in HL-60/MX2 cells, which is also supported by cell cycle profile of HL-60/MX2 cells (Figure 7A and B).

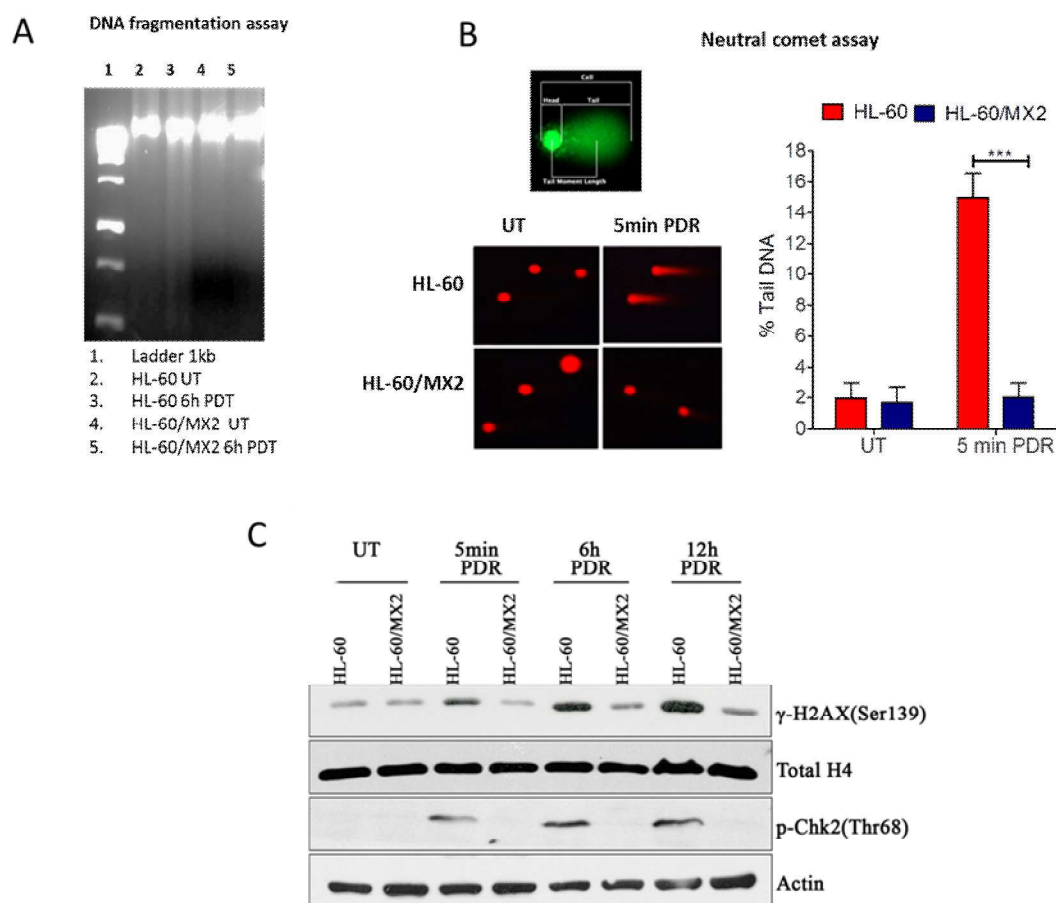


Figure 7: Levels of DNA double strand breaks in HL-60/MX2 cells post mitoxantrone (100nM for 2h) treatment.

Results

*(A) Depicts DNA fragmentation assay on HL-60 and HL-60/MX2 cells. DNA extracted from cells treated with 100nM of mitoxantrone for 6h and run on agarose gel. (B) Bar graph shows % tail DNA versus indicated time points of neutral comet assay for HL-60 and HL-60/MX2 post 2h mitoxantrone treatment (i.e. cells collected 5 min after drug removal post 2h drug treatment). (C) Western blots for p-Chk2, γ -H2AX in HL-60 and HL-60/MX2 cells at indicated time points post 100nM mitoxantrone treatment. Actin and total H4 were used as loading controls. Western blots represent results from at least 3 independent replicates. Results in each bar graph are the composite data from three independent experiments performed in triplicate (mean \pm SEM); * denotes $p \leq .05$, ** denotes $p \leq .01$, *** denotes $p \leq .001$ and **** denotes $p \leq .0001$.*

Phosphorylation of H2AX is the first cellular response to the induction of DSBs and the rate of appearance and resolution of γ -H2AX is considered to be a measure of DSB repair efficiency of a cell [24]. Therefore, we analyzed the activation of γ -H2AX at different time points following the drug treatment. To confirm these results, we performed western blot for γ -H2AX (Ser139) and p-Chk2 (Thr68). HL-60/MX2 cells did not show significant induction of γ -H2AX and p-Chk2 upon mitoxantrone treatment (Figure 7C). These data demonstrate that topoisomerase inhibitor was unable to induce DSBs in HL-60/MX2 cells. As HL-60/MX2 cells were made resistant to mitoxantrone over a period of 2 years we refer to them as Late Drug Resistant Cells (LDRP). The absence of DNA DSBs in HL-60/MX2 cells prompted us to refer through the literature for the cells which were made resistant to DNA damaging drugs for more than 6 months (As most of the drug resistant cells adapt to the drug for at least 6 months).

3.2.2 Absence of DNA damage in highly adapted populations: Various studies those tried to understand the mechanisms of drug resistance found that resistant cells do not show significant DNA damage post drug treatment. Song et al [124] used multidrug resistant

leukemia AML-2/WT cell-line to drugs like doxorubicin, daunorubicin, and Ara-C. DNA fragmentation assay performed post drug treatment shows minimal induction of DNA damage in drug resistant cells. Similarly, to obtain SN-38 (Irinotecan metabolite) resistant cells, HT-29 and HCT-116 cells were exposed to increasing concentrations of SN-38 over 6–9 months. A brief exposure of SN-38 at various doses induced significantly fewer DNA breaks were seen by alkaline comet assay [125]. Wang et al [126] used seven (Bleomycin) BLM-resistant cell lines (ACHN, HOP-62, SF-295, NT/D1, NCCIT, NCI-H322M and MDA-MB-231), established by exposure to escalating BLM concentrations over a period of 16-24 months. Neutral comet assay shows all the BLM resistant cell lines incur significantly less DNA damage than parental cells. Similarly, a panel of NSCLC cell lines (A549, SKMES-1, MOR, H460) were made resistant to cisplatin over a period of twelve months. γ -H2AX staining of these resistant cells shows significantly less DSB induction post cisplatin treatment.[127]. Thus experimental evidence from our work as well as from literature suggest that the late stage drug resistant populations do not incur significant levels of DNA damage and hence are not the appropriate model to evaluate the role of DNA repair mechanisms in chemoresistance. Getting rid of these cells using DNA repair inhibitors doesn't make sense as DNA damage repair response itself is not much activated. However, upregulation of drug transporters and drug efflux was commonly observed in most of the drug resistant models.

3.2.3: Faster DNA repair kinetics in early stage drug resistant population: To understand whether DNA repair mechanisms are requisite during early stage drug resistance, we used EDRP and LDRP derived from K562 and THP-1 cells. To investigate the alteration in DNA repair, we first tested for double strand breaks (DSBs) induced by doxorubicin at different time points (5min, 6h, and 12h) post drug removal (PDR) using neutral comet assay (Figure 8A). As expected, LDRP (for highly adapted cells) showed minimal induction of DSBs while EDRP populations from both the cell lines (K562 and THP-1) showed DSBs similar to the

Results

parent population. However, by 12h EDRP could resolve most of DSBs compared to parent cells suggesting faster DNA repair (Figure 8 B and C).

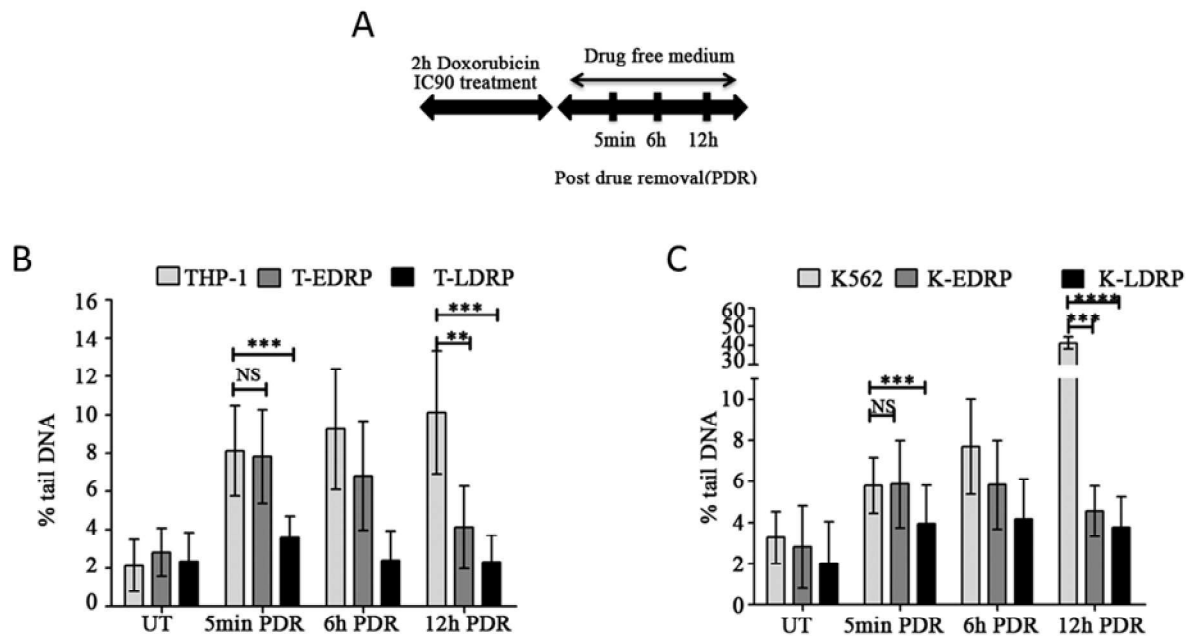


Figure 8: Neutral comet assay in THP-1 and K562 EDRP and LDRP cells.

(A) Schema showing the timeline of doxorubicin treatment and time points of samples collection (B and C) Bar graph shows % tail DNA versus indicated time points of neutral comet assay for K562, THP-1 and their resistant populations. Results in each bar graph are the composite data from three independent experiments performed in triplicate (mean \pm SEM); * denotes $p \leq .05$, ** denotes $p \leq .01$, *** denotes $p \leq .001$ and **** denotes $p \leq .0001$.

Next we analyzed the activation of γ -H2AX at different time points following the drug treatment. We found that immediately after drug removal compared to THP-1 parent cells, T-EDRP cells showed increased H2AX phosphorylation which was mostly resolved by 12h PDR confirming faster DNA repair in EDRP cells (Figure 9A). Concordant with comet assay, T-LDRP cells showed significantly less induction of γ -H2AX indicating the inability of doxorubicin to induce DNA DSBs in these cells (Figure 9B). Similar results were obtained

Results

using K562, K-EDRP and K-LDRP cells (Figure 9C and D). Further higher recruitment of γ -H2AX in K-EDRP cells was confirmed using immunofluorescence assay (Figure 9E)

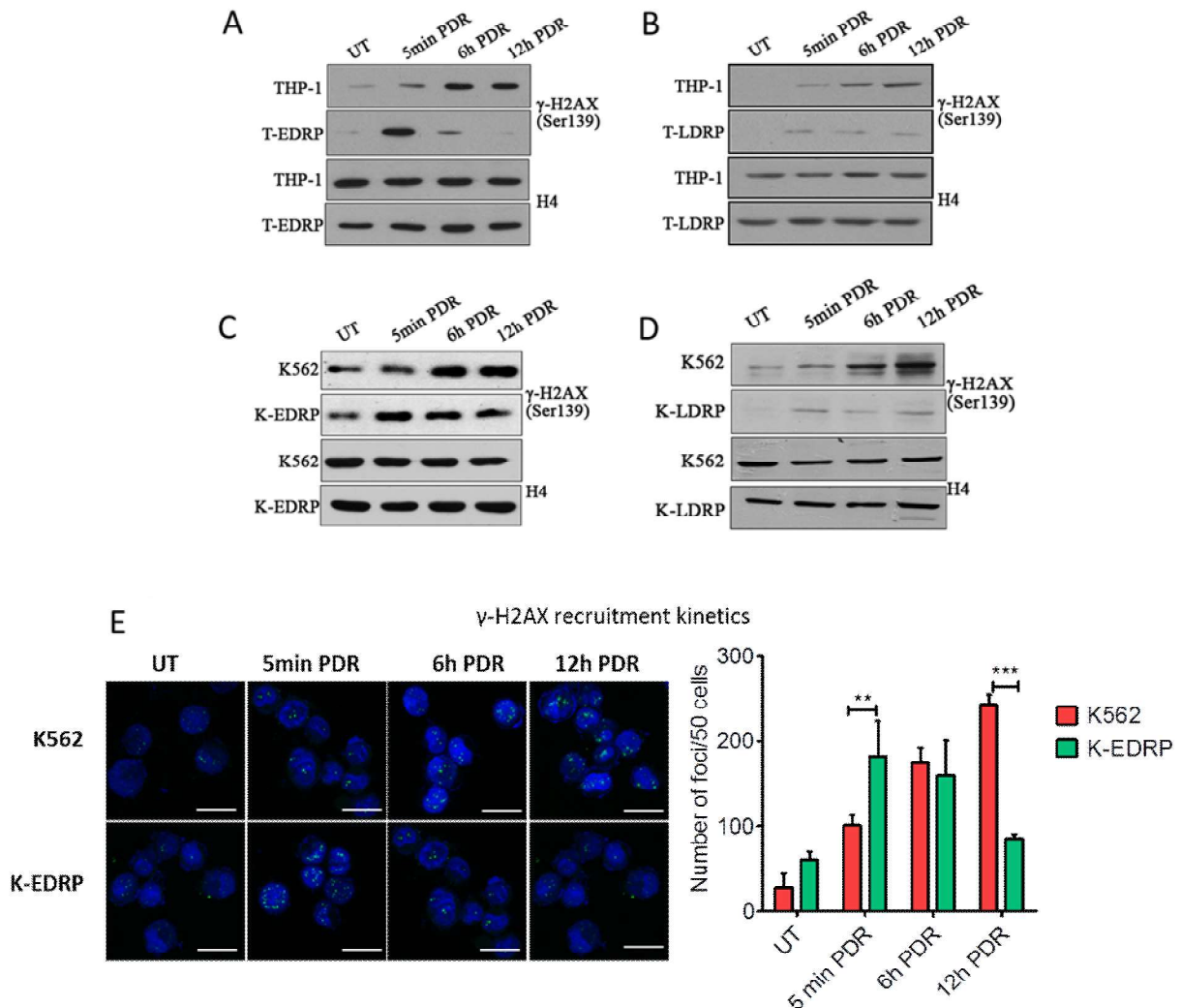


Figure 9: γ -H2AX staining in EDRP and LDRP of K62 and THP-1 cells.

(A and B) Western blot of γ -H2AX in THP-1, T-EDRP and T-LDRP cells at indicated time points post 2h of 1.4 μ M doxorubicin treatment. (C and D) Western blot of γ -H2AX in K562, K-EDRP and K-LDRP cells at indicated time points post 2h of 2.5 μ M doxorubicin treatment. (E) Immunofluorescence staining of γ -H2AX in K562 and K-EDRP cells. Western blots represent results from at least 2 independent replicates. Results are the composite data from three independent experiments (mean \pm SEM); * denotes $p \leq .05$, ** denotes $p \leq .01$, ***denotes $p \leq .001$ and **** denotes $p \leq .0001$. Scale bar 20 μ m.

Further, localization of γ -H2AX (Foci formation) at DSBs was confirmed to be higher in K-EDRP cells than K562 cells by immunofluorescence. Therefore, we found that EDRP cells incur similar levels of DNA DSBs similar to parent cells, however, EDRP repairs their DSBs faster than the parent cells suggesting the importance of DSB repair mechanisms in EDRP cells. Moreover, as EDRP are the earliest cells to exhibit drug resistance, understanding the cause of their resistance offers a much essential strategy to eradicate the very establishment of acquired drug resistance.

3.2.4: EDRP harbors hyperactive ATM kinase signaling and favors HR repair: To investigate whether increased γ -H2AX in EDRP cells could be attributed to ATM activation since ATM (ataxia telangiectasia mutated) is a sensor kinase that phosphorylates H2AX following DNA DSBs [13], levels of p-ATM were analyzed at different time points post doxorubicin treatment using both western blot and immunofluorescence assay. Concordant with γ -H2AX activation kinetics, immunofluorescence and western blot analysis of p-ATM showed more than 2 fold increase in ATM activation in K-EDRP compared to the parent K562 cells (Figure 10A and B). Furthermore, downstream targets of ATM, like p-NBS1 (Ser343), p-BRCA1 (Ser1524) and p-Chk2 (Thr68), also showed higher activation in EDRP cells compared to the K562 cells (Figure 10C). Similar results were obtained for parent THP-1 and T-EDRP (Figure 10D). Additionally, Mcl-1L, an anti-apoptotic protein, whose expression is controlled by ATM [25] showed upregulation in K-EDRP cells (Figure 10E). This confirms hyperactive ATM signaling in EDRP cells. We then wanted to assess the choice of repair pathway (HR or NHEJ) and its efficiency in EDRP cells. For this, we used HR and NHEJ vector activity assay [5].

Results

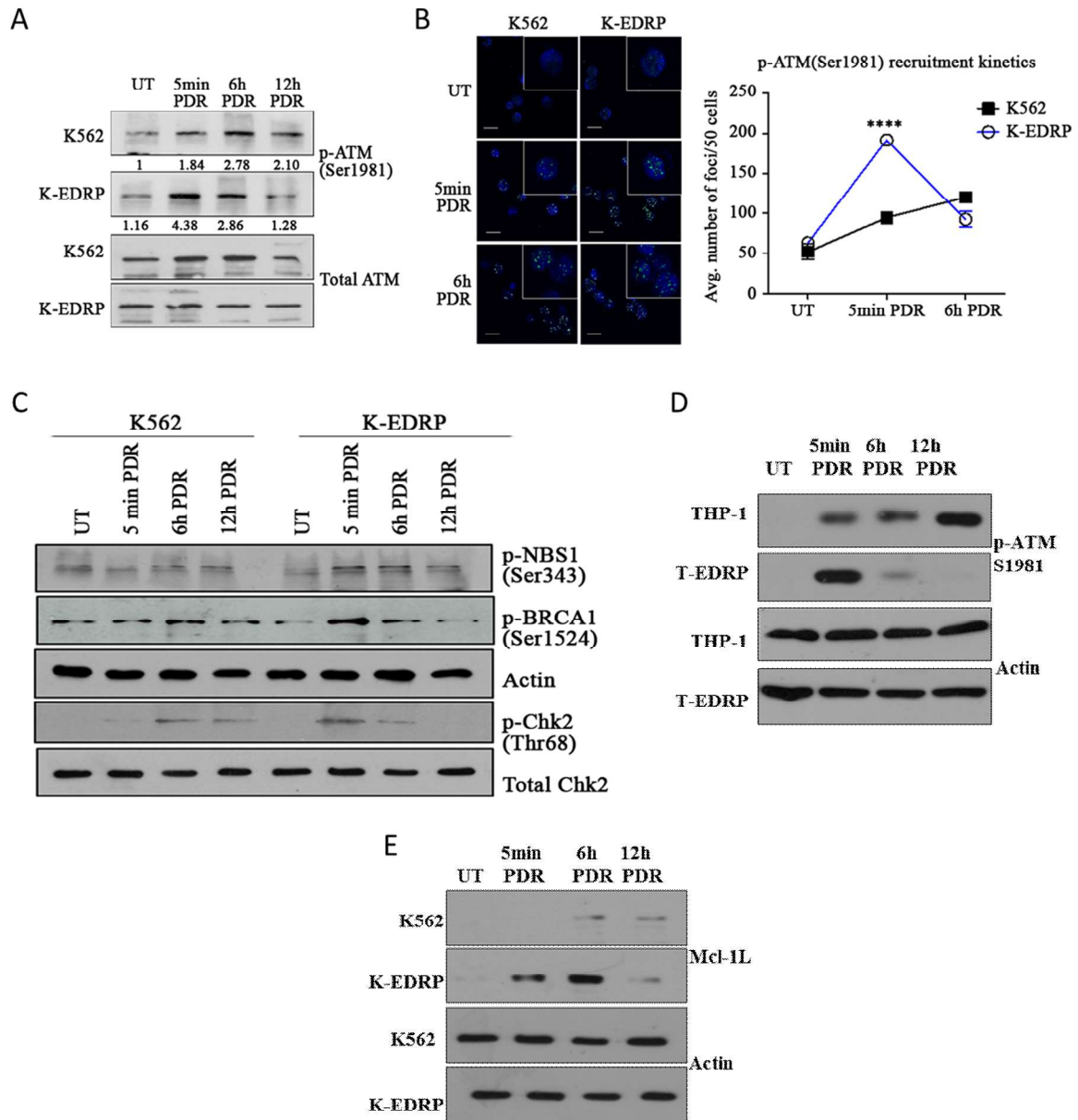


Figure 10: Hyperactive ATM kinase signaling in EDRP cells.

(A) Western blot for p-ATM and total ATM in K562 and K-EDRP cells post 2h of doxorubicin treatment. (B) Representative images of p-ATM foci and nuclei counterstained with DAPI in K562 and K-EDRP cells. The graph represents an average number of p-ATM foci counted per 50 cells from each population (Scale bar=20 μ m). (C) Western blot showing protein expression of p-NBS1, p-BRCA1, p-Chk2 and total Chk2 after 2h of doxorubicin treatment at indicated time points post drug removal. Beta actin is used as a loading control. (D) Western blot for MCL-1L expression in K562 and K-EDRP cells. (E) Western blot for p-ATM and

Results

actin in THP-1 and T-EDRP cells. **(E)** Protein expression of Mcl-1L in K562 and K-EDRP. Western blots represent results from at least 2 independent replicates. Results are the composite data from three independent experiments (mean \pm SEM); * denotes $p \leq .05$, ** denotes $p \leq .01$, ***denotes $p \leq .001$ and **** denotes $p \leq .0001$.

Flow cytometric quantitation of GFP and Td-red quantitation of K562 and K-EDRP cells showed significantly higher HR activity in K-EDRP cells compared to K562 cells (Figure 11A) (For calculations see material and methods). Further, we also found higher recruitment of Rad51, an HR specific protein in K-EDRP compared to the parent K562 (Figure 11B), these data are also in agreement with previous reports, where ATM is shown to prefer resolution of DNA DSBs via HR pathway [26].

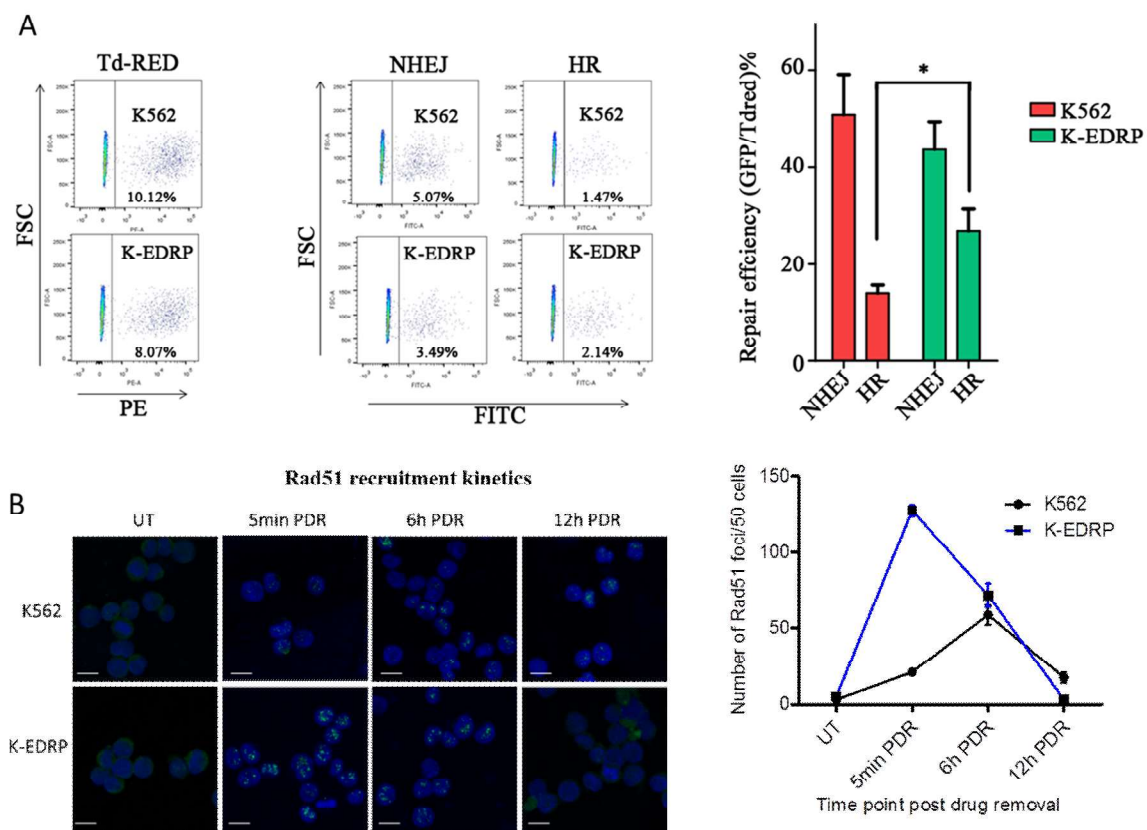


Figure 11: EDRP cells follows HR directed DSB repair.

(A) HR and NHEJ vector reactivation assay performed in K562 and K-EDRP cells. Flow cytometry was done 72h post transfection. Bar graph represents repair efficiency in the

population as indicated. **(B)** *Rad51* is stained in green while nuclei are counterstained with DAPI (blue) in K562 and K-EDRP cells pre and post doxorubicin treatment. (Scale bar 20 μ m). Results in bar and line graph are the composite data from two independent experiments (mean \pm SEM).

3.2.5: ATM kinase inhibition efficiently eliminates EDRP cells, however, fails to

sensitize LDRP cells: The data presented above demonstrates hyperactivation of ATM during the onset of acquired resistance. Accordingly, inhibition of ATM should induce death in residual cells and prevent the emergence of chemoresistance. To test this, parent cells, EDRP and LDRP of K562 and THP-1 were treated with 10 μ M of ATM kinase inhibitor (KU55933) [27] in combination with different concentrations of doxorubicin (0 to 10 μ M) (Figure 12 A). ATM kinase inhibitor induced complete cell death in K-EDRP at 2.5 μ M doxorubicin concentration but only 40% cell death in K-LDRP cells. Importantly, the ATM kinase inhibitor reduced the IC₉₀ concentration of doxorubicin for K-EDRP from 6.93 μ M to 1.39 μ M. Similar results were obtained with THP-1 EDRP and LDRP (Figure 12B). Hence ATM kinase inhibitor is selectively sensitive until the early stages of resistance and moreover, it significantly reduced the drug dose compared to doxorubicin alone.

Specificity of ATM kinase inhibitor was confirmed by quantification of p-ATM and p-Chk2 in K562 and K-EDRP cells following treatment with ATM inhibitor and doxorubicin (Figure 12C). ATM kinase inhibitor in combination with mitoxantrone did not show significant cell death in HL-60/MX2 cells (Figure 12D), this was expected as mitoxantrone fails to induce DSB in these cells.

3.2.6: Plausible reasons for failure of ATM kinase inhibitor in late stage drug resistant

cells: The differential response of EDRP and LDRP cells to ATM kinase inhibitor is

Results

attributed to the fact that, only EDRP but not LDRP cells show the activation of ATM with doxorubicin treatment as LDRP cells showed minimum DNA damage to the drug treatment. Ineffective ATM kinase inhibition facilitated sensitization in LDRP cells can be attributed to the minimal level of DSB induced post-treatment with DNA damaging drugs. However, to confirm this speculation we checked for p-ATM levels in LDRP cells post drug treatment.

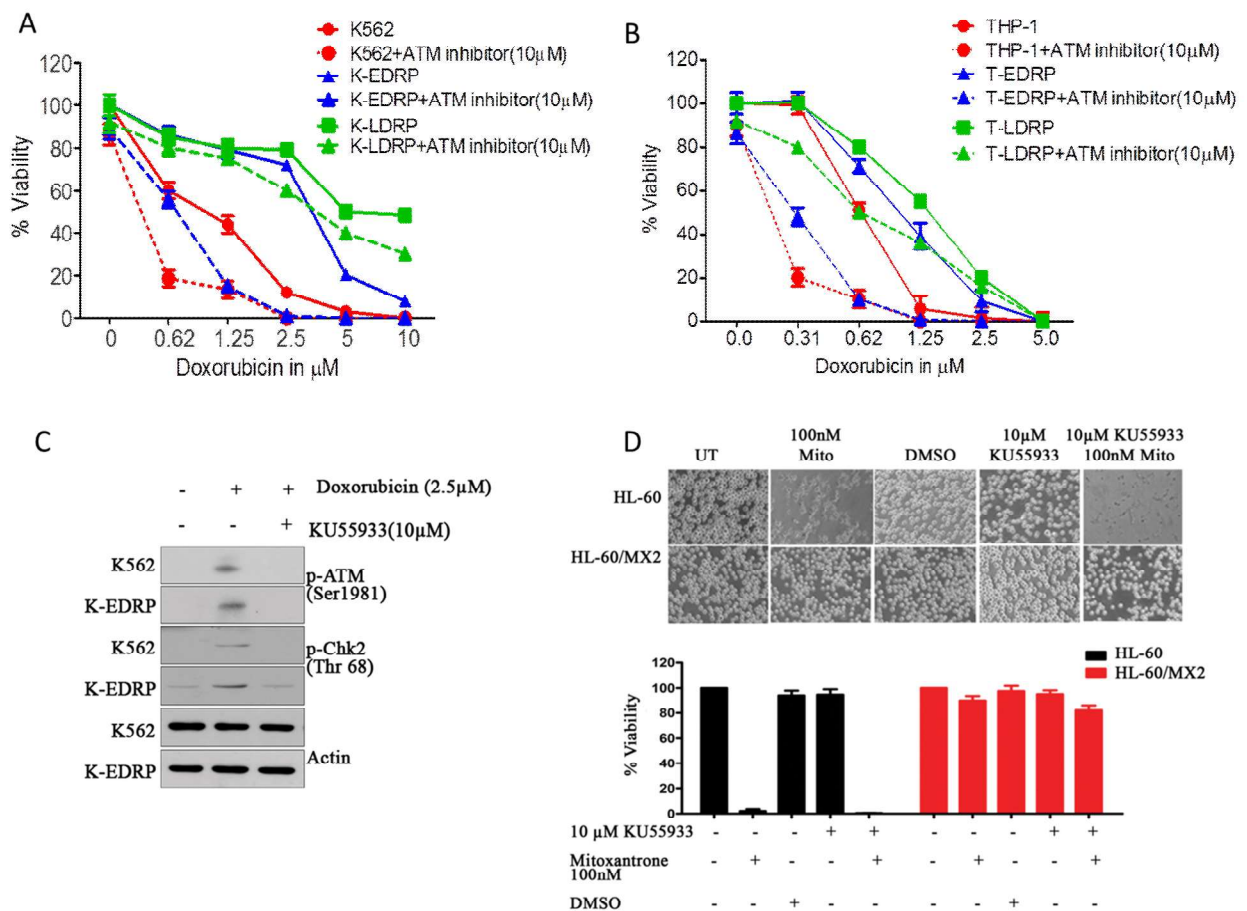


Figure 12: Differential response of early and late stage drug resistant populations to ATM kinase inhibition with DNA damaging drugs.

(A and B) Line plot of cell viability as determined by MTT assay of parent K562, THP-1 and respective EDRP and LDRP cells with 10 μ M of ATM kinase inhibitor and different concentrations of doxorubicin. (C) Western blot of p-ATM and p-Chk2 showing specificity of ATM kinase inhibitor in K562 and K-EDRP cells. Actin was used as loading control. (D)

Results

MTT assay for HL-60 and HL-60/MX2 cells after treatment with ATM kinase inhibitor (10 μ M) and mitoxantrone (100nM). DMSO was used as vehicle control. Results are the composite data from three independent experiments.

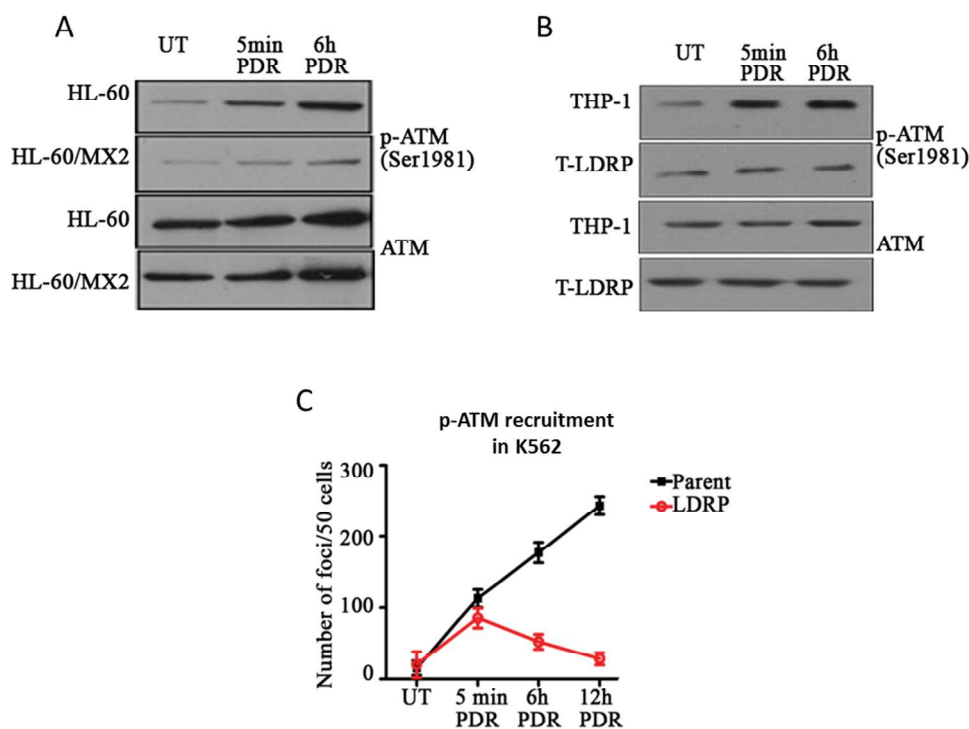


Figure 13: ATM activation kinetics in LDRP cells post drug treatment.

(A) Western blot showing p-ATM and total ATM after mitoxantrone treatment at indicated time points post drug removal in HL-60 and HL-60/MX2. (B) Western blot showing p-ATM and total ATM after doxorubicin treatment at indicated time points post drug removal in THP-1 and T-LDRP. (C) Immunofluorescence staining of p-ATM in K562 and K-EDRP cells.

Western blot (Figure 13A and B) and immunofluorescence (Figure 13C) data from HL-60/MX2, T-LDRP, and K-LDRP clearly show, the absence of ATM activation due to lack of DSBs thus explains the failure of ATM inhibitor to induce apoptosis in late stage drug resistant cells.

3.2.7: LDRP display multifactorial drug resistance: In order to understand how LDRP cells escape DNA damage, we reasoned that this could be because of loss of molecular target or overexpression of drug efflux proteins. Therefore, we checked the expression of *TOP2 β* (molecular target of doxorubicin and mitoxantrone) and drug efflux pump protein *ABCB1* (*MDR1*) in all the three population of cells parent, EDRP and LDRP (Figure 14A). No significant differences were seen in the transcripts of *TOP2 β* in parent and EDRP. However, *TOP2 β* was found to be significantly downregulated in LDRP of both K562 and THP-1 cell line. Similarly, HL-60/MX-2 cells also showed downregulation of *TOP2 β* .

We further examined the drug accumulation capacity of the parent, EDRP, and LDRP of K562 and THP-1 cells (Figure 14B and C). For which cells were treated with IC90 concentrations of doxorubicin and intracellular doxorubicin was measured using flow cytometry at 480nm (excitation wavelength) and 570nm (emission wavelength) [28]. Intracellular drug concentrations were found to be comparable in parent and EDRP but reduced in LDRP cells indicating either reduced uptake or faster efflux of the drug by LDRP.

Results

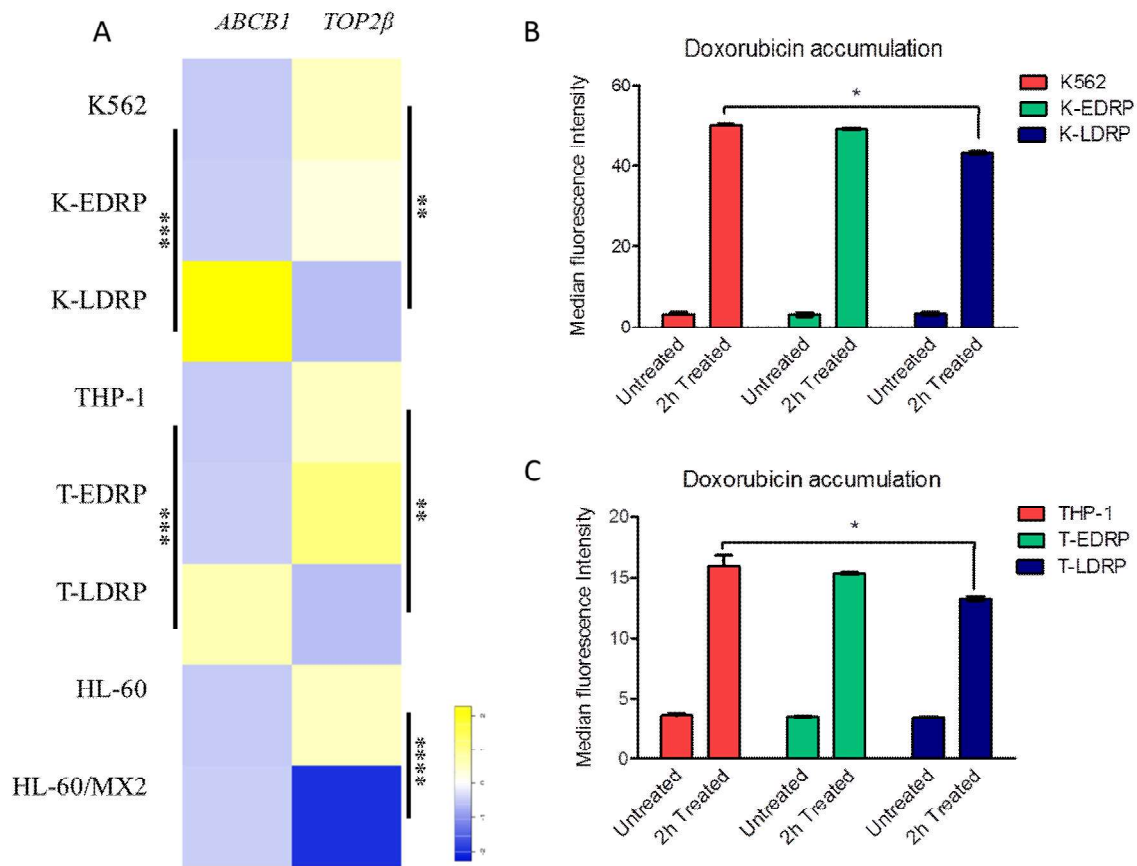


Figure 14: Expression of ABCB1, TOP2β and drug accumulation in early and late stage drug resistant populations.

(A) Heat map represents the mRNA expression of *ABCB1* and *TOP2β* in parent all the drug resistant populations, relative to *GAPDH* mRNA, as measured by SYBR green based real time PCR. (B and C) Doxorubicin accumulation measured by flow cytometry in K562, THP-1 and respective EDRP and LDRP populations. The graph is plotted as median fluorescence intensity v/s different cell lines and conditions as indicated. Results are the composite data from three independent experiments (mean \pm SEM); * denotes $p \leq .05$, ** denotes $p \leq .01$ and ***denotes $p \leq .001$.

We found no significant difference in the transcript levels of *ABCB1* (i.e. *MDR1*) in parent and EDRP but were markedly elevated in LDRP suggesting that reduced drug accumulation in LDRP cells could be due to faster efflux of the drug.

Results

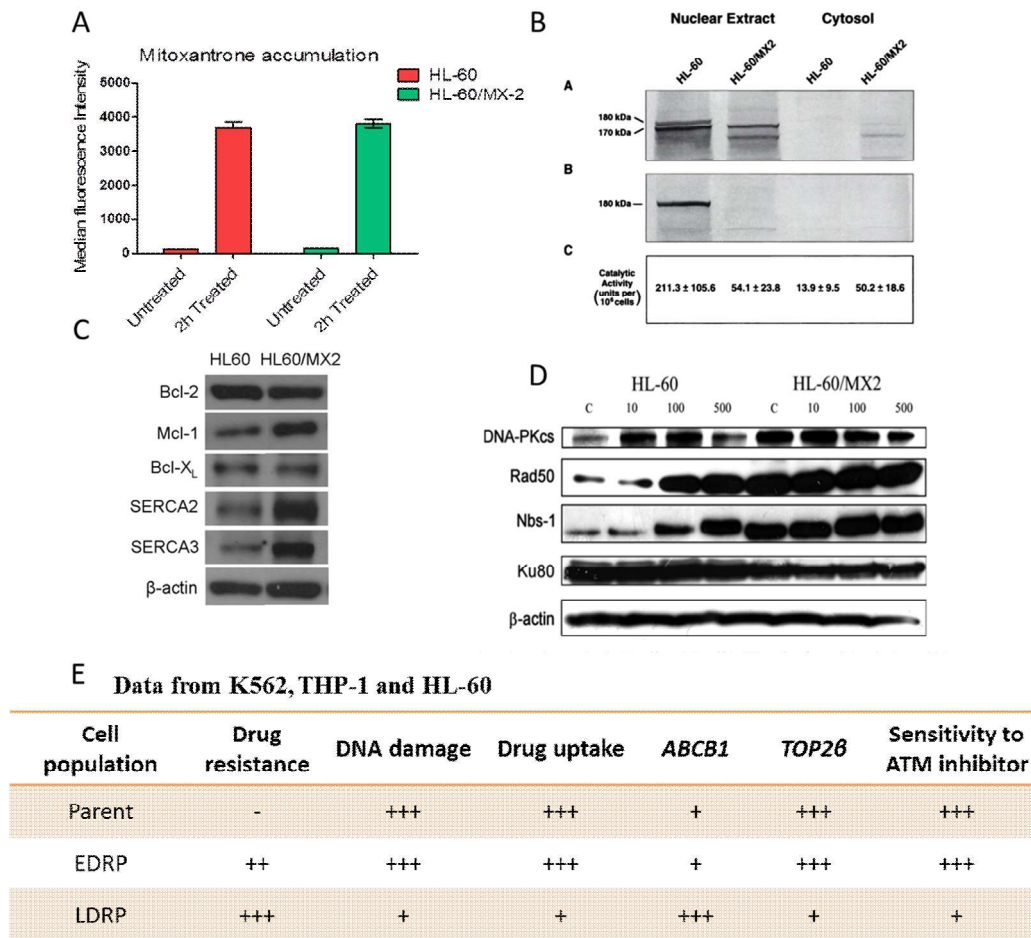


Figure 15: LDRP represents multifactorial drug resistance.

(A) Mitoxantrone accumulation measured by flow cytometry in HL-60 and HL-60/MX2 cells. (B) Literature Data-Expression of an alternative splice variant of TOP2 in HL-60/MX2 cells. (C) Literature data- Expression of different anti-apoptotic proteins by HL-60 and HL-60/MX2 cells. (D) Literature data- Western blot for of DNA repair proteins in HL-60 and HL-60/MX2 cells. (E) Tabular compilation of data from K562, THP-1, and HL-60 drug resistant cells.

Furthermore, we did not observe any downregulation of *ABCB1* transcripts in HL-60/MX2 cells which corroborates with equal mitoxantrone uptake in both HL-60 and HL-60/MX2 cells (Figure 15 A). However, independent reports from HL-60/MX2 cells describe the presence of alternating surviving mechanisms, such as occurrence of an alternate isoform of

TOP2 β [9] (Figure 15B). HL-60/MX2 cells have also been shown to overexpress multiple DNA repair (Figure 15D) [128] and anti-apoptotic proteins (Figure 15C) [129] which help them escape DNA damage induced cell death.

Collectively, data from these experiments prove

1. Evolution of chemoresistance is divided into early and late phase.
2. Only LDRP (not EDRP) cells display cross-resistance to other drugs.
3. Both early and late drug resistant cells show a reversible phenotype in absence of drug.
4. Late drug resistant cells exhibit minimum levels of DSBs induction post drug treatment.
5. Early drug resistant cells show equal induction of DSBs compared to parent cells, however, they resolve their DSBs with faster repair kinetics.
6. EDRP cells hyperactivate ATM signaling following DNA damage and favor homologous Recombination pathway for resolving the damage.
7. ATM kinase inhibitor works efficiently till early phases of drug resistance and fails to eradicate late resistant cells.
8. As cells become more drug resistance they incur lesser DSB with DNA damaging agent which is accompanied by decreased drug uptake, *TOP2 β* and increase expression of *ABCB1* (Figure 15E).
9. The resistance of LDRP is Multifactorial.

However, given the central role of ATM activation in mediating chemoresistance in EDRP, we deemed it important to further understand the mechanism of higher ATM activation in EDRP cells.

3.3: Mechanisms of ATM activation in EDRP cells: Although ATM can be autophosphorylated and activate itself, there are multiple factors which influence ATM activation. ATM activation is known to be largely controlled by the Mre11-Rad50-NBS1 (MRN) sensor complex [17].

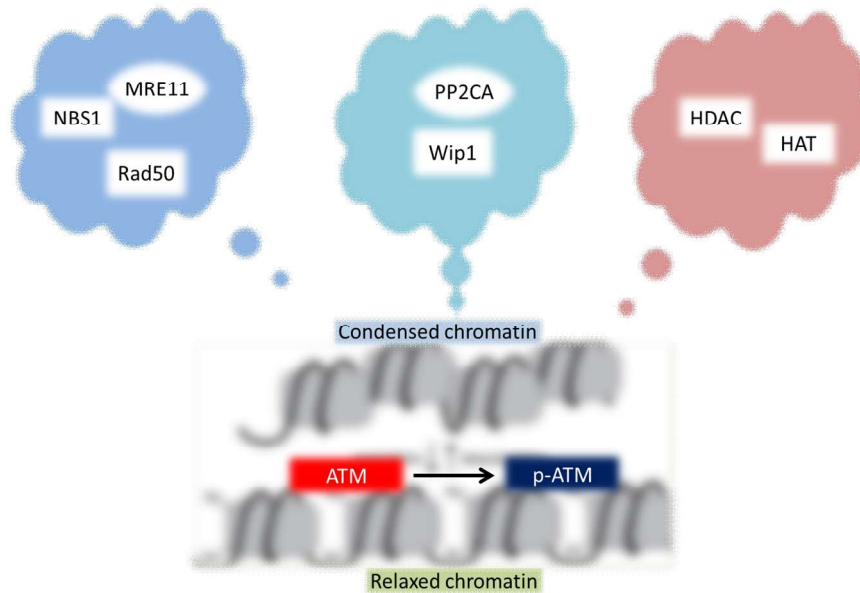


Illustration 14: Mechanisms of ATM activation.

However, we did not find either differential expression or recruitment of Mre11 between parent K562 and K-EDRP, ruling out the possibility of MRN complex mediating differential recruitment of ATM at DSBs in EDRP (Figure 16A and B).

We then reasoned that downregulation of ATM phosphatases (*WIP1* and *PP2CA*) could also maintain high levels of p-ATM [13]. However, we observed no differences at the transcript levels of *WIP1* and *PP2CA* in EDRP cells with respect to parent population (Figure 16C).

3.3.1: EDRP show enrichment of euchromatin rich cells: It is also known that chromatin relaxation triggers higher ATM activation [13]. We, therefore, did immunofluorescence staining for HP1 alpha (heterochromatin-associated protein), indeed we found a significant reduction in the levels of HP1 alpha in K-EDRP compared to the K562 population (Figure

16D). Additionally, transmission electron microscopy of the K562 and K-EDRP also confirmed euchromatinization of K-EDRP cells compared to parent population (Figure 16E).

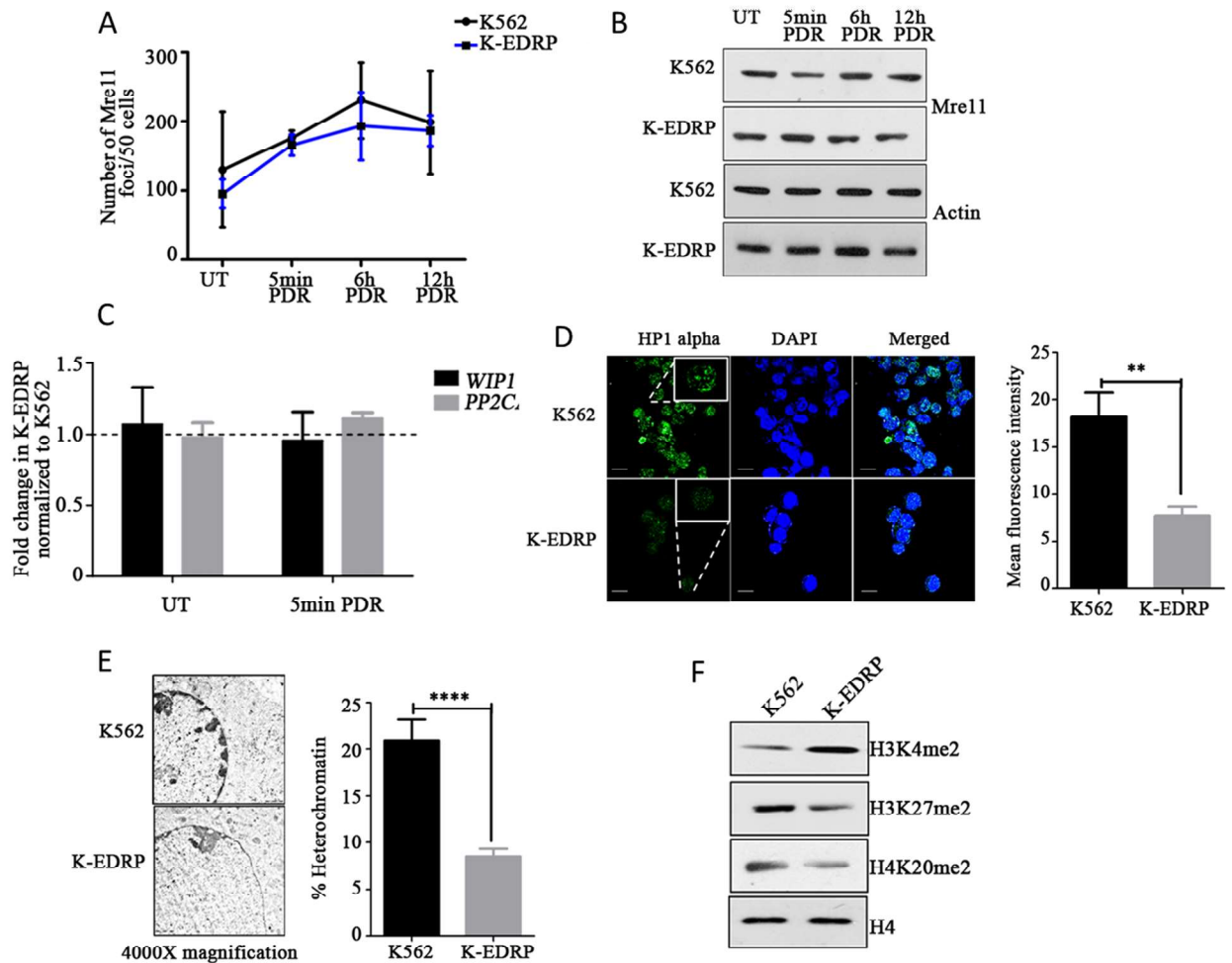


Figure 16: EDRP cells harbors euchromatin rich cells.

(A) Mre11 recruitment kinetics in K562 and K-EDRP cells following 2h of doxorubicin treatment. (B) Western blot for Mre11 with actin as a loading control for parent and EDRP cells at indicated time points post drug removal. (C) SYBR green based real time PCR for WIP1 and PP2CA in parent and EDRP cells before and after 2h of doxorubicin treatment. (D) Immunofluorescence of HP1 alpha in parent and EDRP cells. Nuclei were counter stained with DAPI. Scale bar 20μm. Bar graph shows mean fluorescence intensity of HP-1 alpha staining in K562 and K-EDRP cells as calculated by ImageJ software. (E) Transmission electron micrograph of K562 and K-EDRP cells showing euchromatin and

heterochromatin (dark staining). Bar graph quantifies % heterochromatin from EM images.

(F). Western blot for histone modifications ($H3K27me_2$, $H3K4me_2$ and $H4K20me_2$) in untreated K562 and K-EDRP cells. Total H4 was used as loading control.

Open chromatin in K-EDRP was further confirmed by the presence of increased levels of $H3K4me_2$ and downregulation of $H4K20me_2$ and $H3K27me_2$ (Figure 16F).

3.3.2: GCN5 is upregulated in all the drug resistant populations: HATs (Histone Acetyl Transferases) and HDACs (Histone deacetylases) are important in defining chromatin architecture and DNA repair response [29], also higher expression of *TIP60* and *HMOF* are known to activate ATM. Therefore, to define which HAT/HDAC could be responsible for euchromatization in EDRP cells, we analyzed the transcript levels of *P300*, *GCN5*, *TIP60*, *HMOF*, *HDAC* and *HDAC2* that are well reported to play role in DNA repair and chromatin maintenance[21].

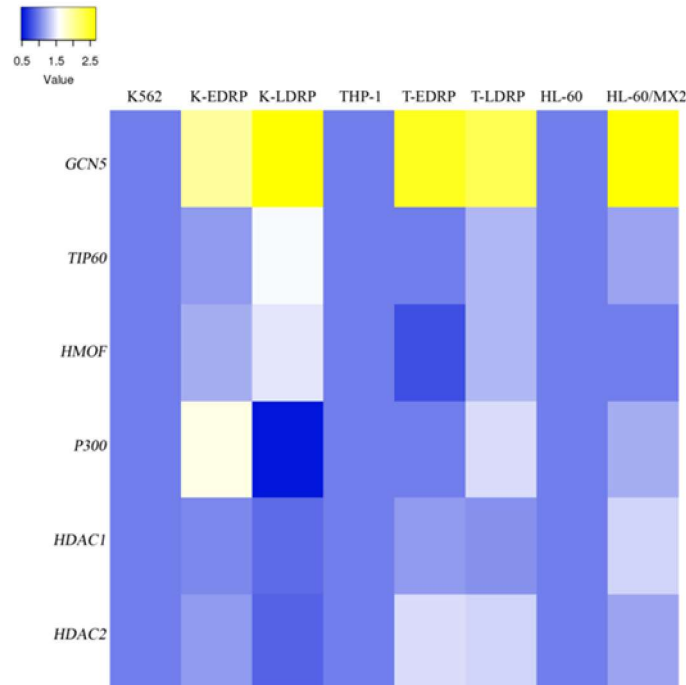


Figure 17: GCN5 is overexpressed by all the drug resistant populations

Expression of HATs and HDAC (GCN5, TIP60, HMOF, P300, HDAC1 and HDAC2)

transcripts in different drug resistant cell lines (K562, THP-1 and HL-60). Heat map represents fold change values from SYBR green quantitative PCR reaction.

We found overexpression of *GCN5* in all the different populations of chemoresistant cell lines (K562, THP-1, and HL-60) (Figure 17).

3.3.3: *GCN5* or *KAT2A* (Lysine Acetyltransferase 2A): *GCN5* is a lysine acetyltransferase involved in post-translational modification of multiple histone and non-histone proteins. *GCN5* acts as a transcription activator and is a part of human ATAC and STAGA complex [33]. *GCN5* is a 94 kDa protein nuclear HAT or A-type HAT composed of 837 amino acids.

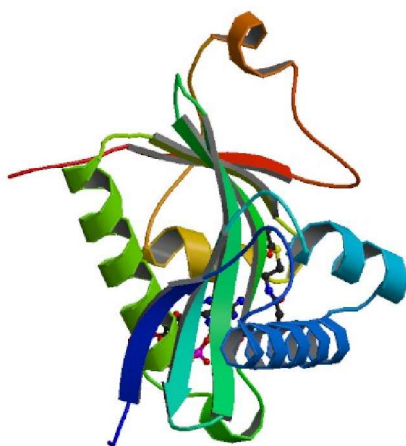


Illustration 15: X-ray crystallographic structure of *GCN5* bound to acetyl coenzyme A (AcCoA)

GCN5 catalyzes the transfer of an acetyl group from AcCoA onto the ϵ -amino group of specific lysine residues of both Histone and non-histone proteins. *GCN5* knockout mice are early embryonic lethal [130]. *GCN5* acetylates and regulates the stability of the oncoprotein *E2A-PBX1* in acute lymphoblastic leukemia [37]. *GCN5* serves as an essential gene for the survival of AML cells [131]. *GCN5* was of key interest as previously, *GCN5* has been shown to interact with DNA repair proteins like DNA-PK, Ku70/80, H2AX [34] and also have been reported to be involved nucleotide excision repair [35].

Results

Gene expression data analysis using firebrowse reveals overexpression of *GCN5* (i.e. *KAT2A*) in most of the available cancer datasets. *GCN5* has already been shown to be essential for the survival of different cancer types. *GCN5* is an exciting target for future therapeutic exploration as; it is a pharmacologically targetable enzyme that is overexpressed in various cancer types (Illustration 16).

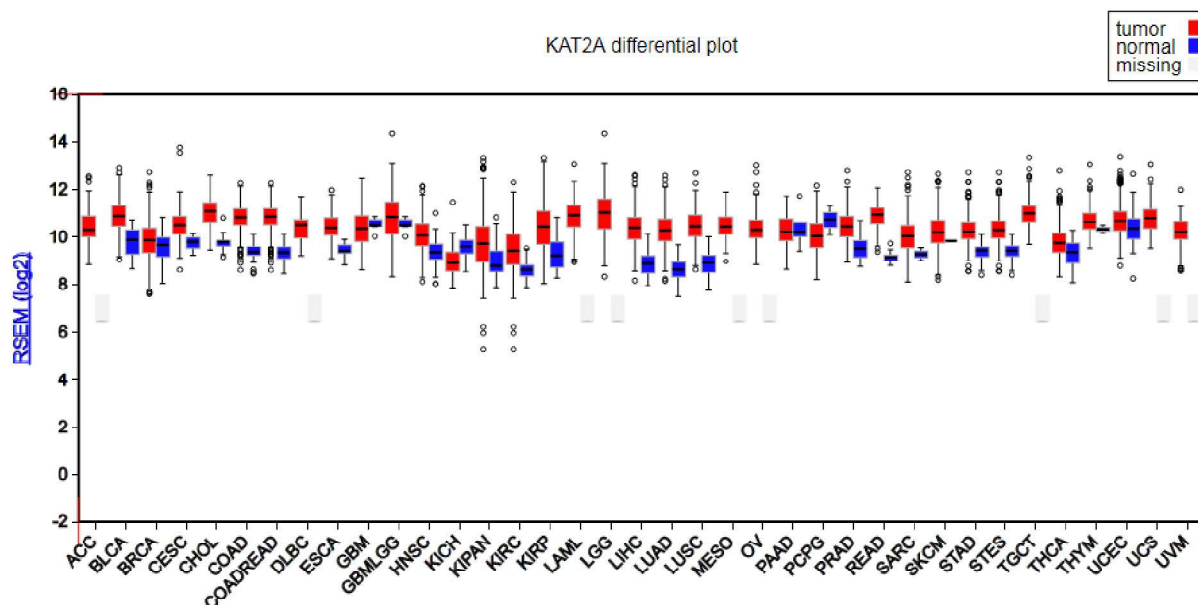


Illustration 16: Expression of KAT2A in various cancer types: Data Source: ©2015 Broad Institute of MIT & Harvard. (<http://firebrowse.org>)

3.3.4: Role of GCN5 in Drug resistance and DNA repair: So to understand the role of *GCN5* in drug resistance and survival we inhibited *GCN5* using a small molecule inhibitor named Butyrolactone 3. We treated EDRP of K562 and THP-1 with different concentrations of *GCN5* inhibitor (Butyrolactone 3 or BL-3) alone and in combination with doxorubicin (Figure 18A and B).

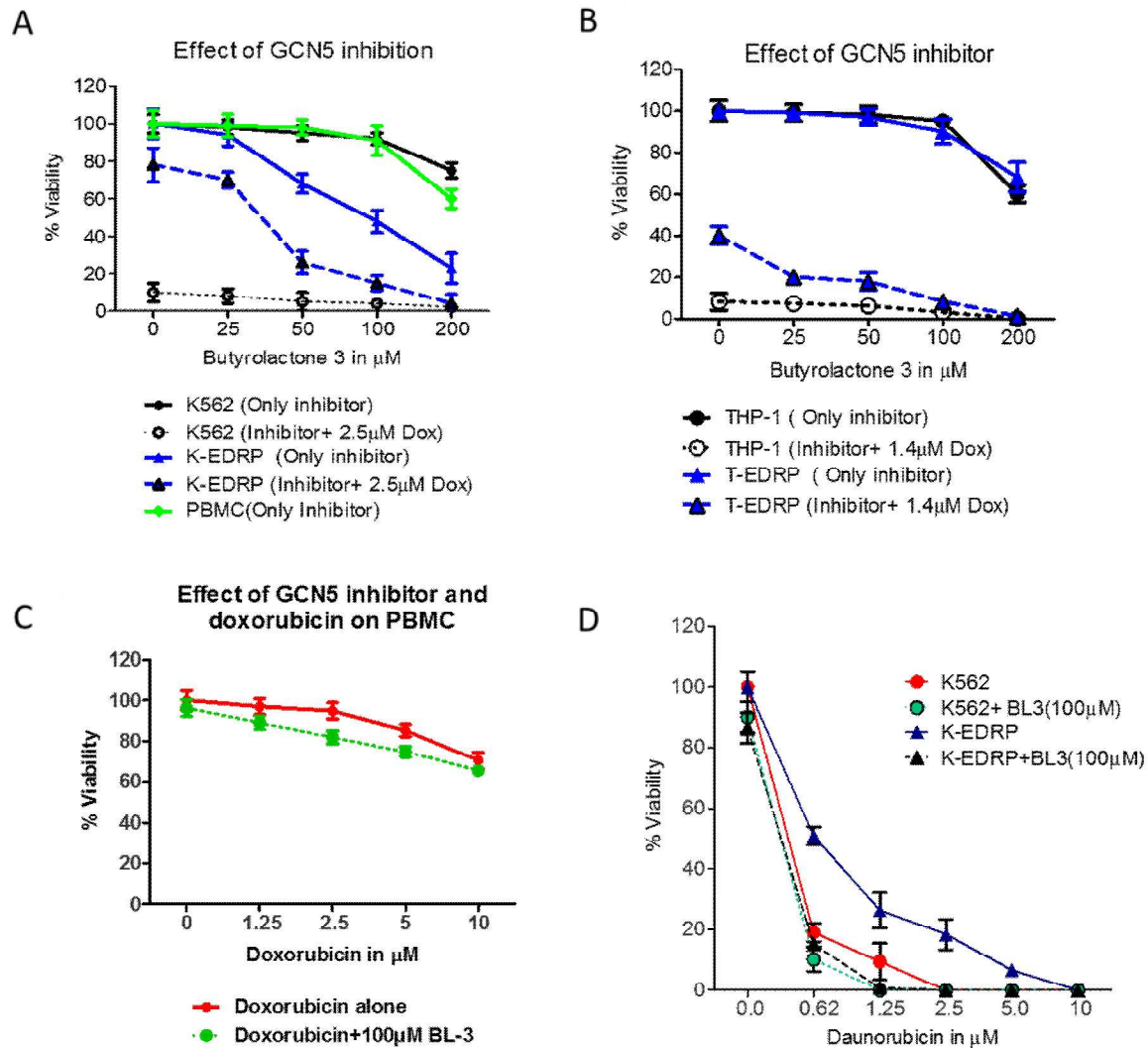


Figure 18: GCN5 inhibition sensitizes EDRP cells to doxorubicin.

(A and B) MTT assay for K562, THP-1 and respective EDRP cells after the treatment of doxorubicin and GCN5 inhibitor (Butyrolactone 3). (C) MTT assay for PBMC treated with different concentration of doxorubicin in combination with 100 μ M Butyrolactone 3. (D) MTT assay for K562 and K-EDRP cells treated with 100 μ M Butyrolactone 3 followed by different concentrations of daunorubicin.

Indeed, inhibition of GCN5 significantly sensitized K-EDRP to doxorubicin. Importantly BL-3 had no effect on the viability of peripheral blood mononuclear cells (PBMCs) at a 100 μ M concentration; this observation is consistent with literature where up to 200 μ M of BL-3 is shown to be insignificantly affecting CFC of CD34⁺ cells [131]. Doxorubicin alone and in

Results

combination with Butyrolactone 3 induced significantly lesser cell death compared to other leukemic cells like K562 and THP-1(Figure 18C). Furthermore, GCN5 inhibition also sensitized K-EDRP cells to daunorubicin suggesting that GCN5 plays a role in resistance to daunorubicin (Figure 18D).

3.3.5: Genetic or pharmacological inhibition of GCN5 perturbs ATM activation: As GCN5 is known to interact with important DSB repair proteins and its inhibition sensitizes EDRP (which depend upon faster DNA repair mechanisms mediated by ATM kinase) cells to doxorubicin, it prompted us to understand if there is a direct role of GCN5 in ATM activation. To understand this, we treated parent and EDRP cells (of K562 and THP-1) with GCN5 inhibitor prior to doxorubicin treatment (Figure 19A and B).

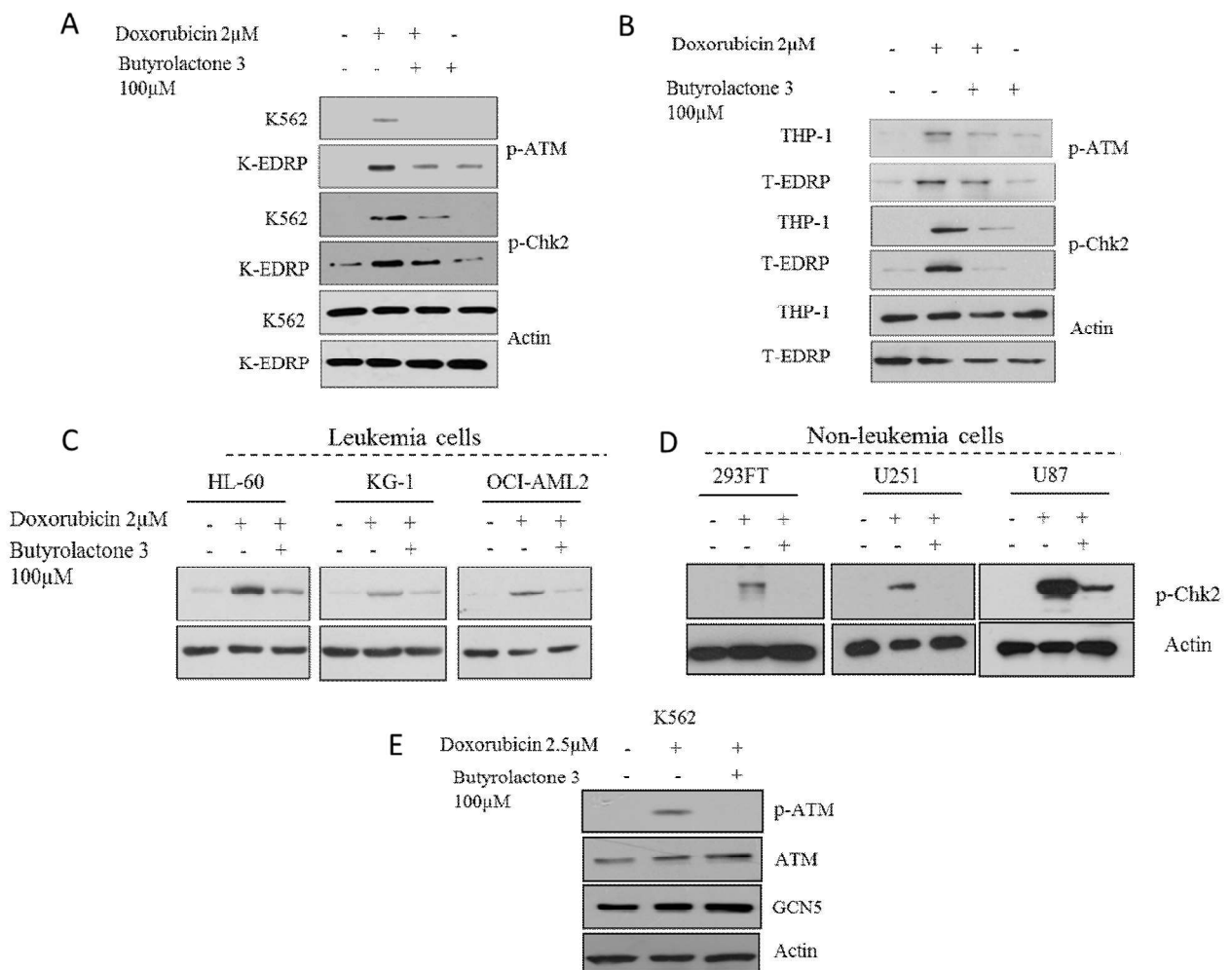


Figure 19: Pharmacological inhibition of GCN5 inhibits ATM activation and downstream pathway in cell type independent manner.

Results

(A and B) Western blots for p-ATM and p-Chk2 from K562, THP-1 parent and EDRP cells treated with different combinations of doxorubicin and Butyrolactone 3 as indicated. Actin was used as loading control. **(C and D)** Western blots for p-Chk2 with actin as a loading control in leukemic (HL-60, OCI-AML2 and KG-1) and non-leukemic (293FT, U251 and U87) cell lines treated with 100 μ M of the GCN5 inhibitor with and without doxorubicin. **(E)** Western blot for p-ATM, ATM and GCN5 in K562 cells when treated with BL-3. Actin as a loading control. Western blots represent results from at least 2 independent replicates.

GCN5 inhibition led to decreased p-ATM and p-Chk2 in doxorubicin treated EDRP and parent cells. Similar results were observed in HL-60, KG-1, OCI-AML2 (leukemic cell lines) (Figure 19C), 293FT and U251 and U87 (Glioblastoma cell lines) (Figure 19D) demonstrating that interaction of GCN5 and ATM is cell type independent. To confirm that reduced p-ATM was not due to reduction in total ATM or GCN5 we performed western blot for total ATM and GCN5 in K562 cells treated with doxorubicin alone and in combination with BL-3 (Figure 19E). Indeed, there wasn't any reduction in total ATM or GCN5 in combination treatment suggesting p-ATM regulation at the level of post-translational modification itself. To confirm, that decreased p-ATM was not because of off-target effect of the inhibitor, we performed siRNA mediated knockdown of GCN5 in THP-1 and U87 cell line. Positively, GCN5 knockdown cells showed reduced p-ATM post doxorubicin treatment compared to control siRNA (Figure 20A and B). To further confirm that GCN5 overexpression can induce higher ATM activation, we overexpressed Flag-tagged and GFP-tagged GCN5 in 293FT cells. These cells, when treated with doxorubicin, showed higher ATM activation compared to doxorubicin treated wildtype 293FT cells (Figure 20C).

Results

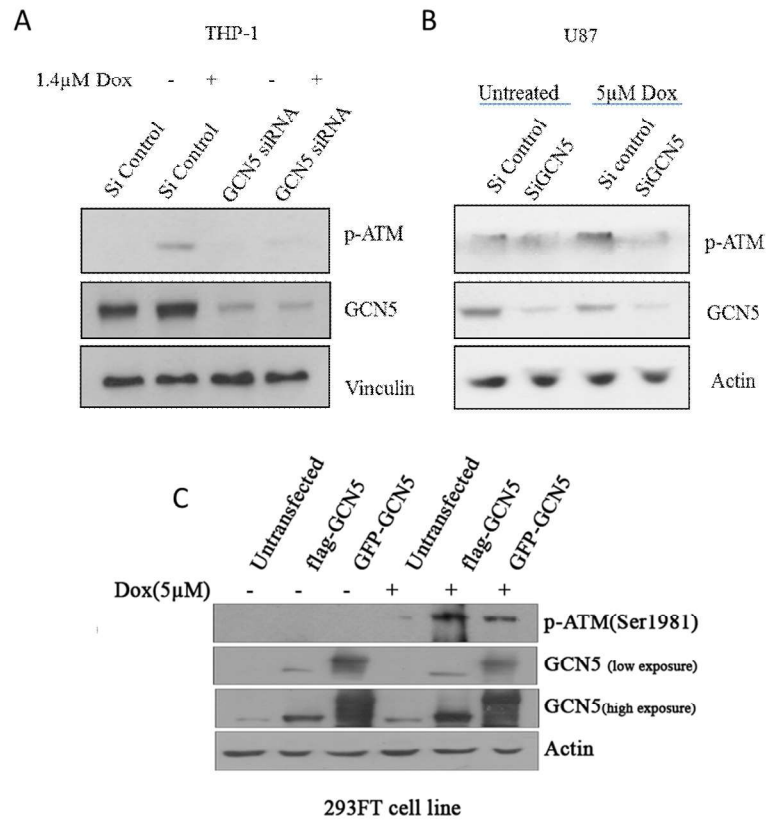


Figure 20: Genetic perturbation of GCN5 influences ATM activation.

(A and B) Western blot for p-ATM, GCN5 of GCN5 knockdown THP-1 and U87 cells pre and post doxorubicin treatment. *(C)* Western blot for p-ATM, GCN5 and actin pre and post doxorubicin treatment in 293FT cells overexpressing Flag-GCN5 and GFP-GCN5

3.3.6: GCN5 colocalizes and interacts with ATM post doxorubicin treatment: Next, to understand if the direct interaction of GCN5 with ATM enhances the recruitment of latter, we first performed colocalization of GCN5 and p-ATM (S1981) in K562 cells following doxorubicin treatment (Figure 21A). GCN5 and p-ATM showed overlapping foci, suggestive of their physical proximity.

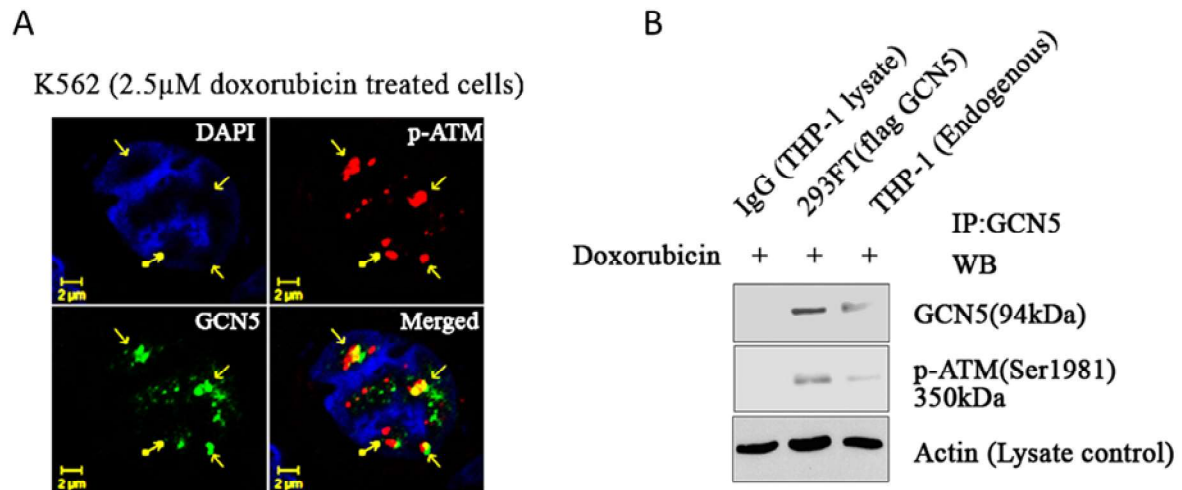


Figure 21: GCN5 interacts with ATM post DNA damage.

(A) Colocalization of GCN5 (green) and p-ATM (S1981) in K562 post 2.5 μ M doxorubicin treatment (Scale bar 2 μ m) **(B)** Immunoprecipitation from THP-1 and 293FT overexpressing Flag-GCN5 cell lysates using anti-GCN5 or normal rabbit IgG antibodies. Western blots show the levels of GCN5 and p-ATM in the immunoprecipitates. Actin shows lysate used per reaction.

Next to examine if GCN5 and ATM physically interact, we immunoprecipitated GCN5 from doxorubicin treated THP-1 and Flag-GCN5 overexpressing 293FT cells. p-ATM (S1981) was co-immunoprecipitated with GCN5 from both the cell lines (Figure 21B). These data confirm that GCN5 physically interacts with ATM kinase post doxorubicin treatment, although we cannot rule out the plausibility of other proteins in the complex that could be mediating the interaction of GCN5 and ATM.

3.3.7: GCN5 overexpression is associated to high risk disease and poor patient survival:

As we found *GCN5* to be overexpressed in all the different populations of chemoresistant cell lines (K562, THP-1, and HL-60) we were intrigued to understand the expression of GCN5 in difficult to treat AML patients. To examine the expression of *GCN5* in AML patient samples,

Results

peripheral blasts of 44 AML patients at baseline (at diagnosis) were collected and immunophenotypically characterized for % blast before and after induction and consolidation therapy. Patient information is provided in Table 7.

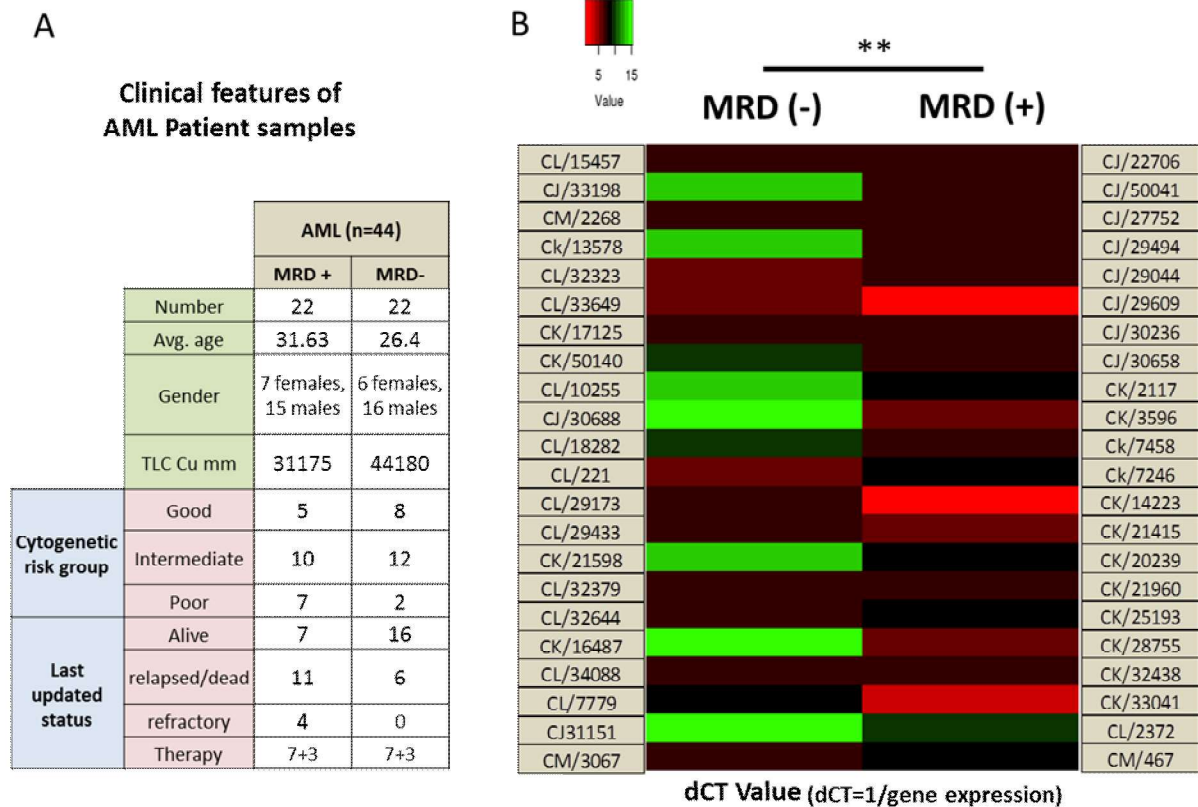


Figure 22: Expression of GCN5/KAT2A in baseline samples of MRD(+) and MRD(-) AML patient samples.

(A) Clinical characteristics of AML patients used for qPCR. (B) Heat map represents transcript levels of GCN5 as detected by SYBR green based real time PCR in baseline samples from MRD negative and MRD positive patients. Data is represented as Δct values versus cohort of patient samples.

Immunophenotyping by multiparametric flow cytometry (MPFC) was used to classify these patients into MRD (Minimal Residual Disease) positive and MRD negative cohorts (Figure 22A). Baseline samples were then analyzed for GCN5 expression by SYBR green based quantitative real time PCR using *RPL19* as an internal control. Absolute Δct values were used

Results

to compare the expression differences of *GCN5* between MRD positive (n=22) and MRD negative (n=22) patients (Figure 22B). We found that MRD positive patients had a significantly higher expression of *GCN5* compared to MRD negative patient samples.

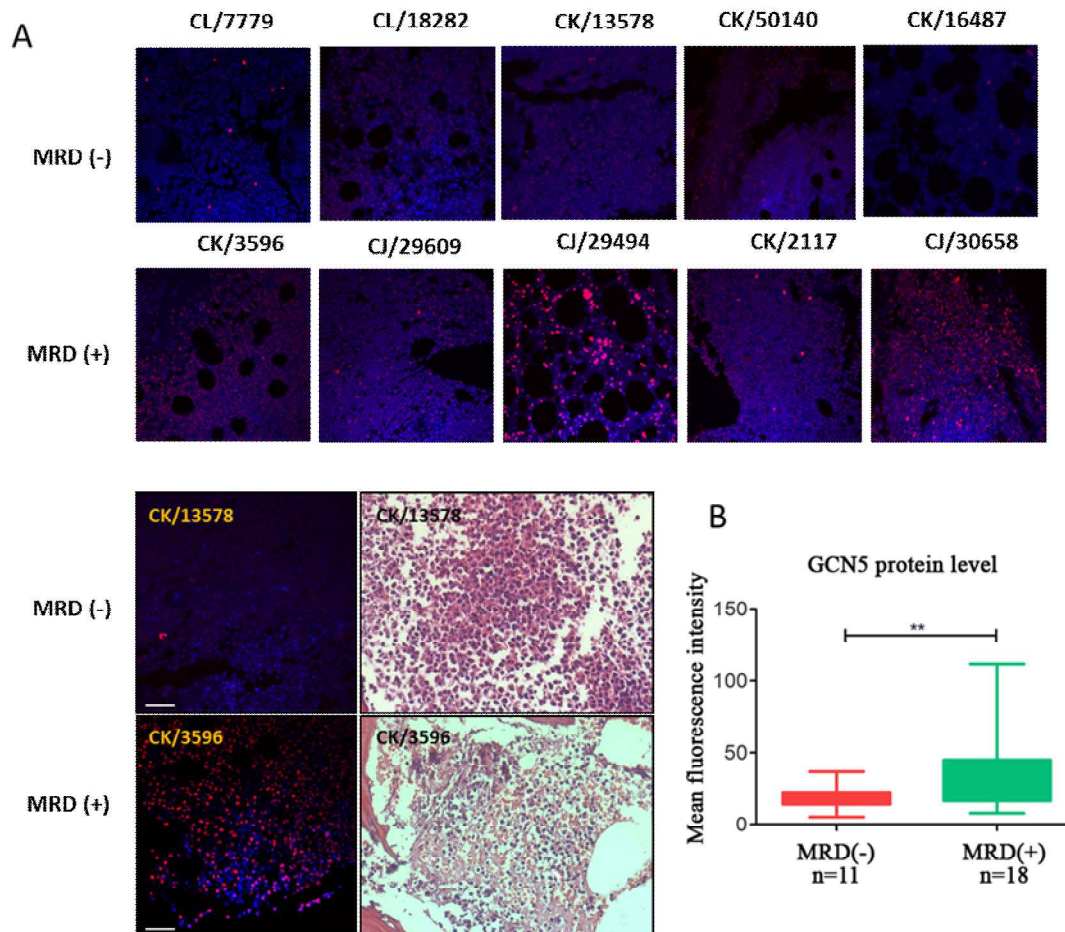


Figure 23: GCN5 protein expression by IHC in bone marrow biopsies of AML patient samples.

(A) Representative images showing immunostaining for *GCN5*, nucleus is counterstained with DAPI (blue) in MRD positive and MRD negative AML bone marrow biopsies. (Scale bar=50µm). **(B)** Graph shows the quantitation of immunostaining for MRD positive (n=18) and MRD negative (n=11) samples. Box and Whisker plot is generated by plotting mean intensity of *GCN5* from at least 20 cells from each section. The variation in *GCN5* intensity of the cohort (MRD + or -) represents whiskers in the plot.

Results

Consequently, protein levels of GCN5 were also significantly higher in MRD positive (n=18) AML baseline bone marrow biopsies compared to MRD negative (n=11) samples as shown by immunostaining (Figure 23 A and B).

Meta-analysis of publically available AML gene expression datasets using SurVExpress analysis [132] revealed *GCN5* overexpression in high-risk AML patient cohort (Figure 24A).

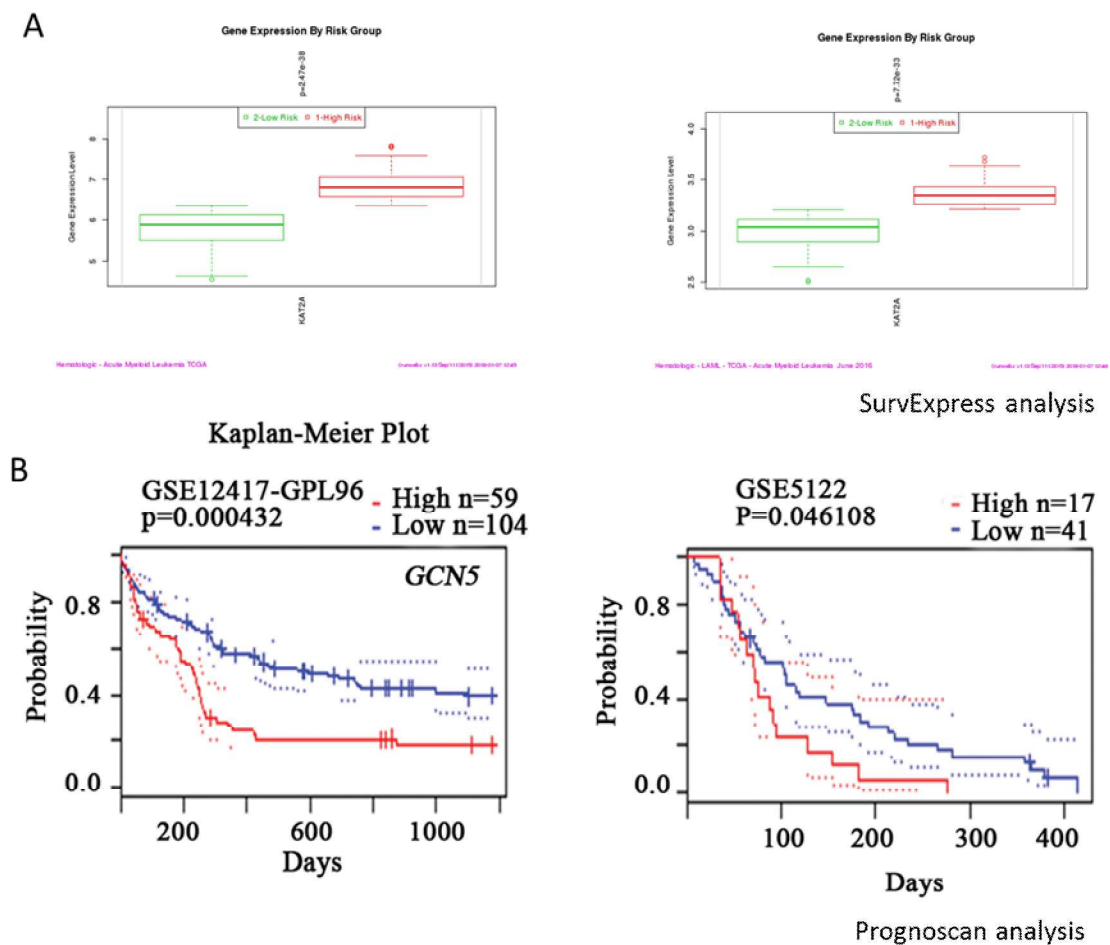


Figure 24: High-risk AML patient show GCN5 upregulation and poor survival.

(A) AML gene expression data analysis with SurVExpress in Acute Myeloid Leukemia TCGA (n=168) and LAML - TCGA - Acute Myeloid Leukemia June 2016 (n=149) samples. (B) Kaplan-Meier overall survival analysis of AML patient samples from GSE12417-GPL96 and GSE5122 dataset that have a high or low expression of GCN5.

Results

Additionally, we analyzed two AML microarray datasets GSE12417-GLP96(n=163) [30] and GSE5122(n=58) [31] using Prognoscan[32] and found that *GCN5* overexpression significantly (Minimum p value= 0.000432 and p= 0.046) correlates with poor patient overall survival (Figure 24B).

Taken together our study showcases the clinical relevance of targeting GCN5 and ATM during early stage resistance to prevent the emergence of difficult to treat stable multifactorial resistance in leukemia.

CHAPTER 4: DISCUSSIONS AND CONCLUSIONS

4.1: Discussion:

Resistance to DNA damaging drugs is the major problem in leukemia treatment as most of the leukemia is treated by conventional chemotherapy. Leukemia treatment involves drugs that inhibit topoisomerases to induce DNA double-strand breaks (DSBs) in rapidly proliferating tumor cells. However, despite initial remission most of the patients experience a relapse. Extensive research on understanding the chemoresistance has been done using cell lines with a high degree of resistance. Since these model systems are not suitable to discern the changes that a population undertakes at the onset of drug resistance, there is limited knowledge regarding the early events during the evolution of acquired resistance. In order to overcome this limitation, we developed *in vitro* cellular models from leukemic cell lines that allowed us to examine the regulation of DNA repair from early drug resistant population (EDRP) to late drug resistant population (LDRP) (Figure 25). We found that with continuous drug treatment, LDRP established themselves in such a way that topoisomerase inhibitors failed to induce significant DNA damage and accordingly ATM activation in these cells which renders them ineffective against ATM inhibitor. However, during the early stages of acquired resistance GCN5/KAT2A (a lysine acetyltransferase) was upregulated in chemoresistant leukemic cells. Upon drug treatment, GCN5 facilitated higher ATM activation leading to faster DNA repair. Inhibition of GCN5 abrogates ATM activation and sensitized EDRP to doxorubicin treatment thus demonstrating that targeting early events during acquired resistance would have maximum clinical benefit. Use of DNA repair inhibitors (ATM or GCN5) could lead to a significant reduction in doses of chemotherapy at induction as seen in our cellular model, ultimately reducing chemotherapy induced side effects. Importantly, baseline AML patient samples (n=44) showed significantly higher GCN5 expression in MRD positive compared to MRD negative samples which are further supported by, a meta-analysis of 221 AML patient samples for GCN5 high expression and

overall survival. Therefore, the *GCN5* expression could be used as a potential biomarker to detect the onset of resistance during induction therapy. Accordingly, inhibition of *GCN5* during early stages is a novel approach to prevent the emergence of difficult to treat stable resistant leukemic clones. Although *GCN5* has earlier been shown as a potential therapeutic target against AML and ALL *in vivo* [37, 131] this is the first report that highlights the role of *GCN5* in the context of AML resistance. Furthermore, this study also demonstrates that *GCN5* is required for efficient ATM activation. However, our understanding of *GCN5* and ATM interaction is inadequate and requires further investigation. In conclusion, this study identifies two important candidates (*ATM* and *GCN5*) that can be targeted during early stages of acquired resistance to prevent relapse and emphasize that *GCN5* can be used as a potential biomarker to detect the onset of resistance in leukemia.

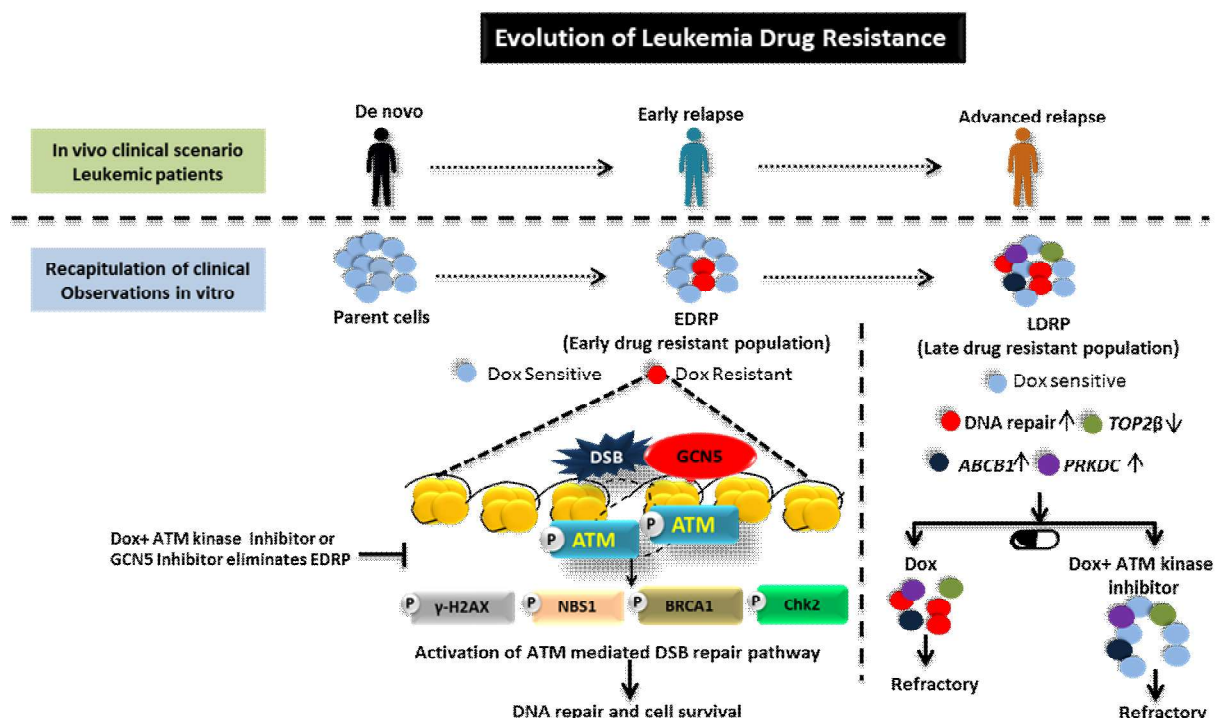


Figure 25: Proposed model for acquired drug resistance in leukemia.

Acquisition of drug resistance is a multistage process. Upper panel shows leukemia chemoresistance as classified in clinics: de novo, early and late stage drug resistance. We

mimicked the clinical scenario in vitro and developed EDRP and LDRP populations which represent early and late stage drug resistance. EDRP cells harbors enhanced DNA repair as the only mechanism of resistance compared to multifactorial drug resistance mechanisms (comprised of enhanced DNA repair, TOP2 β downregulation, ABCB1 upregulation and increased expression of DNA repair proteins like ATM and PRKDC) as shown by different colored cells in LDRP. EDRP population has open chromatin maintained via GCN5. Upon DNA damage GCN5 causes higher recruitment of ATM, consequently activating BRCA1, NBS1, Chk2 and Mcl1, and enhancing DNA repair cell survival. Combination of ATM inhibitor (KU55399) or GCN5 inhibitor and Doxorubicin induce significant apoptosis in EDRP population. However, a combination of ATM inhibitor and Doxorubicin fails to eradicate LDRP cells due to activation of multiple survival mechanisms.

Our work proves that the development of chemoresistance is a complex, multistep evolutionary process and can be grossly divided into early and late phase. Early stage resistance is a phase within which a population is not fully prepared or adapted to thrive against drug pressure by using multiple survival mechanisms, therefore; their dependency on DNA repair mechanisms can be made use of to modify treatment strategy and to have desired results. However, as a cell population is exposed to a drug over a longer duration of time it evolves more than one survival mechanism which is concomitantly active into almost every cell of the population. Results from our study show overexpression of drug transporters (*ABCB1*) or downregulation of *TOP2* or upregulation of anti-apoptotic proteins occurs as late adaptive response and strengthens existing early mechanism (i.e. DNA repair). This change makes it extremely difficult to get rid of such a well-established population by using single inhibitor e.g. DNA repair inhibitor or P-gp inhibitor. This is evident from the failure of clinical trials using DNA repair inhibitors, P-gp inhibitors or apoptosis inducers on relapsed, refractory or advanced stage of cancer patients. For most instances after achieving excellent

success in preclinical trials, failure of these inhibitors in clinical trials raises concerns over either the drug itself or conduct of the preclinical trials. However, it is also extremely imperative to consider the cohort of the patients on which it is being tested. The matter of fact is that in cancer clinical trials patients who are previously exposed to standard chemotherapy may already persist with multifactorial resistant clones which are difficult to get rid of using either monotherapy or combinatorial therapies including inhibitor against only one resistance mechanism. Therefore, it holds true “earliest is the best” not only to start treating the cancer but also to be considerate of such anticipatory changes while devising treatment plan for patients. There are a few drawbacks in this study mainly 1. It is important to use the right model system to have a closer understanding of real life processes. Doing a co-culture of AML cells with stromal cells helps better mimic the microenvironment. Drug sensitivities and survival mechanisms can be altered under such environment. Therefore, use of 3D cultures, co-cultures and ultimately in vivo experimentation gives a more relevant picture of the phenotype. To address this issue we have already initiated development of leukemia mouse model systems to study the mechanisms of resistance in early and advance stage relapse population. 2. I sincerely accept that inclusion of multi-omics (especially phosphoproteome and transcriptome) data would provide a better understanding of the evolution of drug resistance in our model system.

4.2: Summary/ Outcome of the study:

Understanding the mechanisms of therapy resistance:

1. Development of chemoresistance is a **complex, multistep** evolutionary process and can be grossly divided into early and late phase.
2. Efficient **DNA repair is indispensable** for the survival of early stage drug resistant cells while late stage drug resistant cells are characterized by multifactorial resistance.

3. This is again the first study to demonstrate that **GCN5 mediated ATM activation** is responsible for the onset of acquired drug resistance.

In identifying novel therapeutic targets or bringing up the efficacy of currently available therapeutics:

1. Our work demonstrates **GCN5 is overexpressed** in drug resistant cell lines, and patient samples and pharmacological inhibition of GCN5 sensitizes drug resistant cells to DNA damaging drugs by perturbing ATM activation and DNA repair.
2. We prove that the action of ATM kinase inhibitor is limited by induction of DNA damage; hence **targeting the earliest stage** of the disease is beneficial.

In reducing the toxic side effects of standard chemotherapy:

1. Use of DNA repair inhibitors (ATM or GCN5) helps several **fold reduction in chemotherapy dose** without compromising the end result, which would ultimately help in reducing chemotherapy induced side effects.

In Improve disease prognostication:

1. Higher GCN5 could be used **to predict the therapy response** to DNA damaging drugs.

To institute, the early use of ATM kinase inhibitor or the use of GCN5 inhibitor or to establish GCN5 as a marker of drug resistance and poor prognosis it needs rigorous testing in primary patient samples, leukemia naïve and relapse mice models which forms the base for follow-up work to my thesis, however I strongly believe that these findings have potential clinical significance and warrant further investigation.

4.3: Conclusions:

Work done in this thesis tries to understand the holistic picture of acquired drug resistance and not restricted to a particular mechanism. I believe there exists a hierarchy of evolutionary events during acquisition of drug resistance and it is now proved that targeting the earliest evolutionary mechanisms is the effective solution to get rid of drug resistance, as it is not feasible to neutralize advanced stage drug resistance with single target inhibitor/drug.

It is also very important to understand whether DNA repair inhibitors like ATM or GCN5 are able to efficiently eliminate early stage drug resistance in vivo using leukemia mouse models.

Furthermore, a key question like how ATM kinase activation is controlled by GCN5 is still not known. We assume that there can be either direct acetylation of ATM by GCN5 or through intermediate proteins like histone modifications/or chromatin remodeling complexes that help greater ATM activation.

Our work highlights the differential response of early and late stage drug resistant population to ATM kinase inhibition in leukemic cells. Enhanced DNA repair via efficient ATM kinase signaling is indispensable for the survival of early but not late stage resistant cell. Most importantly, we show GCN5 as a novel regulator of ATM activation that significantly contributes to the early stages of acquired resistance in leukemia. Our data provide a plausible mechanistic explanation for the failure of DDR inhibitors that are tested in clinical trial for the relapse, refractory and advanced stage patients.

BIBLIOGRAPHY

Bibliography

1. Velic, D., et al., *DNA Damage Signalling and Repair Inhibitors: The Long-Sought-After Achilles' Heel of Cancer*. *Biomolecules*, 2015. **5**(4): p. 3204-59.
2. Pommier, Y., et al., *DNA topoisomerases and their poisoning by anticancer and antibacterial drugs*. *Chem Biol*, 2010. **17**(5): p. 421-33.
3. Bhatti, S., et al., *ATM protein kinase: the linchpin of cellular defenses to stress*. *Cell Mol Life Sci*, 2011. **68**(18): p. 2977-3006.
4. Stracker, T.H., et al., *The ATM signaling network in development and disease*. *Front Genet*, 2013. **4**: p. 37.
5. Mao, Z., et al., *DNA repair by homologous recombination, but not by nonhomologous end joining, is elevated in breast cancer cells*. *Neoplasia*, 2009. **11**(7): p. 683-91.
6. Kapse-Mistry, S., et al., *Nanodrug delivery in reversing multidrug resistance in cancer cells*. *Front Pharmacol*, 2014. **5**: p. 159.
7. Takimoto, C.H. and S.G. Arbuck, *Clinical status and optimal use of topotecan*. *Oncology (Williston Park)*, 1997. **11**(11): p. 1635-46; discussion 1649-51, 1655-7.
8. Chen, X., et al., *Relation of clinical response and minimal residual disease and their prognostic impact on outcome in acute myeloid leukemia*. *J Clin Oncol*, 2015. **33**(11): p. 1258-64.
9. Harker, W.G., et al., *Alterations in the topoisomerase II alpha gene, messenger RNA, and subcellular protein distribution as well as reduced expression of the DNA topoisomerase II beta enzyme in a mitoxantrone-resistant HL-60 human leukemia cell line*. *Cancer Res*, 1995. **55**(8): p. 1707-16.
10. Marin, J.J., et al., *Role of drug transport and metabolism in the chemoresistance of acute myeloid leukemia*. *Blood Rev*, 2016. **30**(1): p. 55-64.
11. Elliott, S.L., et al., *Mitoxantrone in combination with an inhibitor of DNA-dependent protein kinase: a potential therapy for high risk B-cell chronic lymphocytic leukaemia*. *Br J Haematol*, 2011. **152**(1): p. 61-71.
12. Bian, K., et al., *ERK3 regulates TDP2-mediated DNA damage response and chemoresistance in lung cancer cells*. *Oncotarget*, 2016. **7**(6): p. 6665-75.
13. Paull, T.T., *Mechanisms of ATM Activation*. *Annu Rev Biochem*, 2015. **84**: p. 711-38.
14. Sun, H., et al., *Aurora-A controls cancer cell radio- and chemoresistance via ATM/Chk2-mediated DNA repair networks*. *Biochim Biophys Acta*, 2014. **1843**(5): p. 934-44.
15. Yoon, J.H., et al., *Role of autophagy in chemoresistance: regulation of the ATM-mediated DNA-damage signaling pathway through activation of DNA-PKcs and PARP-1*. *Biochem Pharmacol*, 2012. **83**(6): p. 747-57.
16. te Raa, G.D., et al., *Assessment of p53 and ATM functionality in chronic lymphocytic leukemia by multiplex ligation-dependent probe amplification*. *Cell Death Dis*, 2015. **6**: p. e1852.
17. Lee, J.H. and T.T. Paull, *ATM activation by DNA double-strand breaks through the Mre11-Rad50-Nbs1 complex*. *Science*, 2005. **308**(5721): p. 551-4.
18. Shreeram, S., et al., *Wip1 phosphatase modulates ATM-dependent signaling pathways*. *Mol Cell*, 2006. **23**(5): p. 757-64.
19. McConnell, J.L., et al., *Identification of a PP2A-interacting protein that functions as a negative regulator of phosphatase activity in the ATM/ATR signaling pathway*. *Oncogene*, 2007. **26**(41): p. 6021-30.
20. You, Z., et al., *Rapid activation of ATM on DNA flanking double-strand breaks*. *Nat Cell Biol*, 2007. **9**(11): p. 1311-8.
21. Gong, F. and K.M. Miller, *Mammalian DNA repair: HATs and HDACs make their mark through histone acetylation*. *Mutat Res*, 2013. **750**(1-2): p. 23-30.
22. Sun, Y., et al., *A role for the Tip60 histone acetyltransferase in the acetylation and activation of ATM*. *Proc Natl Acad Sci U S A*, 2005. **102**(37): p. 13182-7.
23. Harker, W.G., et al., *Multidrug resistance in mitoxantrone-selected HL-60 leukemia cells in the absence of P-glycoprotein overexpression*. *Cancer Res*, 1989. **49**(16): p. 4542-9.

Bibliography

24. Podhorecka, M., A. Skladanowski, and P. Bozko, *H2AX Phosphorylation: Its Role in DNA Damage Response and Cancer Therapy*. J Nucleic Acids, 2010. **2010**.
25. Jang, E.R., et al., *ATM modulates transcription in response to histone deacetylase inhibition as part of its DNA damage response*. Exp Mol Med, 2010. **42**(3): p. 195-204.
26. Morrison, C., et al., *The controlling role of ATM in homologous recombinational repair of DNA damage*. EMBO J, 2000. **19**(3): p. 463-71.
27. Hamilton, G., et al., *ATM regulates a RASSF1A-dependent DNA damage response*. Curr Biol, 2009. **19**(23): p. 2020-5.
28. Kim, D.W., et al., *siRNA-based targeting of antiapoptotic genes can reverse chemoresistance in P-glycoprotein expressing chondrosarcoma cells*. Mol Cancer, 2009. **8**: p. 28.
29. Bhoomik, A., et al., *Regulation of TIP60 by ATF2 modulates ATM activation*. J Biol Chem, 2008. **283**(25): p. 17605-14.
30. Metzeler, K.H., et al., *An 86-probe-set gene-expression signature predicts survival in cytogenetically normal acute myeloid leukemia*. Blood, 2008. **112**(10): p. 4193-201.
31. Raponi, M., et al., *Identification of molecular predictors of response in a study of tipifarnib treatment in relapsed and refractory acute myelogenous leukemia*. Clin Cancer Res, 2007. **13**(7): p. 2254-60.
32. Mizuno, H., et al., *PrognScan: a new database for meta-analysis of the prognostic value of genes*. BMC Med Genomics, 2009. **2**: p. 18.
33. Nagy, Z. and L. Tora, *Distinct GCN5/PCAF-containing complexes function as co-activators and are involved in transcription factor and global histone acetylation*. Oncogene, 2007. **26**(37): p. 5341-57.
34. Chatr-Aryamontri, A., et al., *The BioGRID interaction database: 2017 update*. Nucleic Acids Res, 2017. **45**(D1): p. D369-D379.
35. Zhao, M., et al., *PCAF/GCN5-Mediated Acetylation of RPA1 Promotes Nucleotide Excision Repair*. Cell Rep, 2017. **20**(9): p. 1997-2009.
36. Tzelepis, K., et al., *A CRISPR Dropout Screen Identifies Genetic Vulnerabilities and Therapeutic Targets in Acute Myeloid Leukemia*. Cell Rep, 2016. **17**(4): p. 1193-1205.
37. Holmlund, T., et al., *GCN5 acetylates and regulates the stability of the oncoprotein E2A-PBX1 in acute lymphoblastic leukemia*. Leukemia, 2013. **27**(3): p. 578-85.
38. Siegel, R.L., K.D. Miller, and A. Jemal, *Cancer statistics, 2016*. CA Cancer J Clin, 2016. **66**(1): p. 7-30.
39. Kadia, T.M., et al., *New drugs in acute myeloid leukemia*. Ann Oncol, 2016. **27**(5): p. 770-8.
40. Bejanyan, N., et al., *Survival of patients with acute myeloid leukemia relapsing after allogeneic hematopoietic cell transplantation: a center for international blood and marrow transplant research study*. Biol Blood Marrow Transplant, 2015. **21**(3): p. 454-9.
41. Jabbour, E., et al., *Targeted therapy in chronic myeloid leukemia*. Expert Rev Anticancer Ther, 2008. **8**(1): p. 99-110.
42. Yang, F., et al., *Doxorubicin, DNA torsion, and chromatin dynamics*. Biochim Biophys Acta, 2014. **1845**(1): p. 84-9.
43. Motlagh, N.S., et al., *Fluorescence properties of several chemotherapy drugs: doxorubicin, paclitaxel and bleomycin*. Biomed Opt Express, 2016. **7**(6): p. 2400-6.
44. Wang, S.L., J.J. Lee, and A.T. Liao, *Comparison of efficacy and toxicity of doxorubicin and mitoxantrone in combination chemotherapy for canine lymphoma*. Can Vet J, 2016. **57**(3): p. 271-6.
45. Ravandi, F., *Primary refractory acute myeloid leukaemia - in search of better definitions and therapies*. Br J Haematol, 2011. **155**(4): p. 413-9.
46. Syed, S.B., et al., *Targeting P-glycoprotein: Investigation of piperine analogs for overcoming drug resistance in cancer*. Sci Rep, 2017. **7**(1): p. 7972.
47. Thomas, H. and H.M. Coley, *Overcoming multidrug resistance in cancer: an update on the clinical strategy of inhibiting p-glycoprotein*. Cancer Control, 2003. **10**(2): p. 159-65.

48. Shukla, S., S. Ohnuma, and S.V. Ambudkar, *Improving cancer chemotherapy with modulators of ABC drug transporters*. Curr Drug Targets, 2011. **12**(5): p. 621-30.
49. Kathawala, R.J., et al., *The modulation of ABC transporter-mediated multidrug resistance in cancer: a review of the past decade*. Drug Resist Updat, 2015. **18**: p. 1-17.
50. Binkhathlan, Z. and A. Lavasanifar, *P-glycoprotein inhibition as a therapeutic approach for overcoming multidrug resistance in cancer: current status and future perspectives*. Curr Cancer Drug Targets, 2013. **13**(3): p. 326-46.
51. Choi, Y.H. and A.M. Yu, *ABC transporters in multidrug resistance and pharmacokinetics, and strategies for drug development*. Curr Pharm Des, 2014. **20**(5): p. 793-807.
52. Ferry, D.R., H. Traunecker, and D.J. Kerr, *Clinical trials of P-glycoprotein reversal in solid tumours*. Eur J Cancer, 1996. **32A**(6): p. 1070-81.
53. Amin, M.L., *P-glycoprotein Inhibition for Optimal Drug Delivery*. Drug Target Insights, 2013. **7**: p. 27-34.
54. Kelly, R.J., et al., *A pharmacodynamic study of docetaxel in combination with the P-glycoprotein antagonist tariquidar (XR9576) in patients with lung, ovarian, and cervical cancer*. Clin Cancer Res, 2011. **17**(3): p. 569-80.
55. Kuppens, I.E., et al., *A phase I, randomized, open-label, parallel-cohort, dose-finding study of elacridar (GF120918) and oral topotecan in cancer patients*. Clin Cancer Res, 2007. **13**(11): p. 3276-85.
56. Sandler, A., et al., *A Phase I trial of a potent P-glycoprotein inhibitor, zosuquidar trihydrochloride (LY335979), administered intravenously in combination with doxorubicin in patients with advanced malignancy*. Clin Cancer Res, 2004. **10**(10): p. 3265-72.
57. Matsumoto, Y., H. Takano, and T. Fojo, *Cellular adaptation to drug exposure: evolution of the drug-resistant phenotype*. Cancer Res, 1997. **57**(22): p. 5086-92.
58. Mo, Y.Y., Q. Wang, and W.T. Beck, *Down-regulation of topoisomerase IIalpha in CEM cells selected for merbarone resistance is associated with reduced expression of Sp3*. Cancer Res, 1997. **57**(22): p. 5004-8.
59. Binaschi, M., et al., *Relationship between lethal effects and topoisomerase II-mediated double-stranded DNA breaks produced by anthracyclines with different sequence specificity*. Mol Pharmacol, 1997. **51**(6): p. 1053-9.
60. Drake, F.H., et al., *In vitro and intracellular inhibition of topoisomerase II by the antitumor agent merbarone*. Cancer Res, 1989. **49**(10): p. 2578-83.
61. Potmesil, M., et al., *Resistance of human leukemic and normal lymphocytes to drug-induced DNA cleavage and low levels of DNA topoisomerase II*. Cancer Res, 1988. **48**(12): p. 3537-43.
62. Lyu, Y.L., et al., *Topoisomerase IIbeta mediated DNA double-strand breaks: implications in doxorubicin cardiotoxicity and prevention by dexrazoxane*. Cancer Res, 2007. **67**(18): p. 8839-46.
63. Tewey, K.M., et al., *Adriamycin-induced DNA damage mediated by mammalian DNA topoisomerase II*. Science, 1984. **226**(4673): p. 466-8.
64. Calabrese, C.R., et al., *Anticancer chemosensitization and radiosensitization by the novel poly(ADP-ribose) polymerase-1 inhibitor AG14361*. J Natl Cancer Inst, 2004. **96**(1): p. 56-67.
65. Donawho, C.K., et al., *ABT-888, an orally active poly(ADP-ribose) polymerase inhibitor that potentiates DNA-damaging agents in preclinical tumor models*. Clin Cancer Res, 2007. **13**(9): p. 2728-37.
66. Jiang, H., et al., *The combined status of ATM and p53 link tumor development with therapeutic response*. Genes Dev, 2009. **23**(16): p. 1895-909.
67. Mir, S.E., et al., *In silico analysis of kinase expression identifies WEE1 as a gatekeeper against mitotic catastrophe in glioblastoma*. Cancer Cell, 2010. **18**(3): p. 244-57.
68. Karimi-Busheri, F., et al., *Human polynucleotide kinase participates in repair of DNA double-strand breaks by nonhomologous end joining but not homologous recombination*. Cancer Res, 2007. **67**(14): p. 6619-25.

Bibliography

69. Srivastava, M., et al., *An inhibitor of nonhomologous end-joining abrogates double-strand break repair and impedes cancer progression*. *Cell*, 2012. **151**(7): p. 1474-87.
70. Shuck, S.C. and J.J. Turchi, *Targeted inhibition of Replication Protein A reveals cytotoxic activity, synergy with chemotherapeutic DNA-damaging agents, and insight into cellular function*. *Cancer Res*, 2010. **70**(8): p. 3189-98.
71. Polo, S.E. and S.P. Jackson, *Dynamics of DNA damage response proteins at DNA breaks: a focus on protein modifications*. *Genes Dev*, 2011. **25**(5): p. 409-33.
72. Bhaskara, S., et al., *Deletion of histone deacetylase 3 reveals critical roles in S phase progression and DNA damage control*. *Mol Cell*, 2008. **30**(1): p. 61-72.
73. Bhaskara, S., et al., *Hdac3 is essential for the maintenance of chromatin structure and genome stability*. *Cancer Cell*, 2010. **18**(5): p. 436-47.
74. Ni, X., L. Li, and G. Pan, *HDAC inhibitor-induced drug resistance involving ATP-binding cassette transporters (Review)*. *Oncol Lett*, 2015. **9**(2): p. 515-521.
75. Davis, A.J. and D.J. Chen, *DNA double strand break repair via non-homologous end-joining*. *Transl Cancer Res*, 2013. **2**(3): p. 130-143.
76. Clouaire, T., A. Marnef, and G. Legube, *Taming Tricky DSBs: ATM on duty*. *DNA Repair (Amst)*, 2017. **56**: p. 84-91.
77. Czornak, K., S. Chughtai, and K.H. Chrzanowska, *Mystery of DNA repair: the role of the MRN complex and ATM kinase in DNA damage repair*. *J Appl Genet*, 2008. **49**(4): p. 383-96.
78. Ceccaldi, R., B. Rondinelli, and A.D. D'Andrea, *Repair Pathway Choices and Consequences at the Double-Strand Break*. *Trends Cell Biol*, 2016. **26**(1): p. 52-64.
79. Abuzeid, W.M., et al., *Molecular disruption of RAD50 sensitizes human tumor cells to cisplatin-based chemotherapy*. *J Clin Invest*, 2009. **119**(7): p. 1974-85.
80. Ewald, B., D. Sampath, and W. Plunkett, *ATM and the Mre11-Rad50-Nbs1 complex respond to nucleoside analogue-induced stalled replication forks and contribute to drug resistance*. *Cancer Res*, 2008. **68**(19): p. 7947-55.
81. Takata, M., et al., *Homologous recombination and non-homologous end-joining pathways of DNA double-strand break repair have overlapping roles in the maintenance of chromosomal integrity in vertebrate cells*. *EMBO J*, 1998. **17**(18): p. 5497-508.
82. Lim, D.S., et al., *ATM phosphorylates p95/nbs1 in an S-phase checkpoint pathway*. *Nature*, 2000. **404**(6778): p. 613-7.
83. Williams, R.S., J.S. Williams, and J.A. Tainer, *Mre11-Rad50-Nbs1 is a keystone complex connecting DNA repair machinery, double-strand break signaling, and the chromatin template*. *Biochem Cell Biol*, 2007. **85**(4): p. 509-20.
84. Golub, E.I., et al., *Interaction of human rad51 recombination protein with single-stranded DNA binding protein, RPA*. *Nucleic Acids Res*, 1998. **26**(23): p. 5388-93.
85. Baumann, P., F.E. Benson, and S.C. West, *Human Rad51 protein promotes ATP-dependent homologous pairing and strand transfer reactions in vitro*. *Cell*, 1996. **87**(4): p. 757-66.
86. Takata, M., et al., *Chromosome instability and defective recombinational repair in knockout mutants of the five Rad51 paralogs*. *Mol Cell Biol*, 2001. **21**(8): p. 2858-66.
87. Buisson, R., et al., *Cooperation of breast cancer proteins PALB2 and piccolo BRCA2 in stimulating homologous recombination*. *Nat Struct Mol Biol*, 2010. **17**(10): p. 1247-54.
88. Swagemakers, S.M., et al., *The human RAD54 recombinational DNA repair protein is a double-stranded DNA-dependent ATPase*. *J Biol Chem*, 1998. **273**(43): p. 28292-7.
89. Van Dyck, E., et al., *Binding of double-strand breaks in DNA by human Rad52 protein*. *Nature*, 1999. **398**(6729): p. 728-31.
90. Duckett, D.R., et al., *The structure of the Holliday junction, and its resolution*. *Cell*, 1988. **55**(1): p. 79-89.
91. Valerie, K. and L.F. Povirk, *Regulation and mechanisms of mammalian double-strand break repair*. *Oncogene*, 2003. **22**(37): p. 5792-812.

Bibliography


92. Walker, J.R., R.A. Corpina, and J. Goldberg, *Structure of the Ku heterodimer bound to DNA and its implications for double-strand break repair*. Nature, 2001. **412**(6847): p. 607-14.
93. Yoo, S. and W.S. Dynan, *Geometry of a complex formed by double strand break repair proteins at a single DNA end: recruitment of DNA-PKcs induces inward translocation of Ku protein*. Nucleic Acids Res, 1999. **27**(24): p. 4679-86.
94. Karmakar, P., et al., *Werner protein is a target of DNA-dependent protein kinase in vivo and in vitro, and its catalytic activities are regulated by phosphorylation*. J Biol Chem, 2002. **277**(21): p. 18291-302.
95. Ma, Y., et al., *Hairpin opening and overhang processing by an Artemis/DNA-dependent protein kinase complex in nonhomologous end joining and V(D)J recombination*. Cell, 2002. **108**(6): p. 781-94.
96. Broderick, S., et al., *Eukaryotic single-stranded DNA binding proteins: central factors in genome stability*. Subcell Biochem, 2010. **50**: p. 143-63.
97. Mahajan, K.N., et al., *Association of DNA polymerase mu (pol mu) with Ku and ligase IV: role for pol mu in end-joining double-strand break repair*. Mol Cell Biol, 2002. **22**(14): p. 5194-202.
98. Chen, L., et al., *Interactions of the DNA ligase IV-XRCC4 complex with DNA ends and the DNA-dependent protein kinase*. J Biol Chem, 2000. **275**(34): p. 26196-205.
99. Chan, D.W. and S.P. Lees-Miller, *The DNA-dependent protein kinase is inactivated by autophosphorylation of the catalytic subunit*. J Biol Chem, 1996. **271**(15): p. 8936-41.
100. Perlman, S., S. Becker-Catania, and R.A. Gatti, *Ataxia-telangiectasia: diagnosis and treatment*. Semin Pediatr Neurol, 2003. **10**(3): p. 173-82.
101. Peterson, R.D., et al., *Cancer susceptibility in ataxia-telangiectasia*. Leukemia, 1992. **6 Suppl 1**: p. 8-13.
102. Chen, X., et al., *CAND3: A ubiquitously expressed gene immediately adjacent and in opposite transcriptional orientation to the ATM gene at 11q23.1*. Mamm Genome, 1997. **8**(2): p. 129-33.
103. Prokopcova, J., et al., *The role of ATM in breast cancer development*. Breast Cancer Res Treat, 2007. **104**(2): p. 121-8.
104. Morgan, S.E., et al., *Fragments of ATM which have dominant-negative or complementing activity*. Mol Cell Biol, 1997. **17**(4): p. 2020-9.
105. Savitsky, K., et al., *A single ataxia telangiectasia gene with a product similar to PI-3 kinase*. Science, 1995. **268**(5218): p. 1749-53.
106. Shafman, T., et al., *Interaction between ATM protein and c-Abl in response to DNA damage*. Nature, 1997. **387**(6632): p. 520-3.
107. Bakkenist, C.J. and M.B. Kastan, *DNA damage activates ATM through intermolecular autophosphorylation and dimer dissociation*. Nature, 2003. **421**(6922): p. 499-506.
108. Kozlov, S.V., et al., *Involvement of novel autophosphorylation sites in ATM activation*. EMBO J, 2006. **25**(15): p. 3504-14.
109. Burma, S., et al., *ATM phosphorylates histone H2AX in response to DNA double-strand breaks*. J Biol Chem, 2001. **276**(45): p. 42462-7.
110. Dantuma, N.P. and H. van Attikum, *Spatiotemporal regulation of posttranslational modifications in the DNA damage response*. EMBO J, 2016. **35**(1): p. 6-23.
111. Seeber, A., M. Hauer, and S.M. Gasser, *Nucleosome remodelers in double-strand break repair*. Curr Opin Genet Dev, 2013. **23**(2): p. 174-84.
112. Kruhlak, M.J., et al., *Changes in chromatin structure and mobility in living cells at sites of DNA double-strand breaks*. J Cell Biol, 2006. **172**(6): p. 823-34.
113. Kim, Y.C., et al., *Activation of ATM depends on chromatin interactions occurring before induction of DNA damage*. Nat Cell Biol, 2009. **11**(1): p. 92-6.
114. Ziv, Y., et al., *Chromatin relaxation in response to DNA double-strand breaks is modulated by a novel ATM- and KAP-1 dependent pathway*. Nat Cell Biol, 2006. **8**(8): p. 870-6.

Bibliography

115. Goodarzi, A.A., et al., *ATM signaling facilitates repair of DNA double-strand breaks associated with heterochromatin*. Mol Cell, 2008. **31**(2): p. 167-77.
116. Verma, D., et al., *Late relapses in acute myeloid leukemia: analysis of characteristics and outcome*. Leuk Lymphoma, 2010. **51**(5): p. 778-82.
117. Sawicka, M., et al., *A review of selected anti-tumour therapeutic agents and reasons for multidrug resistance occurrence*. J Pharm Pharmacol, 2004. **56**(9): p. 1067-81.
118. Minotti, G., et al., *Anthracyclines: molecular advances and pharmacologic developments in antitumor activity and cardiotoxicity*. Pharmacol Rev, 2004. **56**(2): p. 185-229.
119. Olson, R.D. and P.S. Mushlin, *Doxorubicin cardiotoxicity: analysis of prevailing hypotheses*. FASEB J, 1990. **4**(13): p. 3076-86.
120. Boutet-Robinet, E., Trouche, D. and Canitrot, Y., *Neutral Comet Assay*. Bio-protocol 3(18): e915., 2013.
121. Hickson, I., et al., *Identification and characterization of a novel and specific inhibitor of the ataxia-telangiectasia mutated kinase ATM*. Cancer Res, 2004. **64**(24): p. 9152-9.
122. Crescenzi, E., et al., *Ataxia telangiectasia mutated and p21CIP1 modulate cell survival of drug-induced senescent tumor cells: implications for chemotherapy*. Clin Cancer Res, 2008. **14**(6): p. 1877-87.
123. Biel, M., et al., *Design, synthesis, and biological evaluation of a small-molecule inhibitor of the histone acetyltransferase Gcn5*. Angew Chem Int Ed Engl, 2004. **43**(30): p. 3974-6.
124. Song, J.H., et al., *Enhanced invasiveness of drug-resistant acute myeloid leukemia cells through increased expression of matrix metalloproteinase-2*. Int J Cancer, 2009. **125**(5): p. 1074-81.
125. Petitprez, A., et al., *Acquired irinotecan resistance is accompanied by stable modifications of cell cycle dynamics independent of MSI status*. Int J Oncol, 2013. **42**(5): p. 1644-53.
126. Wang, Q., et al., *Resistance to bleomycin in cancer cell lines is characterized by prolonged doubling time, reduced DNA damage and evasion of G2/M arrest and apoptosis*. PLoS One, 2013. **8**(12): p. e82363.
127. Barr, M.P., et al., *Generation and characterisation of cisplatin-resistant non-small cell lung cancer cell lines displaying a stem-like signature*. PLoS One, 2013. **8**(1): p. e54193.
128. Mikusova, V., et al., *Mitoxantrone in combination with a DNA-PK inhibitor: possible therapy of promyelocytic leukaemia resistant forms*. Folia Biol (Praha), 2011. **57**(5): p. 200-5.
129. Hermanson, D.L., et al., *Overexpression of Mcl-1 confers multidrug resistance, whereas topoisomerase IIbeta downregulation introduces mitoxantrone-specific drug resistance in acute myeloid leukemia*. Mol Pharmacol, 2013. **84**(2): p. 236-43.
130. Xu, W., et al., *Loss of Gcn5l2 leads to increased apoptosis and mesodermal defects during mouse development*. Nat Genet, 2000. **26**(2): p. 229-32.
131. Tzelepis, K., et al., *A CRISPR Dropout Screen Identifies Genetic Vulnerabilities and Therapeutic Targets in Acute Myeloid Leukemia*. Cell Rep, 2016. **17**(4): p. 1193-1205.
132. Aguirre-Gamboa, R., et al., *SurvExpress: an online biomarker validation tool and database for cancer gene expression data using survival analysis*. PLoS One, 2013. **8**(9): p. e74250.

PUBLICATIONS

Inhibition of novel GCN5–ATM axis restricts the onset of acquired drug resistance in leukemia

Sameer Salunkhe^{1,3}, Saket V. Mishra^{1,3}, Jyothi Nair^{1,3}, Samadri Ghosh¹, Neha Choudhary¹, Ekjot Kaur^{1,3}, Sanket Shah¹, Ketaki Patkar¹, Dev Anand², Navin Khattry², Syed K. Hasan² and Shilpee Dutt^{1,3} 

¹ Shilpee Dutt laboratory, Tata Memorial Centre, Advanced Centre for Treatment, Research and Education in Cancer, Navi Mumbai 410210, India

² Department of Medical Oncology, Tata Memorial Centre, Advanced Centre for Treatment, Research and Education in Cancer, Navi Mumbai 410210, India

³ Homi Bhabha National Institute, Training School Complex, Anushakti Nagar, Mumbai 400085, India

Leukemia is majorly treated by topoisomerase inhibitors that induce DNA double strand breaks (DSB) resulting in cell death. Consequently, modulation of DSB repair pathway renders leukemic cells resistant to therapy. As we do not fully understand the regulation of DSB repair acquired by resistant cells, targeting these cells has been a challenge. Here we investigated the regulation of DSB repair pathway in early drug resistant population (EDRP) and late drug resistant population (LDRP). We found that doxorubicin induced equal DSBs in parent and EDRP cells; however, cell death is induced only in the parent cells. Further analysis revealed that EDRP cells acquire relaxed chromatin via upregulation of lysine acetyl transferase *KAT2A* (*GCN5*). Drug treatment induces *GCN5* interaction with ATM facilitating its recruitment to DSB sites. Hyperactivated ATM maximize H2AX, NBS1, BRCA1, Chk2, and Mcl-1 activation, accelerating DNA repair and survival of EDRP cells. Consequently, inhibition of *GCN5* significantly reduces ATM activation and survival of EDRP cells. Contrary to EDRP, doxorubicin failed to induce DSBs in LDRP because of reduced drug uptake and downregulation of *TOP2β*. Accordingly, ATM inhibition prior to doxorubicin treatment completely eliminated EDRP but not LDRP. Furthermore, baseline AML samples ($n = 44$) showed significantly higher *GCN5* at mRNA and protein levels in MRD positive compared to MRD negative samples. Additionally, meta-analysis ($n = 221$) showed high *GCN5* expression correlates with poor overall survival. Together, these results provide important insights into the molecular mechanism specific to EDRP and will have implications for the development of novel therapeutics for AML.

Leukemia chemotherapy involves drugs that inhibit topoisomerases to induce DNA double strand breaks (DSBs) in rapidly dividing cells. However, despite initial remission most of patients experience relapse.¹ Apart from mechanisms like downregulation of topoisomerases² and upregulation of drug transporters,³ modulation of DNA repair pathway is known to play a major role in acquiring drug resistance in different cancer types.^{4,5} As topoisomerase inhibitors induce DNA DSBs, we focused on understanding the regulation of DNA repair mechanisms in chemoresistant leukemic cells.

Key words: leukemia, chemoresistance, DNA repair, ATM, *GCN5*

Abbreviations: EDRP: early drug-resistant population; LDRP: late drug-resistant population; MRD: minimal residual disease; DDR: DNA damage and repair; DSB: double strand break; PDR: post drug removal

Additional Supporting Information may be found in the online version of this article.

Grant sponsor: Indian Council of Medical Research; **Grant number:** 90/04/2012–STM(TF)/BMS

DOI: 10.1002/ijc.31242

History: Received 2 June 2017; Accepted 20 Dec 2017; Online 3 Jan 2018

Correspondence to: Shilpee Dutt, Ph.D., Principal Investigator, KS 326, Tata Memorial Centre, ACTREC, Navi Mumbai, Maharashtra, India, E-mail: sdutt@actrec.gov.in; Tel: +91-22-2740-5394

ATM, a master regulator kinase involved in DNA DSBs repair,⁶ is known as an important mediator of drug resistance.^{7–9} Although ATM can get activated by autophosphorylation, mechanisms like higher recruitment via Mre11 proteins, relaxed chromatin architecture, downregulation of its phosphatases (*WIP1* and *PP2CA*), direct acetylation by *TIP-60*- and *HMOF*-induced H4K16ac-mediated recruitment^{6,10–15} have been shown to further enhance its activity.

Extensive research on understanding the role of DNA DSB repair in chemoresistance in leukemia has been done using cell lines with high-resistance indices-based model systems. As these model systems cannot be used for comparative studies between the early and late stages of drug resistance, there is limited knowledge regarding the evolution of DNA repair mechanism during acquired resistance. Therefore, we developed *in vitro* cellular models that allowed us to examine regulation of DNA repair from an initial drug-tolerant state to late drug-resistant state. We found that with continuous drug treatment, LDRP evolved such that topoisomerase inhibitors failed to induce significant DNA damage and ATM activation, rendering these cells ineffective against ATM inhibitor. However, during early stages of acquired resistance *GCN5/KAT2A* (a lysine acetyltransferase) was upregulated in chemoresistant leukemic cells. Upon drug treatment *GCN5* facilitated higher ATM activation leading to faster DNA repair. Inhibition of *GCN5* inhibited ATM activation and

What's new?

Leukemia is mainly treated by topoisomerase inhibitors that induce DNA double strand breaks (DSB) resulting in cell death. Modulation of DSB repair pathway, however, renders leukemic cells resistant to therapy, and the underlying mechanisms remain unclear. This work highlights the differential response of early- and late-stage drug-resistant populations to ATM kinase inhibition in leukemic cells. Enhanced DNA repair via efficient ATM kinase signaling is indispensable for survival of early-stage, but not late-stage resistant cells. Importantly, the findings suggest GCN5 as a novel ATM activation regulator that significantly contributes to the early stages of acquired resistance in leukemia.

sensitized EDRP to doxorubicin treatment thus demonstrating that targeting early events during acquired resistance would have maximum clinical benefit. Furthermore, GCN5 expression could be used as a potential biomarker to detect onset of resistance during induction therapy. Accordingly, inhibition of GCN5 during early stages is a novel approach to prevent emergence of difficult to treat stable resistant leukemic clones.

Material and Methods**Cells lines, cell culture and vector transfections**

K562, THP-1, KG-1 and HL-60 cell lines were obtained from NCCS Pune, HL-60/MX2 cell line was obtained from ATCC (CRL 2257TM). All the cell lines were maintained in RPMI with 10% FBS and antibiotics. 293FT cells (a kind gift from Dr Amit Dutt, ACTREC) were cultured in DMEM with 10% FBS and antibiotics. Cell lines were authenticated by STR profiling using PROMEGA STR profiling kit using 10 markers (Supporting Information, Table 1). GFP-GCN5 was purchased from Addgene (plasmid # 65386). pEBB Flag GCN5 was a gift from Dr Ezra Burstein (UT Southwestern Medical Centre). 293FT cells were transfected with GCN5 overexpression vectors using lipofectamine 3000 reagent according to manufacturer's protocol.

Immunofluorescence/colocalization

Methanol-fixed cells were spread on coverslips. Cells were then permeabilized and blocked followed by overnight incubation with primary antibody. Following PBS washes, cells were incubated with secondary antibody (Alexa Fluor 488/633). Cells were mounted with vectashield mounting medium containing DAPI and imaged using Zeiss LSM 780 Confocal Microscope. For colocalization, $\sim 0.5 \times 10^6$ K562 cells treated with 2.5 μ M of doxorubicin for 2 hr prior to fixing with 100% methanol for 2 hr in -20°C and dispensed on a poly-lysine coated coverslips. Dual staining with anti-GCN5 and anti-p-ATM (S1981) was performed as mentioned above. Staining was quantitated using ImageJ software.

Co-immunoprecipitation

THP-1 and Flag-GCN5 overexpressing 293FT cells were treated with doxorubicin for 2 hr. Cells were fixed with formaldehyde and then lysed in EBC lysis buffer. Approximately 300 μ g of lysates were incubated overnight on rotating shaker

at 4°C with 5 μ g GCN5 antibody and appropriate IgG Iso-type control. Equilibrated agarose-G beads were added to immuno-complexes and incubated for 2 hr on rotating shaker at 4°C . Immunoprecipitated proteins was loaded on 10% SDS-PAGE and probed with anti-GCN5 and anti-p-ATM (S1981) antibodies.

HR and NHEJ vector reactivation assay

HR and NHEJ activity assay vectors were a kind gift from Dr Vera Gorbunova (University of Rochester Department of Biology). Cells were transfected with 1 μ g of I-SceI endonuclease digested vectors with X-treme GENE HP DNA Transfection Reagent (Roche). Transfection was done in three biological replicates including Td-Red as transfection control. Flow cytometry was done 72 hr post transfection. Percent repair efficiency was calculated by taking ratio of % of GFP (HR or NHEJ) positive cells to % of Td-Red-positive cells.

Ethics statement and patient samples

Blood samples from AML patients were accrued after approval by the institutional ethics committee (TMC-IEC III) DCGI registration number: IEC III: ECR/149/Inst/MH/2013. A written informed consent was taken in language understood by the patients. Following FAB diagnosis, AML cases were characterized by immunophenotyping using multiparametric flow cytometry. Patient information is provided in Supporting Information, Table 4.

MTT assay and drugs

Approximately 5×10^3 cells were treated with doxorubicin (Pfizer Laboratories), mitoxantrone (Sun pharmaceuticals), KU55933 (Calbiochem), Daunorubicin (Pfizer Laboratories), Cytarabine (Fresenius Kabi), and Butyrolactone 3 (ab141255) at different concentrations. MTT Assay was performed as per manufacturer's instructions (Himedia).

Cell cycle and drug uptake analysis

Cells treated with IC90 concentration of doxorubicin were acquired at different time points and stained with propidium iodide. Cell cycle analysis was done by flow cytometry (BD FACS CaliburTM). For drug uptake, cells were analyzed by flow cytometry at 480/580 nm wavelengths.

Western blotting

Cells were lysed in laemmli lysis buffer, proteins separated on SDS-PAGE and transferred on to nitrocellulose membrane. Membranes were probed with different primary antibodies (Supporting Information, Table 2). Blots were developed using ECL reagent (Thermo Fischer). Densitometric analysis was done using ImageJ software as per the instructions of the software manual. Western blot densitometric data are provided in Supporting Information.

SYBR green-based quantitative real-time PCR

RNA was extracted using TRI Reagent (Thermo Fisher) and cDNA made using Superscript III First-Strand kit (Invitrogen). Quantitative real-time PCR was performed using SYBR green (Roche) in a Roche Life Cyclor 480. *GAPDH* or *RPL19* was used as internal control. Primer sequences are given in Supporting Information, Table 3.

Clonogenic assay

1×10^3 cells were treated with drug and seeded directly in 1 ml of methyl cellulose agar (1.6%) with 1 ml of $2\times$ RPMI containing 20% FBS and $2\times$ antibiotic cocktail in 1:1 ratio. Colonies (>40 cells) were scored under inverted optical microscope (Olympus model IX 51) on the 12th day.

Neutral comet assay

The protocol used for neutral comet assay was modified from E. Boutet-Robinet *et al.*¹⁶ Briefly, 1×10^4 cells were mixed in LMPA at 42°C , spread on agarose-coated slides and incubated with lysis buffer. Following electrophoresis, slides were dehydrated and stained with propidium iodide. Images were taken and comets scored using Open Comet software.

Transmission electron microscopy (TEM)

Cells were fixed with 3% glutaraldehyde and treated with 0.1% osmium tetroxide. Subsequently, cells were dehydrated and treated with absolute alcohol, araldite A and araldite B. Sections of 70 nm were made and stained in 10% of alcoholic uranyl acetate incubated with lead acetate. The sections were imaged on transmission electron microscope (Jeol 1400 plus).

TEM image quantitation

Images were analyzed on the basis of their gray-scale intensity using MATLAB (Mathworks) computing software. To obtain the distribution of gray scale values at a given offset, the gray-level co-occurrence matrix (GLCM) was used.¹⁷

siRNA knockdown of GCN5

THP-1 cells were seeded at 0.3 million/ml density per well in a 6-well plate and transfected with siRNA (Invitrogen Cat no. 4390824) at 30 pmols per well concentration using standard 6-well protocol for RNAiMax reagent. Cells were collected 72 hr post transfection and tested for GCN5 knockdown by western blotting.

AML bone marrow immunohistochemistry

Bone marrow sections of 4 μM thickness were fixed on poly-L-lysine-coated glass slides. Sections were rehydrated by passing through xylene and ethanol gradient for 10 min each. Tris-EDTA buffer (pH = 9) was used for antigen retrieval with moist heat for 15 min. Sections were blocked with serum for 30 min at room temperature. Sections were incubated overnight with anti-GCN5 antibody at 1:100 dilution. After PBS washes, sections were incubated with secondary antibody tagged with Alexa 633 dye for 1 hr at RT. Unbound antibodies were removed by PBS wash and sections were mounted with mounting medium containing DAPI. Sections were imaged using Zeiss LSM 780 Confocal Microscope. Median fluorescence intensity was calculated using ImageJ software.

Statistical analysis

The two-tailed Student's *t* test was applied for statistical analysis. Results were considered significant in all experiments at $p < 0.05$. When representing quantitative data, * means $p < 0.05$, ** means $p < 0.01$ and *** means $p < 0.001$.

RESULTS

Recapitulating clinical scenario of acquired resistance in a cellular model

We modeled acquired resistance to DNA damaging agent doxorubicin using leukemic cell lines K562 and THP-1. The overall schema for the development of the resistance model is shown in Figure 1a. First, the lethal dose (where $\geq 90\%$ cells die) of doxorubicin for K562 and THP-1 was determined to be 2.5 and 1.4 μM , respectively, by cell viability assay (Figs. 1b and 1c). Cells were then treated with their respective lethal dose of doxorubicin for 48 hr. We found that a small percentage ($<10\%$) of cells survived (persisters or residual cells, equivalent to the minimal residual disease observed in the patients) high concentrations of doxorubicin in both the cell lines. These persisters were allowed to grow. The first relapsed population (R) was termed K562-R1 and THP-1 R1. K562 cells were treated with doxorubicin for 10 cycles (over 8 months) while THP-1 for 7 cycles (over 6 months) to obtain the cells with the high drug resistance index. We collected the relapsed cells after every round of drug treatment, that is, R1, R2, R5, R7 and R10 for K562 and R1, R2, R3, R5 and R7 for THP-1 cell line. Resistance to doxorubicin for each population was analyzed by MTT cell viability assay (Figs. 1b and 1c). We found that R1 population of K562 and R1 and R2 population of THP-1 cell line showed similar sensitivity to doxorubicin as the parent population. However, K562-R2 cells (1.97-fold resistance) and THP-1-R3 cells (1.46-fold resistance) were earliest relapses that showed significantly better survival to doxorubicin than their respective parent populations (Figs. 1d and 1e). As K562-R2 and THP-1-R3 were the first populations to show significant resistance to doxorubicin, we refer to these populations as early drug resistant population (EDRP) cells and K562-R10

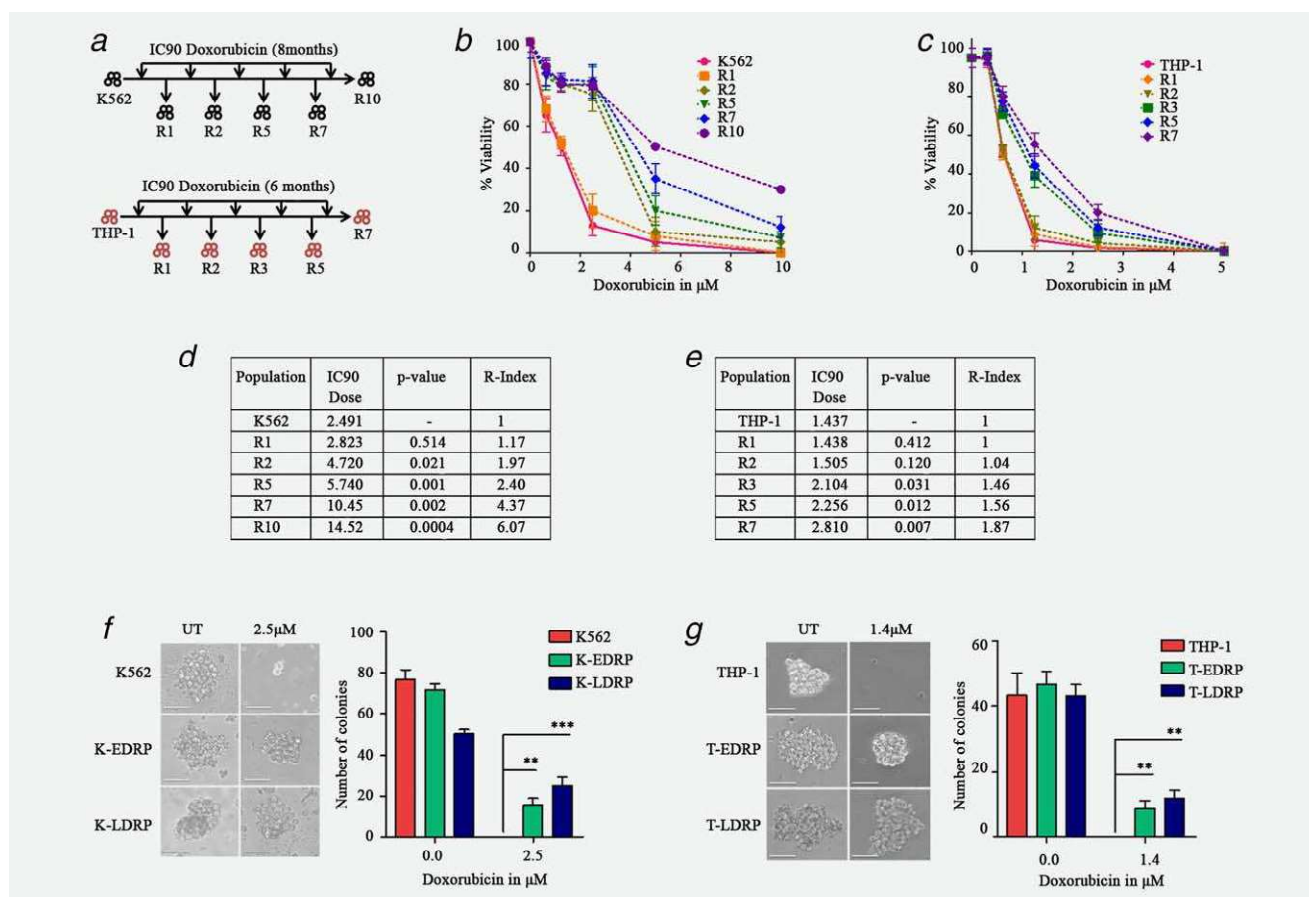


Figure 1. Recapitulating clinical scenario of acquired resistance in a cellular model. (a) Schema represents development of acquired chemoresistance model using K562 and THP-1 cell lines. (b and c) Cytotoxicity evaluation by MTT assay after treatment of K562, THP-1 and their resistant derivatives to increasing concentrations of doxorubicin for 48 h. (d and e) Resistance indices of different resistant populations developed from K562 and THP-1 cells following increasing cycles of doxorubicin treatment. (f and g) Representative images of a typical cell colony observed by bright-field microscopy (20 \times objective) at day 12 of growth in soft agar (Scale bar = 50 μm). Bar graph quantifies the number of colonies formed in different cell populations after doxorubicin treatment. Results in each bar and line graph are the composite data from three independent experiments performed in triplicate (mean \pm SEM); * denotes $p \leq .05$, ** denotes $p \leq .01$ and *** denotes $p \leq .001$. PDR, post drug removal.

and THP-1-R7 as late drug resistant population (LDRP) cells. EDRP and LDRP of both the cell lines were analyzed for their clonogenic ability in the presence of IC90 concentration of doxorubicin. As shown in Figures 1f and 1g, both EDRP and LDRP formed significantly higher number of colonies compared to parent cells, indicating the enrichment of cells with colony forming capacity (unlimited cell growth) in these populations. Similar results were obtained with HL-60 and its mitoxantrone-resistant subcell line HL-60/MX2 (representing LDRP of HL-60), which is 35-fold more resistant than parent HL-60 cells¹⁸ (Supporting Information, Fig. 1a). We further tested the cross resistance of K562, K-EDRP and K-LDRP to DNA-damaging drugs daunorubicin and cytarabine and found that both the populations were resistant to daunorubicin, whereas cytarabine resistance was shown only by K-LDRP (Supporting Information, Fig. 1b).

Interestingly, the chemoresistant populations showed reversibility to resistance when cultured in drug-free media.

EDRP cells showed loss of resistance faster (10–12 days) than LDRP cells (30–40 days) (Supporting Information, Fig. 1c). Similarly, chemoresistance is shown to be reversible in HL-60/MX2 cells as well (ATCC CRL 2257). These data are suggestive of nongenetic mechanisms of acquired chemoresistance, especially during early stages of drug resistance.

EDRP shows faster DNA repair while LDRP do not incur significant DSBs post doxorubicin treatment

To investigate the alteration in DNA repair, we first checked for double strand breaks (DSBs) induced by doxorubicin at different time points (5 min, 6 hr, and 12 hr) post drug removal (PDR) using neutral comet assay (Fig. 2a). Interestingly, LDRP showed minimal induction of DSBs while EDRP populations from both the cell lines (K562 and THP-1) showed DSBs similar to the parent population (Figs. 2b and 2c). However, by 12 hr EDRP could resolve most of DSBs compared to parent cells suggesting faster DNA repair. Similar

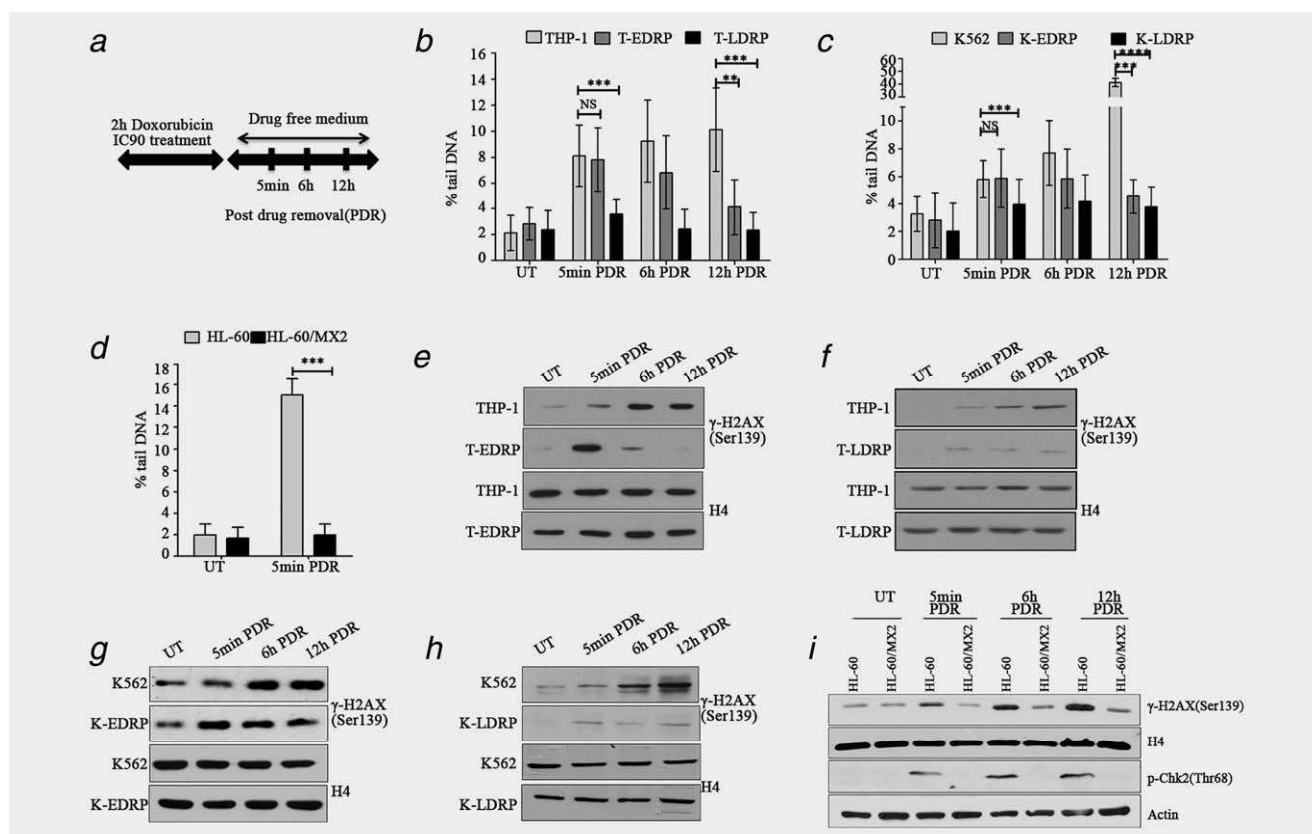


Figure 2. EDRP shows faster DNA repair while LDRP do not incur significant DSBs post doxorubicin treatment. (a) Schema showing the timeline of drug treatment and time points of samples collection. (b–d) Bar graph shows % tail DNA versus indicated time points of neutral comet assay for K562, THP-1, HL-60 and their resistant populations. (e and f) Western blot of γ -H2AX in THP-1 and T-EDRP cells at indicated time points post 2 h of 1.4 μ M doxorubicin treatment. (g and h) Western blot of γ -H2AX in K562 and K-EDRP cells at indicated time points post 2 h of 2.5 μ M doxorubicin treatment. (i) Western blots for p-Chk2, γ -H2AX in HL-60 and HL-60/MX2 cells at indicated time points post 100 nM mitoxantrone treatment. Actin and total H4 were used as loading controls. Western blots represent results from at least 3 independent replicates. Results in each bar graph are the composite data from three independent experiments performed in triplicate (mean \pm SEM); * denotes $p \leq .05$, ** denotes $p \leq .01$, *** denotes $p \leq .001$ and **** denotes $p \leq .0001$.

to LDRP of K562 and THP-1 post mitoxantrone treatment, HL-60/MX2 cells also induced minimal DNA DSBs (Fig. 2d).

Phosphorylation of H2AX is the first cellular response to the induction of DSBs and the rate of appearance and resolution of γ -H2AX is considered to be a measure of DSB repair efficiency of a cell.¹⁹ Therefore, we analyzed the activation of γ -H2AX at different time points following the drug treatment. We found that immediately after drug removal compared to the parent cells, EDRP cells showed increased H2AX phosphorylation which was mostly resolved by 12 hr PDR (Figs. 2e and 2g) confirming faster DNA repair in EDRP cells. Concordant with comet assay, LDRP cells showed significantly less induction of γ -H2AX indicating inability of doxorubicin to induce DNA DSBs in these cells (Figs. 2f and 2h). Similarly, HL-60/MX2 cells also did not show significant induction of γ -H2AX and p-Chk2 upon mitoxantrone treatment (Fig. 2i). These data demonstrate that topoisomerase inhibitors were unable to induce DSBs in LDRP cells. We then sought to elucidate the mechanism of DSB repair in EDRP cells.

EDRP harbors hyperactive ATM kinase signaling

Because cell cycle arrest and DNA repair is interlinked, we analyzed cell cycle profile of parent and EDRP with and without doxorubicin treatment. Post drug treatment, K562 and THP-1 parent and respective EDRP cells showed S and G2/M arrest at 24 and 48 hr, respectively. Although, the parent populations remained arrested, EDRP cells could overcome S and G2/M cell cycle arrest (Fig. 3a and Supporting Information, Fig. 2a). Similarly, mitoxantrone treatment induced cell cycle arrest in HL-60 cells but not in HL-60/MX2 cells (Supporting Information, Fig. 2b). These data demonstrate that EDRP cells were able to resolve cell cycle arrest and do not elicit an apoptotic response.

ATM (ataxia telangiectasia mutated) is a sensor kinase that phosphorylates H2AX following DNA DSBs.⁶ To investigate whether increased γ -H2AX in EDRP cells could be attributed to ATM activation, levels of p-ATM were analyzed at different time points post doxorubicin treatment. Concordant with γ -H2AX activation kinetics, immunofluorescence and western blot analysis of p-ATM showed >2-fold increase

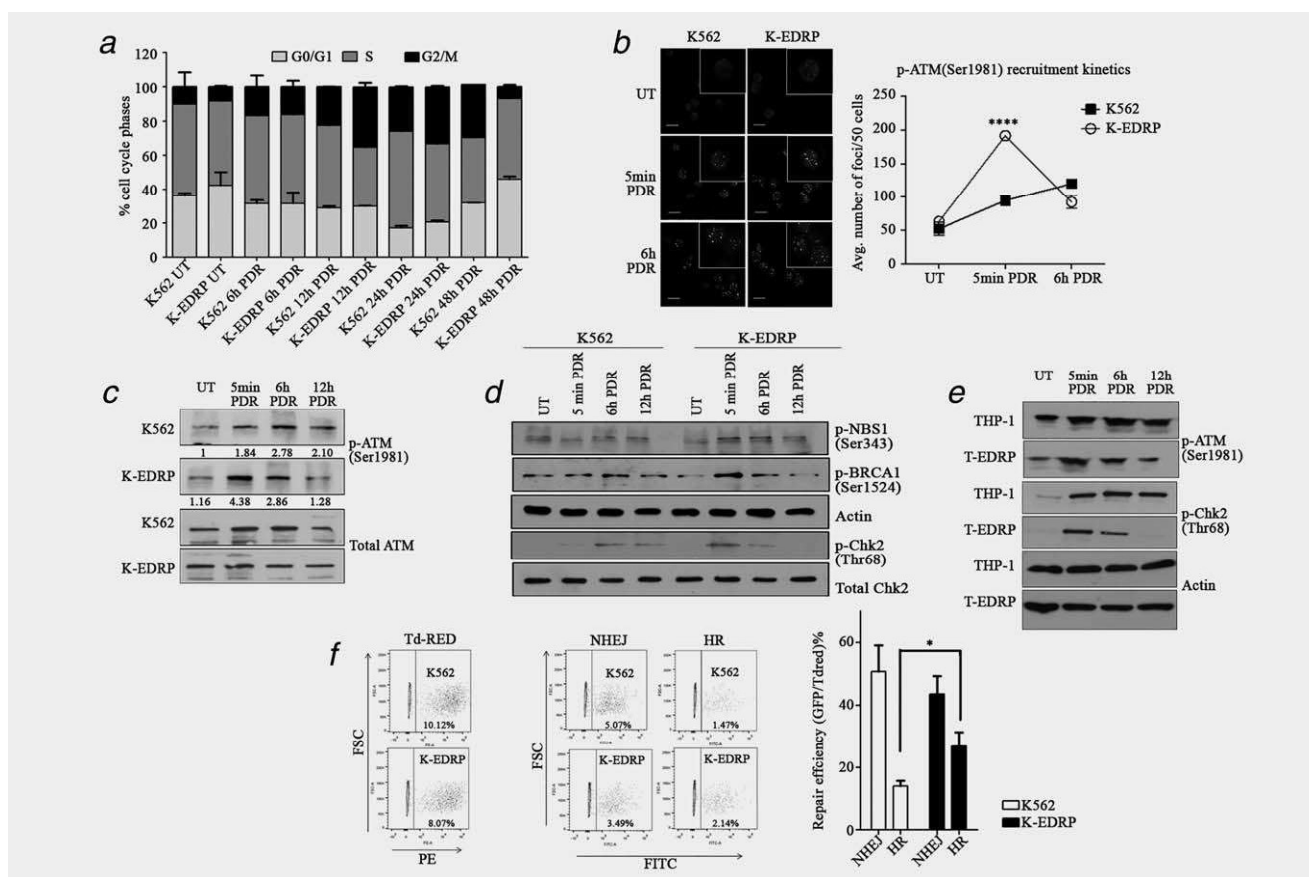


Figure 3. EDRP harbors hyperactive ATM kinase signaling. (a) Cell cycle analysis of the parent K562 and K-EDRP cells with doxorubicin treatment. Bar graph shows relative percentage of cells at G0/G1, S and G2/M phase of the cell cycle at indicated time points. (b) Representative images of p-ATM foci and nuclei counterstained with DAPI in K562 and K-EDRP cells. Graph represents average number of p-ATM foci counted per 50 cells from each population (scale bar = 20 μm). (c) Western blot for p-ATM and total ATM in K562 and K-EDRP cells post 2h of doxorubicin treatment. (d) Western blot showing protein expression of p-NBS1, p-BRCA1, p-Chk2 and total Chk2 after 2 h of doxorubicin treatment at indicated time points post drug removal. Beta actin is used as loading control. (e) Western blot showing protein expression of p-ATM and p-Chk2 in THP-1 and T-EDRP after 2 h of doxorubicin treatment at indicated time points post drug removal. Beta actin is used as loading control. (f) HR and NHEJ vector reactivation assay performed in K562 and K-EDRP cells. Flow cytometry was done 72 h post transfection. Bar graph represents repair efficiency in the population as indicated. Western blots represent results from at least 2 independent replicates. Results are the composite data from three independent experiments (mean ± SEM); * denotes $p \leq .05$, ** denotes $p \leq .01$, *** denotes $p \leq .001$ and **** denotes $p \leq .0001$. Scale bar 20 μm.

in ATM activation in K-EDRP compared to the parent K562 cells (Figs. 3b and 3c). Furthermore, downstream targets of ATM, like p-NBS1 (Ser343), p-BRCA1 (Ser1524) and p-Chk2 (Thr68), also showed higher activation in EDRP cells compared to the parent K562 cells (Fig. 3d). Additionally Mcl-1 L, an antiapoptotic protein, whose expression is controlled by ATM²⁰ showed upregulation in K-EDRP cells (Supporting Information, Fig. 2c). Similar results were obtained for parent THP-1 and T-EDRP (Fig. 4e). We then wanted to assess the choice of repair pathway (HR or NHEJ) and its efficiency in EDRP cells, for which we used HR and NHEJ vector activity assay.²¹ Results showed significantly higher HR activity in K-EDRP cells compared to K562 cells (Fig. 3f). Furthermore, we also found higher recruitment of Rad51, an HR-specific protein in K-EDRP compared to the parent K562 (Supporting Information, Fig. 3a), these data are

in agreement with previous reports where ATM is shown to prefer resolution of DNA DSBs via HR pathway.²²

ATM kinase inhibition eliminates EDRP but not LDRP cells

The data presented above demonstrates hyperactivation of ATM during the onset of acquired resistance. Accordingly, inhibition of ATM should induce death in residual cells and prevent emergence of chemoresistance. To test this, parent cells, EDRP and LDRP of K562 and THP-1 were treated with 10 μM of ATM kinase inhibitor (KU55933)²³ in combination with different concentrations of doxorubicin (0–10 μM). ATM kinase inhibitor induced complete cell death in K-EDRP at 2.5 μM doxorubicin concentration but only 40% cell death in K-LDRP cells. Importantly, ATM inhibitor reduced the IC₉₀ concentration of doxorubicin for K-EDRP from 6.93 to 1.39 μM. Similar results were obtained with

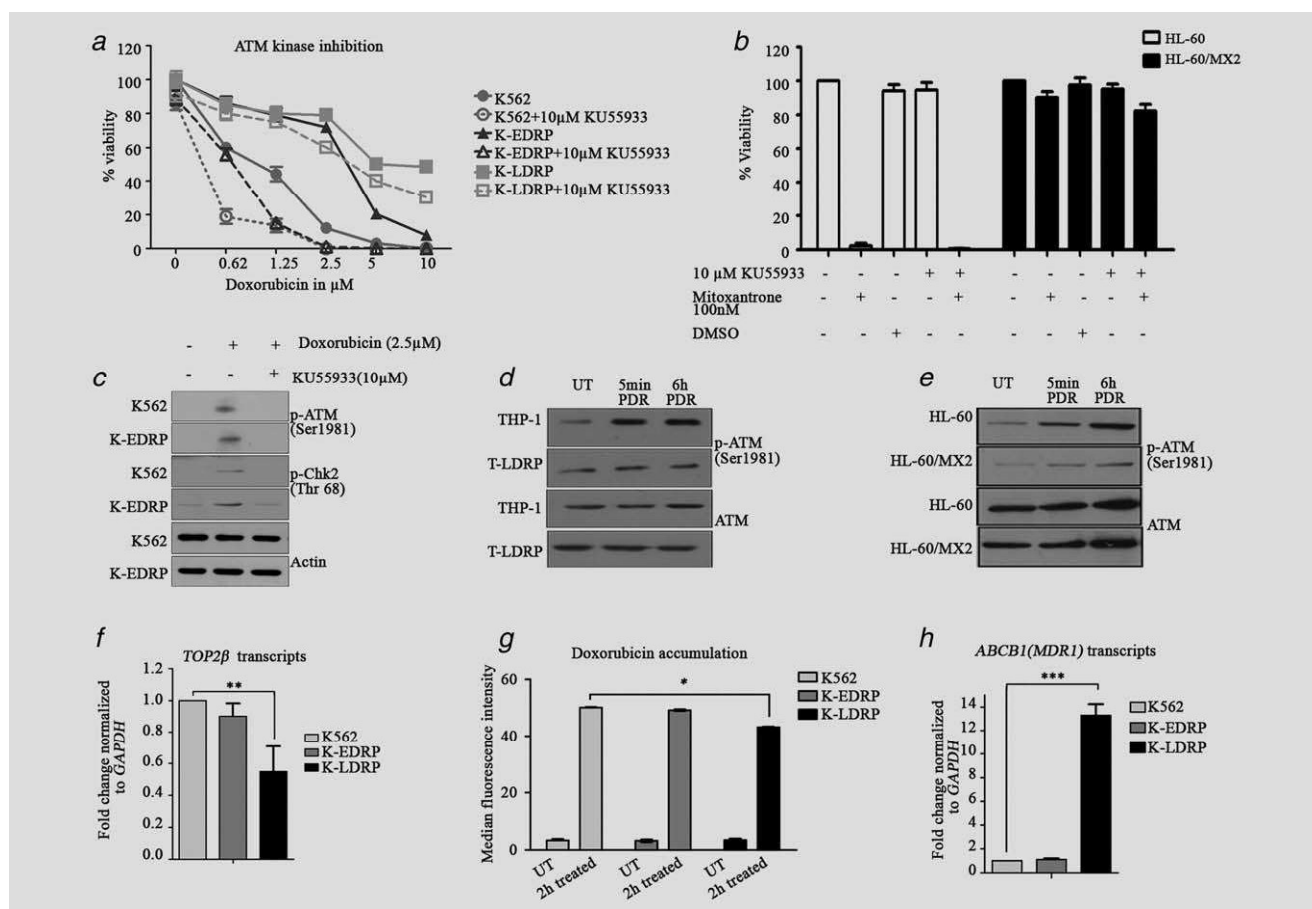


Figure 4. ATM kinase inhibition eliminates EDRP but not LDRP cells. (a) Line plot of cell viability as determined by MTT assay of parent K562, K-EDRP and K-LDRP cells with 10 μM of ATM kinase inhibitor and different concentrations of doxorubicin. (b) MTT assay for HL-60 and HL-60/MX2 cells after treatment with ATM kinase inhibitor (10 μM) and mitoxantrone (100 nM). DMSO was used as vehicle control. (c) Western blot of p-ATM and p-Chk2 showing specificity of ATM kinase inhibitor in K562 and K-EDRP cells. Actin was used as loading control. (d) Western blot showing p-ATM and total ATM after doxorubicin treatment at indicated time points post drug removal in THP-1 and T-LDRP. (e) Western blot showing p-ATM and total ATM after mitoxantrone treatment at indicated time points post drug removal in HL-60 and HL-60/MX2. (f) The mRNA expression of *TOP2 β* in parent K562, K-EDRP and K-LDRP cells, relative to *GAPDH* mRNA, as measured by SYBR green-based real-time PCR. (g) Doxorubicin accumulation measured by flow cytometry in K562 populations. Graph is plotted as median fluorescence intensity v/s different cell lines and conditions as indicated. (h) The mRNA expression of *ABCB1* in parent K562, K-EDRP and K-LDRP cells, relative to *GAPDH* mRNA, as measured by SYBR green based real-time PCR. Western blots represent results from at least 3 independent replicates. Results are the composite data from three independent experiments (mean \pm SEM); * denotes $p \leq .05$, ** denotes $p \leq .01$ and ***denotes $p \leq .001$.

THP-1 EDRP and LDRP (Fig. 4a and Supporting Information, Fig. 4a). As expected, ATM kinase inhibitor in combination with mitoxantrone did not show significant cell death in HL-60/MX2 cells (Fig. 4b). Specificity of ATM kinase inhibitor was confirmed by quantification of p-ATM and p-Chk2 (Fig. 4c). The differential response of EDRP and LDRP cells to ATM kinase inhibitor is attributed to the fact that, only EDRP but not LDRP cells show the activation of ATM with doxorubicin treatment (Figs. 4d and 4e). This was expected as the LDRP cells showed minimum DNA damage to the drug treatment. To understand how LDRP cells escape DNA damage, we reasoned that this could be because of loss of its molecular target or over expression of drug efflux proteins. Therefore, we checked the expression of *TOP2 β* (molecular target of doxorubicin and mitoxantrone) and drug

efflux pump protein *ABCB1* (*MDR1*) in all the three population of cells: parent, EDRP and LDRP. No significant differences were seen in the transcripts of *TOP2 β* in parent and EDRP. However, *TOP2 β* was found to be significantly down-regulated in LDRP of both K562 and THP-1 cell line (Fig. 4f and Supporting Information, Fig. 4b). Similarly, HL-60/MX-2 cells also showed downregulation of *TOP2 β* (Supporting Information, Fig. 4c). We further examined the drug accumulation capacity of the parent, EDRP and LDRP of K562 and THP-1 cells. For which cells were treated with IC90 concentrations of doxorubicin and intracellular doxorubicin was measured using flow cytometry at 480 nm (excitation wavelength) and 570 nm (emission wavelength).²⁴ Intracellular drug concentrations were found to be comparable in parent and EDRP but reduced in LDRP cells indicating either

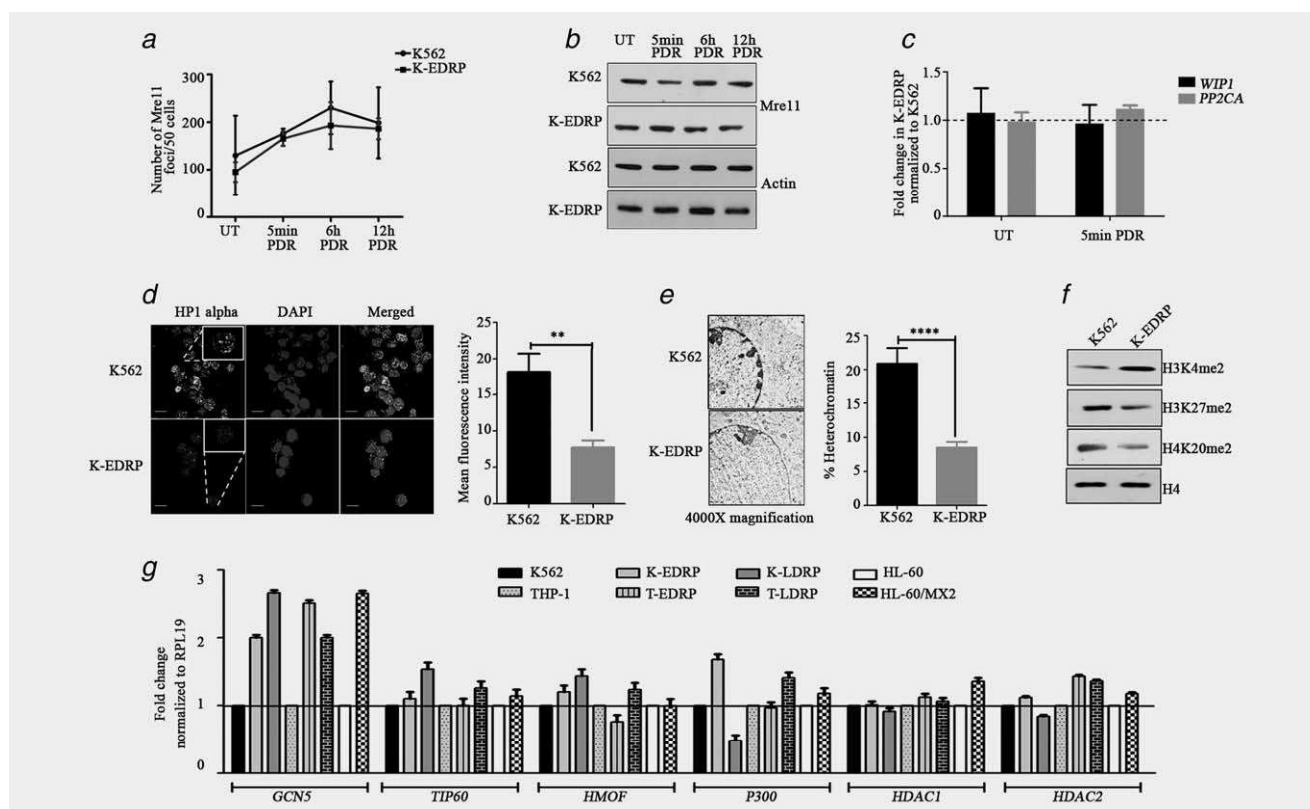


Figure 5. EDRP cells show GCN5 upregulation. (a) Mre11 recruitment kinetics in K562 and K-EDRP cells following 2 h of doxorubicin treatment. (b) Western blot for Mre11 with actin as loading control for parent and EDRP cells at indicated time points post drug removal. (c) SYBR green-based real-time PCR for *WIP1* and *PP2CA* in parent and EDRP cells before and after 2 h of doxorubicin treatment. (d) Immunofluorescence of HP1 alpha in parent and EDRP cells. Nuclei were counterstained with DAPI. Scale bar 20 μ m. Bar graph shows mean fluorescence intensity of HP-1 alpha staining in K562 and K-EDRP cells as calculated by ImageJ software. (e) Transmission electron micrograph of K562 and K-EDRP cells showing euchromatin and heterochromatin (dark staining). Bar graph quantifies % heterochromatin from EM images. (f) Western blot for histone modifications (H3K27me2, H3K4me2 and H4K20me2) in untreated K562 and K-EDRP cells. Total H4 was used as loading control. (g) Expression of HATs and HDAC (*GCN5*, *TIP60*, *HMOF*, *P300*, *HDAC1* and *HDAC2*) transcripts in different drug-resistant cell lines (K562, THP-1 and HL-60). Western blots represent results from at least 3 independent replicates. Results in bar and line graph are the composite data from three independent experiments (mean \pm SEM); ** denotes $p \leq .01$. Scale bar 20 μ m.

reduced uptake or faster efflux of drug by LDRP (Fig. 4g and Supporting Information, Fig. 4d). We found no significant difference in the transcript levels of *ABCB1* (i.e., *MDR1*) in parent and EDRP, but they were markedly elevated in LDRP (Fig. 4h and Supporting Information, Fig. 4e) suggesting that reduced drug accumulation in LDRP cells could be due to faster efflux of the drug. Collectively, these data showed that LDRP cells had evolved multiple mechanisms to escape drug induced DNA damage. However, given the central role of ATM activation in mediating chemoresistance in EDRP, we deemed it important to further understand the mechanism of higher ATM activation in EDRP cells.

EDRP cells show GCN5 upregulation

ATM activation is known to be controlled by the Mre11-Rad50-NBS1 (MRN) sensor complex.¹⁰ However, we did not find either differential expression or recruitment of Mre11 between parent K562 and K-EDRP, ruling out the possibility of MRN complex mediating differential recruitment of ATM

at DSBs in EDRP (Figs. 5a and 5b). We then reasoned that downregulation of ATM phosphatases (*WIP1* and *PP2CA*) could also maintain high levels of p-ATM.⁶ However, no differences in the transcript levels of *WIP1* and *PP2CA* in EDRP cells with respect to parent population were observed (Fig. 5c). It is also known that chromatin relaxation triggers higher ATM activation.⁶ We therefore did immunofluorescence staining for HP1 alpha (heterochromatin associated protein), indeed we found significant reduction in the levels of HP1 alpha in K-EDRP compared to the K562 population (Fig. 5d). Additionally, transmission electron microscopy of the K562 and K-EDRP also confirmed euchromatinization of K-EDRP (Fig. 5e) cells compared to parent population. Open chromatin in K-EDRP was further confirmed by the presence of increased levels of H3K4me2 and downregulation of H4K20me2 and H3K27me2 (Fig. 5f). HATs (Histone Acetyl Transferases) and HDACs (Histone deacetylases) are important in defining chromatin architecture and DNA repair response,²⁵ also higher expression of *TIP60* and *HMOF* are

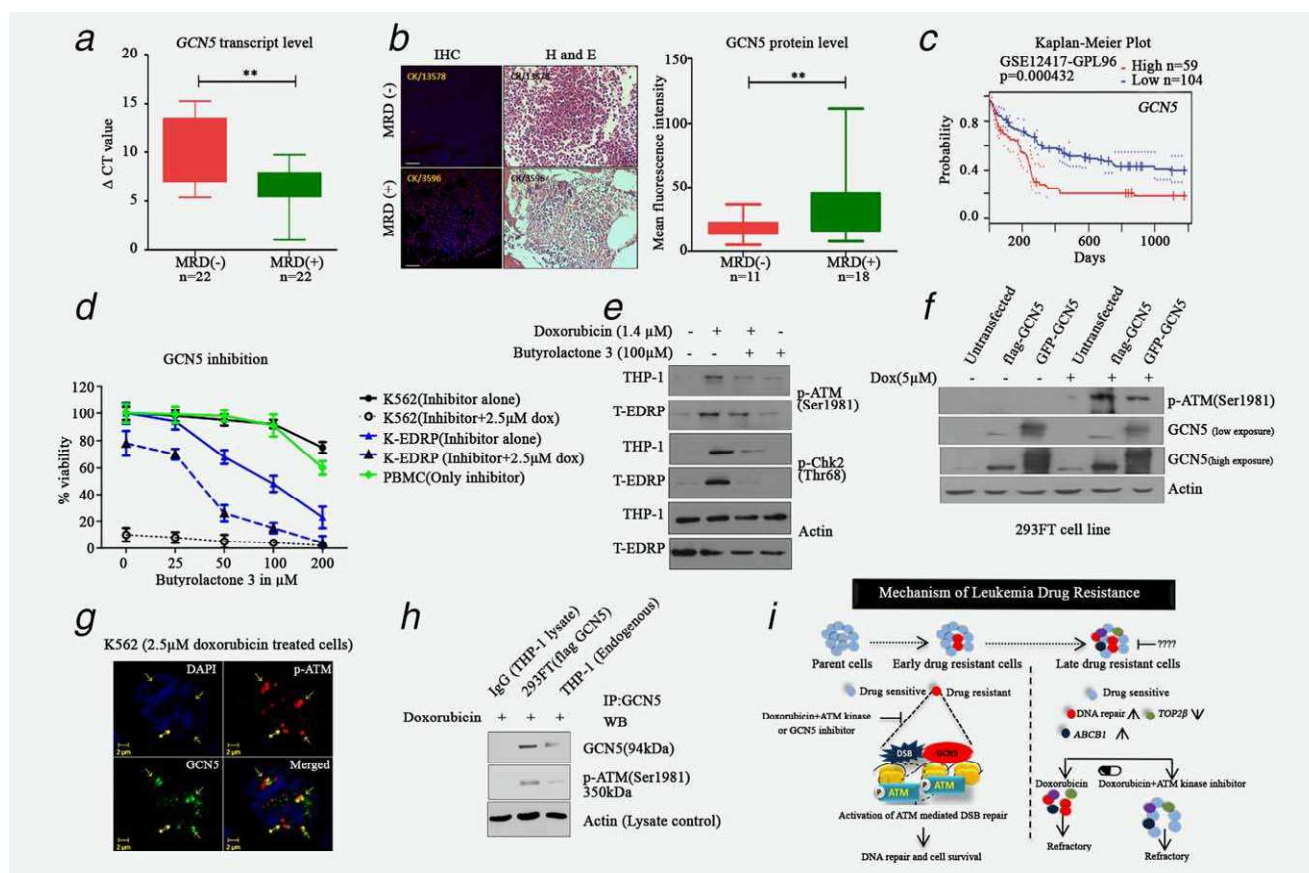


Figure 6. GCN5-mediated ATM hyperactivation causes onset of acquired drug resistance in leukemia. (a) Box plot represents transcript levels of *GCN5* as detected by SYBR green-based real-time PCR in baseline samples from MRD-negative and MRD-positive patients. Graph represents Δ ct values versus cohort of patient samples. (b) Representative images showing H and E staining and immunostaining for GCN5 (red). Nucleus is counterstained with DAPI (blue) in MRD-positive and MRD-negative AML bone marrow biopsies (scale bar = 50 μm). Graph shows the quantitation of immunostaining for MRD-positive ($n = 18$) and MRD-negative ($n = 11$) samples. (c) Kaplan–Meier survival analysis of AML patient samples from GSE12417-GLP96 dataset that have high or low expression of *GCN5*. (d) MTT assay for K562 and K-EDRP cells after the treatment of doxorubicin and GCN5 inhibitor (Butyrolactone 3). (e) Western blots for p-ATM and p-Chk2 from THP-1 parent and T-EDRP cells treated with different combinations of doxorubicin and Butyrolactone 3 as indicated. Actin was used as loading control. (f). Western blot for p-ATM, GCN5 and actin pre and post doxorubicin treatment in 293FT cells overexpressing Flag-GCN5 and GFP-GCN5. (g) Colocalization of GCN5 (green) and p-ATM (S1981) (red) in K562 post 2.5 μM doxorubicin treatment (scale bar = 2 μm). (h) Immunoprecipitation from THP-1 and 293FT overexpressing Flag-GCN5 cell lysates using anti-GCN5 or normal rabbit IgG antibodies. Western blots show the levels of GCN5 and p-ATM in the immunoprecipitates. Actin shows lysate used per reaction. Western blots represent results from at least 3 independent replicates. Results in bar and line graph are the composite data from three independent experiments (mean \pm SEM); * denotes $p \leq .05$ and ** denotes $p \leq .01$. (i) We mimicked the clinical scenario of resistance *in vitro* and developed EDRP and LDRP representing early and late stages of drug resistance. Enhanced DNA repair is the only mechanism of resistance in EDRP cells, whereas multiple mechanisms (enhanced DNA repair, *TOP2β* downregulation and *ABCB1* upregulation) are active in LDRP. EDRP cells show higher euchromatin. Upon DNA damage, GCN5 cause higher recruitment of ATM, consequently activating BRCA1, NBS1, Chk2 and Mcl-1L and enhancing DNA repair and cell survival. Combination of ATM inhibitor (KU55399) or GCN5 inhibitor and doxorubicin induce significant apoptosis in EDRP but fail to eradicate LDRP cells due to activation of multiple survival mechanisms.

known to activate ATM. Therefore, to define which HAT/HDAC could be responsible for euchromatinization in EDRP cells, we analyzed the transcript levels of *P300*, *GCN5*, *TIP60*, *HMOF*, *HDAC* and *HDAC2* in all the chemoresistant populations. We found *GCN5* to be overexpressed in all the different populations of chemoresistant cell lines (K562, THP-1 and HL-60) (Fig. 5g).

To examine the expression of *GCN5* in AML patient samples, peripheral blasts of 44 AML patients at baseline (at diagnosis) were collected and immunophenotypically

characterized. Patient information is provided in Supporting Information, Table 4. Immunophenotyping by multiparametric flow cytometry (MPFC) was used to classify these patients into MRD-positive and MRD-negative cohorts post induction and consolidation therapy. Baseline samples were then analyzed for *GCN5* expression by SYBR green-based quantitative real-time PCR using *RPL19* as internal control. Absolute Δ ct values were used to compare the expression differences of *GCN5* between MRD-positive ($n = 22$) and MRD-negative ($n = 22$) patients (Fig. 6a). We found that MRD-positive

patients had significantly higher expression of *GCN5* compared to MRD-negative patient samples. Consequently, protein levels of *GCN5* were also significantly higher in MRD-positive ($n = 18$) AML baseline bone marrow biopsies compared to MRD-negative ($n = 11$) samples as shown by immunostaining (Fig. 6b). Additionally, we analyzed two AML microarray datasets GSE12417-GLP96 ($n = 163$)²⁶ and GSE5122 ($n = 58$)²⁷ using Prognoscan²⁸ and found that *GCN5* overexpression significantly (minimum p values = 0.000432 and $p = 0.046$) correlates with poor patient survival (Fig. 6c and Supporting Information, Fig. 5a). These results suggest that *GCN5* expression could be used to predict therapy response in AML patients.

GCN5-mediated ATM hyperactivation causes onset of acquired drug resistance in leukemia

Although *GCN5* upregulation was associated with chemoresistant population, however, to analyze if *GCN5* also contributed to the chemoresistance, we treated EDRP of K562 and THP-1 with different concentrations of *GCN5* inhibitor (Butyrolactone 3) alone and in combination with doxorubicin. Indeed, inhibition of *GCN5* significantly sensitized K-EDRP to doxorubicin. Importantly, Butyrolactone 3 had no effect on the viability of peripheral blood mononuclear cells (PBMCs) at 100 μ M concentration (Fig. 6d and Supporting Information, Fig. 5b). Furthermore, *GCN5* inhibition also sensitized K-EDRP cells to daunorubicin suggesting that *GCN5* plays a role in resistance to daunorubicin (Supporting Information, Fig. 5c). We next examined whether *GCN5* inhibition is linked with ATM activation in leukemia cells. For this, we treated parent and EDRP cells with *GCN5* inhibitor prior to doxorubicin treatment. As evident from Figure 6e and Supporting Information, Fig. 5d, *GCN5* inhibition led to decreased p-ATM and p-Chk2 in doxorubicin-treated EDRP and parent cells. To confirm that decreased p-ATM was due to loss of *GCN5* and not because of off-target effect of the inhibitor, we performed siRNA-mediated knockdown of *GCN5* in THP-1 cell line. Indeed, THP-1 *GCN5* knockdown cells showed reduced p-ATM post doxorubicin treatment compared to control siRNA (Supporting Information, Fig. 6a). Similar results were also observed in HL-60, KG-1 (leukemic cell lines) and 293FT (nontransformed cell line) (Supporting Information, Figs. 6b and 6c), demonstrating that interaction of *GCN5* and ATM is not restricted to a specific cell type.

GCN5 colocalizes and interacts with ATM post doxorubicin treatment

To further confirm that *GCN5* over expression can induce higher ATM activation, we overexpressed Flag-tagged and GFP-tagged *GCN5* in 293FT cells. These cells when treated with doxorubicin showed higher ATM activation compared to doxorubicin treated non *GCN5* overexpressing 293FT cells (Fig. 6f). Next to understand, if the direct interaction of *GCN5* with ATM enhances its recruitment, we first

performed colocalization of *GCN5* and p-ATM (S1981) in K562 cells following doxorubicin treatment. As seen from Figure 6g, *GCN5* and p-ATM showed overlapping foci, suggestive of their physical interaction. To further examine if *GCN5* and ATM physically interact, we immunoprecipitated *GCN5* from doxorubicin treated THP-1 and Flag-*GCN5* overexpressing 293FT cells. As can be seen from Figure 6h, p-ATM (S1981) was co-immunoprecipitated with *GCN5* from both the cell lines. These data confirm that *GCN5* physically interacts with ATM kinase post doxorubicin treatment, although we cannot rule out the plausibility of other proteins in the complex that could be mediating the interaction of *GCN5* and ATM. Taken together, this is the first study that shows *GCN5* interacts with ATM and inhibition of *GCN5* activity inhibits ATM activation.

DISCUSSION

Collectively, the data summarized in Figure 6i show that early drug-resistant cells survive by modulating DNA repair via higher activation of ATM kinase mediated by *GCN5*. Accordingly, these cells can be efficiently targeted by *GCN5* and ATM inhibitors. In contrast, LDRP cells undergo several rounds of drug selection and acquire more than one bona fide drug-resistance mechanisms and therefore do not respond to ATM inhibitor. These findings provide a plausible mechanistic explanation for the failure of DDR inhibitors that are tested in clinical trial for the relapse, refractory and advanced stage patients.

We observed that both early and late acquired drug resistance was reversible in absence of drug, which indicates non-genetic routes of resistance. We demonstrate that modulation of DNA repair pathway is the first response of the cells toward development of resistance to DNA-damaging drugs and over multiple rounds of drug treatment, there is a gradual accumulation of molecular events that leads to difficult to treat highly resistant cells. At least during the early drug resistant stage as defined by our studies, there are no multiple clones with different mechanisms of resistance, because ATM inhibitor with doxorubicin in EDRP kills all the cells. However, we cannot rule out the fact that there are different mechanisms in different clones all requiring ATM activation for their survival. *GCN5* is a lysine acetyl transferase involved in post translational modification of multiple histone and nonhistone proteins. *GCN5* acts as a transcription activator and is a part of human ATAC and STAGA complex.²⁹ *GCN5* have been shown to interact with DNA repair proteins like DNA-PK, Ku70/80, H2AX³⁰ and also have been reported to be involved nucleotide excision repair.³¹ This is the first report showing *GCN5* is required for efficient ATM activation. However, our understanding of *GCN5* and ATM interaction is inadequate and requires further investigation. This study identifies two important candidates (ATM and *GCN5*) that can be targeted during early stages of acquired resistance to prevent relapse. Recently, *GCN5* is shown as potential therapeutic target against AML and ALL *in vivo*.^{32,33}

Moreover, our data demonstrate GCN5 to be an important drug target that precludes leukemia drug resistance. Most importantly, we also demonstrate that GCN5 expression can be used as an indicator to detect onset of acquired drug resistance. We show that ATM inhibition in the EDRP along with doxorubicin not only induce apoptosis in EDRP but also significantly lower the concentration of doxorubicin required to induce complete cell death thus, increasing the efficacy of doxorubicin many folds. In conclusion, our data provides mechanistic explanation to clinical observations and demonstrate that preventing emergence of resistance by targeting early drug-resistant population would be more effective therapeutic approach in leukemia treatment. We believe that these findings are clinically significant and warrant further studies to establish their *in vivo* significance.

References

- Chen X, Xie H, Wood BL, et al. Relation of clinical response and minimal residual disease and their prognostic impact on outcome in acute myeloid leukemia. *JCO* 2015;33:1258–64.
- Harker WG, Slade DL, Parr RL, Feldhoff PW, Sullivan DM, Holguin MH. Alterations in the topoisomerase II alpha gene, messenger RNA, and subcellular protein distribution as well as reduced expression of the DNA topoisomerase II beta enzyme in a mitoxantrone-resistant HL-60 human leukemia cell line. *Cancer Res* 1995;55:1707–16.
- Marin JJ, Briz O, Rodriguez-Macias G, et al. Role of drug transport and metabolism in the chemoresistance of acute myeloid leukemia. *Blood Rev* 2016;30:55–64.
- Elliott SL, Crawford C, Mulligan E, et al. Mitoxantrone in combination with an inhibitor of DNA-dependent protein kinase: a potential therapy for high risk B-cell chronic lymphocytic leukaemia. *Br J Haematol* 2011;152:61–71.
- Bian K, Muppani NR, Elkhadragy L, et al. ERK3 regulates TDP2-mediated DNA damage response and chemoresistance in lung cancer cells. *Oncotarget* 2016;7:6665–75.
- Paull TT. Mechanisms of ATM activation. *Annu Rev Biochem* 2015;84:711–38.
- SunWang H, Wang Y, Meng Z, Qi J, Yang ZG. Aurora-A controls cancer cell radio- and chemoresistance via ATM/Chk2-mediated DNA repair networks. *Biochim Biophys Acta* 2014;1843:934–44.
- Yoon JH, Ahn SG, Lee BH, et al. Role of autophagy in chemoresistance: regulation of the ATM-mediated DNA-damage signaling pathway through activation of DNA-PKcs and PARP-1. *Biochem Pharmacol* 2012;83:747–57.
- Te Raa GD, Moerland PD, Leeksa AC, et al. Assessment of p53 and ATM functionality in chronic lymphocytic leukemia by multiplex ligation-dependent probe amplification. *Cell Death Dis* 2015;6:e1852.
- Lee JH, Paull TT. ATM activation by DNA double-strand breaks through the Mre11-Rad50-Nbs1 complex. *Science* 2005;308:551–4.
- Shreeram S, Demidov ON, Hee WK, et al. Wip1 phosphatase modulates ATM-dependent signaling pathways. *Mol Cell* 2006;23:757–64.
- McConnell JL, Gomez RJ, McCorvey LR, et al. Identification of a PP2A-interacting protein that functions as a negative regulator of phosphatase activity in the ATM/ATR signaling pathway. *Oncogene* 2007;26:6021–30.
- You Z, Bailis JM, Johnson SA, et al. Rapid activation of ATM on DNA flanking double-strand breaks. *Nat Cell Biol* 2007;9:1311–8.
- Gong F, Miller KM. Mammalian DNA repair: HATs and HDACs make their mark through histone acetylation. *Mutat Res* 2013;750:23–30.
- Sun Y, Jiang X, Chen S, et al. A role for the Tip60 histone acetyltransferase in the acetylation and activation of ATM. *Proc Natl Acad Sci USA* 2005;102:13182–7.
- Boutet-Robinet E, Trouche D, Canitrot Y. Neutral comet assay. *Bio-protocol* 2013;3:e915.
- Singh KSHR. A comparison of gray-level run length matrix and gray-level co-occurrence matrix towards cereal grain classification. *Int J Comput Eng Technol* 2016;7: (November–December).
- Harker WG, Slade DL, Dalton WS, Meltzer PS, Trent JM. Multidrug resistance in mitoxantrone-selected HL-60 leukemia cells in the absence of P-glycoprotein overexpression. *Cancer Res* 1989;49:4542–9.
- PodhoreckaSkładanowski M, Bozko AP. H2AX phosphorylation: its role in DNA damage response and cancer therapy. *J Nucleic Acids* 2010;2010.
- Jang ER, Choi JD, Park MA, et al. ATM modulates transcription in response to histone deacetylase inhibition as part of its DNA damage response. *Exp Mol Med* 2010;42:195–204.
- Mao Z, Jiang Y, Liu X, et al. DNA repair by homologous recombination, but not by nonhomologous end joining, is elevated in breast cancer cells. *Neoplasia* 2009;11:683–91.
- Morrison C, Sonoda E, Takao N, et al. The controlling role of ATM in homologous recombinational repair of DNA damage. *Embo J* 2000;19:463–71.
- Hamilton G, Yee KS, Scrase S, et al. ATM regulates a RASSF1A-dependent DNA damage response. *Curr Biol* 2009;19:2020–5.
- Kim DW, Kim KO, Shin MJ, et al. siRNA-based targeting of antiapoptotic genes can reverse chemoresistance in P-glycoprotein expressing chondrosarcoma cells. *Mol Cancer* 2009;8:28.
- Bhoomik A, Singha N, O'connell MJ, et al. Regulation of TIP60 by ATF2 modulates ATM activation. *J Biol Chem* 2008;283:17605–14.
- Metzeler KH, Hummel M, Bloomfield CD, et al. An 86-probe-set gene-expression signature predicts survival in cytogenetically normal acute myeloid leukemia. *Blood* 2008;112:4193–201.
- Raponi M, Harousseau JL, Lancet JE, et al. Identification of molecular predictors of response in a study of tipifarnib treatment in relapsed and refractory acute myelogenous leukemia. *Clin Cancer Res* 2007;13:2254–60.
- Mizuno H, Kitada K, Nakai K, et al. PrognosScan: a new database for meta-analysis of the prognostic value of genes. *BMC Med Genomics* 2009;2:18.
- Nagy Z, Tora L. Distinct GCN5/PCAF-containing complexes function as co-activators and are involved in transcription factor and global histone acetylation. *Oncogene* 2007;26:5341–57.
- Chatr-Aryamontri A, Oughtred R, Boucher L, et al. The BioGRID interaction database: 2017 update. *Nucleic Acids Res* 2017;45:D369–79.
- Zhao M, Geng R, Guo X, et al. PCAF/GCN5-mediated acetylation of RPA1 promotes nucleotide excision repair. *Cell Rep* 2017;20:1997–2009.
- Tzelepis K, Koike-Yusa H, De Braekeleer E, et al. A CRISPR dropout screen identifies genetic vulnerabilities and therapeutic targets in acute myeloid leukemia. *Cell Rep* 2016;17:1193–205.
- Holmlund T, Lindberg MJ, Grandér D, et al. GCN5 acetylates and regulates the stability of the oncoprotein E2A-PBX1 in acute lymphoblastic leukemia. *Leukemia* 2013;27:578–85.

FINANCIAL SUPPORT

This work was supported by Indian Council of Medical Research (grant no. 90/04/2012-STM(TF)/BMS) to Dr Shilpee Dutt.

Disclosure of Potential Conflicts of Interest

The authors declare no conflict of interests.

Acknowledgement

The authors thank Dr Amit Dutt and Pawan Upadhyay for STR profiling of the cell lines used in this study, Dr Epari Shridhar for providing AML patient bone marrow biopsy samples and Dr Saurabh Mishra (LPU Punjab) for his help in quantitation of heterochromatin from electron microscopy images.